Delft University of Technology
Faculty of Civil Engineering and Geosciences
Department of Design & Construction – Concrete Structures

Universidad San Francisco de Quito
Politecnico

Report nr. 25.5-14-04

July 2nd 2014

Fatigue of concrete under compression
Database and proposal for high strength concrete

Auteur:
Dr. ir. E.O.L. Lantsoght

Delft University of Technology Report nr. 25.5-14-04
Faculty of Civil Engineering and Geosciences
Department of Design & Construction – Concrete Structures

Universidad San Francisco de Quito
Politecnico

July 2nd 2014

Fatigue of concrete under compression
Database and proposal for high strength concrete

Auteur:
Dr. ir. E.O.L. Lantsoght

Delft University of Technology
Faculty of Civil Engineering and Geosciences
Department of Design & Construction – Concrete Structures
Stevinlaboratorium
Postbus 5048
2600 GA Delft
Telephone 015 2783990/4578
Telefax 015 2785895/7438

Contents

1 Introduction

The compressive strength of concrete decreases as an element is subjected to cycles of loading. In a typical fatigue test for the concrete compressive strength, a concrete specimen (typically a cylinder) is loaded between a lower and upper stress limit. These limits are expressed as a fraction of the concrete compressive strength, and can be written as $S_{min}f_{ck}$ and $S_{max}f_{ck}$. The value of S_{min} and S_{max} are thus between 0 and 1. The upper limit for S_{max} in experiments is typically 0,95 and S_{min} can be as low as 0,02. Experiments in which alternating tensile and compressive stresses are applied can also be executed, but this loading case is not considered in the current study.

The result of fatigue tests on concrete cylinders in compression is the so-called Wöhler-curve, or *S-N* curve. In this graph, a (linear) relation is found between the logarithm of the number of cycles N and the maximum fraction of the static compressive strength S_{max}. In the codes, different expressions are given for the relation between N and S_{max}. The codes that are studied in this report are the Dutch Code NEN 6723:2009 (Code Committee 351 001 "Technical Foundations for Structures", 2009), the Eurocode suite for concrete: NEN-EN 1992-1-1+C2:2011 (CEN, 2011a) with the Dutch National Annex NEN-EN 1992-1-1+C2:2011/NB:2011 (Code Committee 351 001, 2011a) and NEN-EN 1992-2+C1:2011 (CEN, 2011b) and the Dutch National Annex NEN-EN 1992-2+C1:2011/NB:2011 (Code Committee 351 001, 2011b), the new Model Code 2010 (fib, 2012). Some expressions from the literature are considered as well, such as the proposal by Hans Bongers (Snijders, 2013) and an expression suitable for higher strengths concrete (Kim and Kim, 1996).

The expression for concrete under compression subjected to cycles of loading from NEN-EN 1992-1-1+C2:2011 is more conservative than previously used expressions in the Netherlands. Therefore, different expressions are given in the National Annex NEN-EN 1992-1-1+C2:2011/NB:2011. The *S-N* relationship given in the Dutch National Annex consists of two equations: the first branch is valid for $N \leq 10^6$ cycles and the second branch for $N > 10^6$ cycles. The transition between these two expressions is not smooth, but instead causes a jump in the Wöhler-curve.

Because of this anomaly in the current code provisions, it is necessary to propose a new expression for concrete under cycles of compressive loading. Moreover, the proposed expression should be valid, yet not overly conservative, for high strength concrete. The current Eurocode NEN-EN 1992-1-1+C2:2011 is limited to concrete class C90/105. The *fib* Model Code goes up to C120. The goal of this report is to develop an expression that is valid up to C120. To check the quality of the proposed expression, it should be compared to experimental results. For this purpose, a database of experiments on (ultra) high strength concrete tested in compressive fatigue is developed first, and then used to validate the new proposal for concrete under cycles of compression.

2 Literature survey on fatigue of concrete under compression

2.1 Basics of compressive fatigue

This chapter aims at giving an overview on the fatigue strength of concrete under compression, with an emphasis on the important parameters that affect the fatigue life and the recent results and development with respect to high strength concrete.

The current study focuses on compression fatigue. However, it appears that the same equations can be used for flexural fatigue if the concrete compressive strength f_{ck} is replaced by the modulus of rupture f_r (Hsu, 1981).

Fatigue is of importance for structures subjected to repetitive loading, such as bridges. Static actions not repeated more than 10^4 times, for which $\psi_1 = 0$, are considered unable to produce fatigue failure. Examples of actions able to cause fatigue are loads due to vehicles, moving machinery, wind (gusts, turbulence, vortices, etc.) and wave action (fib, 2012). However, fatigue cracking in concrete is not as easy and straightforward to determine as fatigue cracks in, for example, steel. As such, it is difficult to identify fatigue distress in concrete structures (CEB Committee GTG 15, 1988). It is nonetheless evident, that each of the following, when present, significantly influence the behavior of the structure or element:

1. Repeated deflections leading to secondary stresses.
2. Increased traffic stresses and rolling loads of increased frequency and/or magnitude on bridges, pavements and slabs.
3. Live load stresses much greater than dead load stresses.
4. Repeated impact and other forces on bridge bearings, pavement joints and elsewhere in structures.
5. Vibration, particularly when associated with contaminants and dynamically lively elements.
6. Unconfined or poorly confined points of application of repeated loads.
7. Fretting, pitting and chemical attack, particularly in prestressed concrete.
8. Carbonation attack, particularly in reinforced concrete.

As explained in the introduction, the fatigue behavior (of, among other, concrete in compression) is expressed by the Wöhler-curve which shows a (linear) relationship between the logarithm of the number of cycles to failure N and the fraction of the static compressive strength S_{max} to which the element is subjected, as given for example in Fig. 1. The general methods to find the relation between S_{max} and N are based on the assumption of a linear relationship between S_{max} and $\log N$. From experiments, it is known that the S-N curve for concrete is approximately linear starting at 100 cycles (Kim and Kim, 1996).

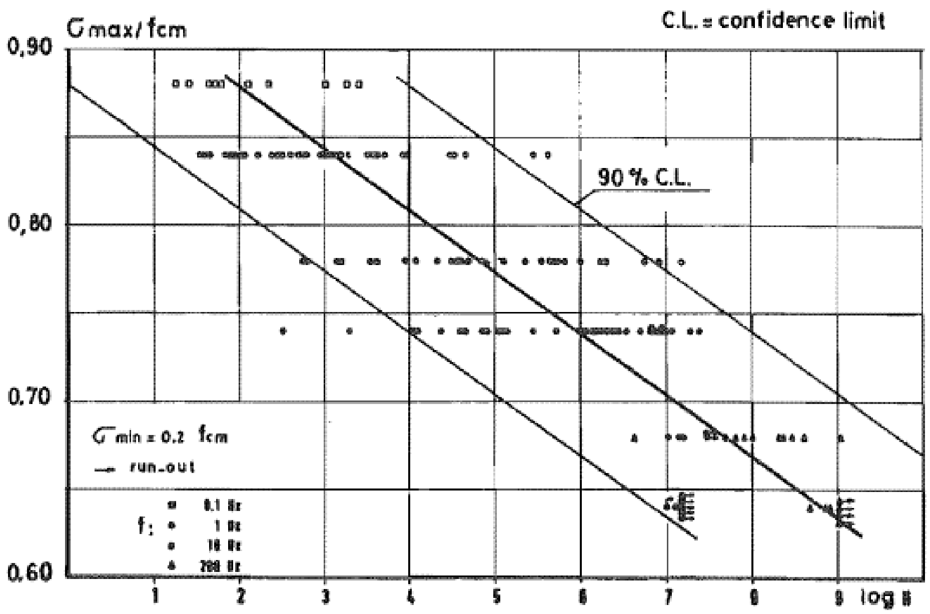

Fig. 1: Typical S-N line for concrete in compression (CEB Committee GTG 15, 1988).

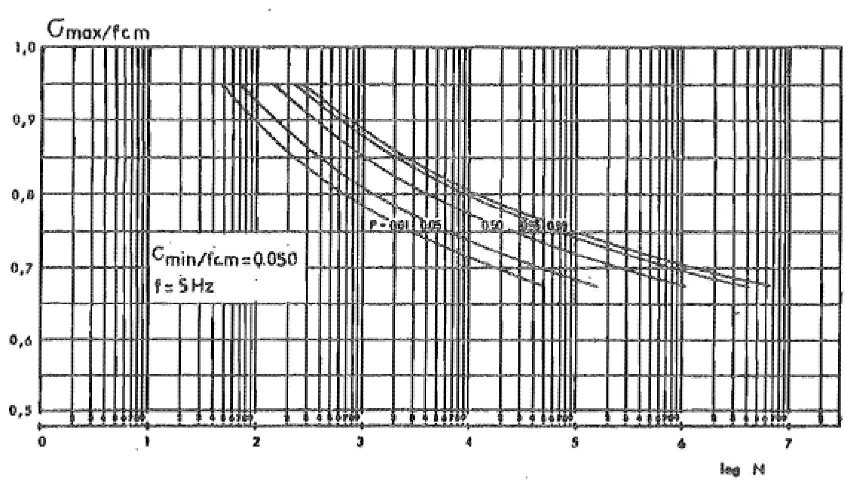

Fig. 2: Probability of failure lines in S-N diagram (CEB Committee GTG 15, 1988).

2.2 Parameters determing the fatigue strength

The fatigue strength depends on the maximum as well as on the minimum stress in the cycle, an effect that can be represented by a Goodmann diagram (Fig. 3a), or Smith diagram (Fig. 3b). An increase of the minimum stress level S_{min} typically results in an increased fatigue strength for a given number of cycles (CEB Committee GTG 15, 1988). Sometimes the stress ratio $R = S_{min}/S_{max}$ is included in the relationship describing the fatigue life of concrete under compression. In that case it is possible to express both the

S-N curve and the Smith diagram in a single equation and graph (CEB Committee GTG 15, 1988), Fig. 4. The expression then looks as follows:

$$S_{max} = 1 - \beta(1-R)\log N$$

in which β = 0,064 – 0,08, a material constant. The scatter on this expression, when derived from experimental results, can be described by a dependence of the standard deviation of log*N* on the fatigue stresses (expressed as *R* and S_{max}) and the scatter on the concrete compressive strength (CEB Committee GTG 15, 1988), Fig. 5. The scatter on the number of cycles to failure for a given stress level can be explained by the scatter on the static compressive strength (Holmen, 1982). This scatter is nonetheless signifciant, and therefore it is necessary to test a number of specimens at each of different levels of S_{max} to determine the *S-N* curve. With the use of probabilistic methods, a relation between the probability of failure and the number of cycles to failure can be obtained, It must be noted as well that the static strength usually is determined from tests in which the rate of load application may be several orders of magnitude less than the rate of loading in the fatigue test. As the static strength of concrete is influenced by the rate of loading and the shape of the test specimen, the resulting values for the compressive capacity should be considered as nominal values related to convential strength properties which may not truly reflect the conditions in the loaded structure (CEB Committee GTG 15, 1988). Variables such as water-cement ratio, cement content, amount of entrained air, curing conditions and age at loading do not seem to influence the fatigue strength when expressed as S_{max} and S_{min}. These conclusions were based on extensive experimental research for concrete compressive strengths up to 60 MPa (CEB Committee GTG 15, 1988).

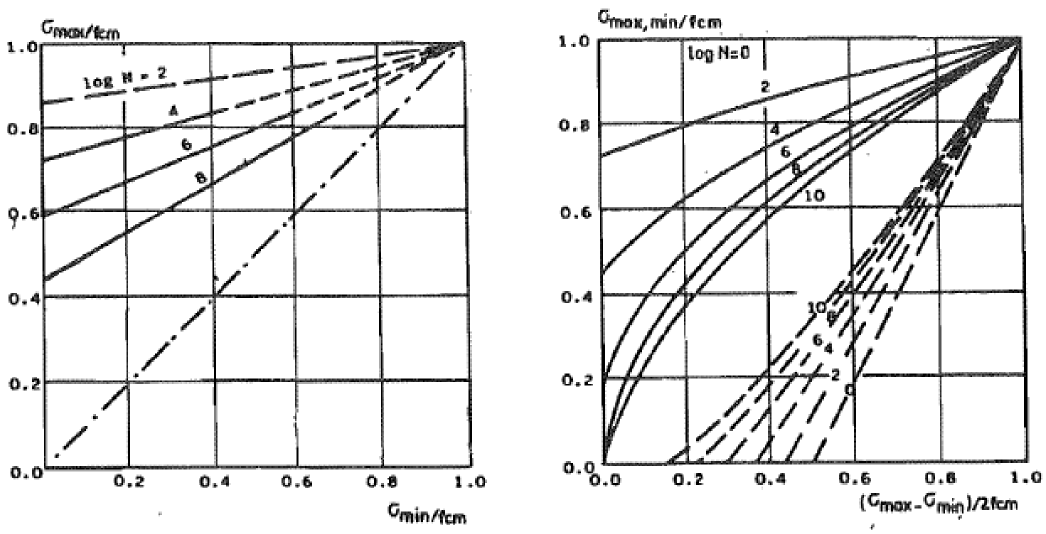

Fig. 3: (a) Goodman diagram; (b) Smith diagram (CEB Committee GTG 15, 1988).

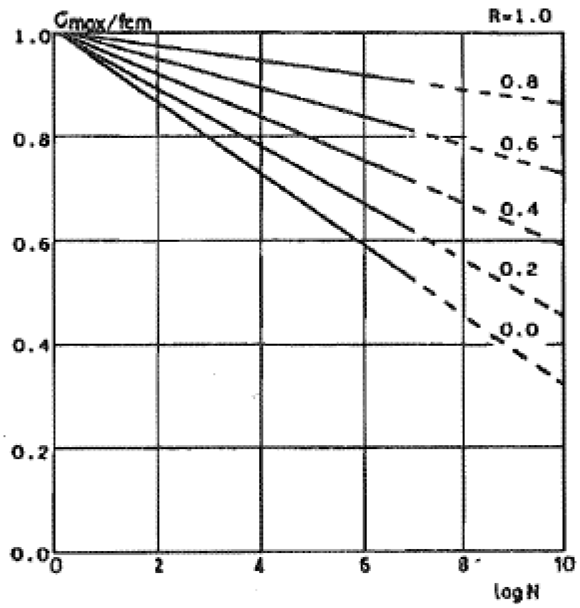

Fig. 4: S-N lines for various R values (CEB Committee GTG 15, 1988).

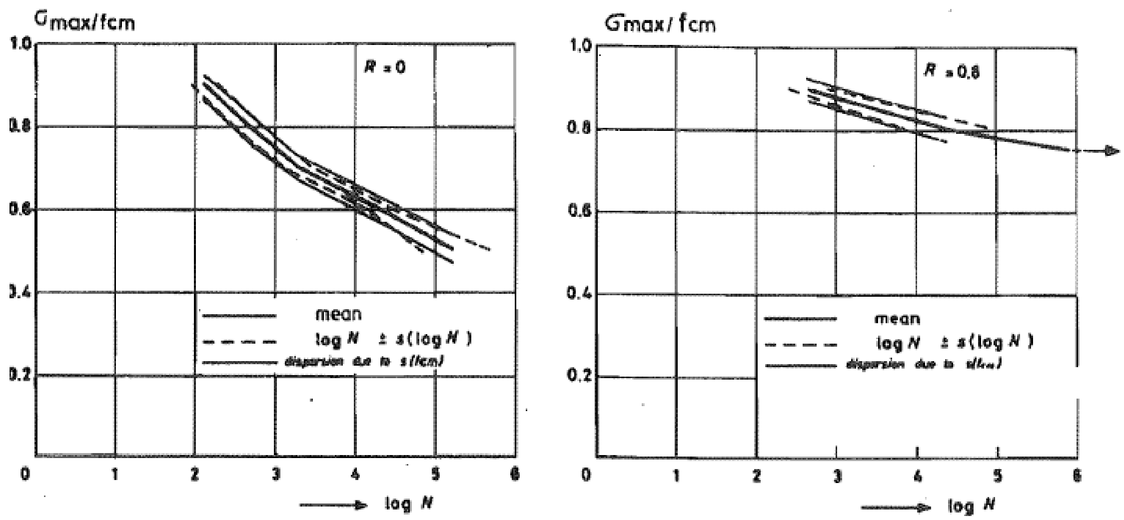

Fig. 5: Scatter in S-N diagrams explained by the dispersion due to the concrete compressive strength (CEB Committee GTG 15, 1988).

Another property that is typically studied in fatigue experiments and research, is the increase of the strain (sum of elastic and inelastic strain) at the maximum stress during the load cycles ($S_{max}f_{ck} = \sigma_{max}$). This strain typically shows an increase as the number of cycles increases as shown in Fig. 6. The number of cycles in this figure is expressed as a ratio between the number of cycles and the number of cycles to failure N/N_f, which is sometimes also described as the accumulated damage. The strain as a function of N/N_f goes through 3 stages: the first stage (from 0 to 10 percent of the total life) is characterized by a quick increase of the strain as the number of cycles increase, the second stage (from 10 to 80% of the total life) has a slow, steady and linear increase for the strain with the number of cycles, and in the third and final stage, the strain increases rapidly with the number of cycles, indicating that failure is imminent – until failure occurs. The variation of the total strain seems to be a function of the stress level, but independent of the number of cycles to failure at a constant stress level, provided that the duration of the test is less than a few hours. If the test takes more time, the total strain increases with the time as a function of the stress level. The total maximum strain can be written as the sum of two components $\varepsilon_{max} = \varepsilon_e + \varepsilon_t$ with ε_e related to the endurance of the specimen (including the elastic strain) and ε_t the time dependent strain, which is mostly determined by the creep deformation. By measuring the variation of the total maximum strain, it should be possible to assess the remaining life of a partially fatigued specimen and the ultimate strain can be used as a fatigue criterion for concrete. On the other hand, the residual strain reflects the development of damage, and as such it can be used to measure fatigue damage of concrete and fatigue life under various loading conditions (CEB Committee GTG 15, 1988). It is the strain development in the secondary branch (Fig. 6) that is of importance for the fatigue life prediction: the relation between the secondary cyclic strain rate and the number of cycles to failure can be used. This relation is found to be independent of the testing frequency, but depending on the type of aggregate (CEB Committee GTG 15, 1988).

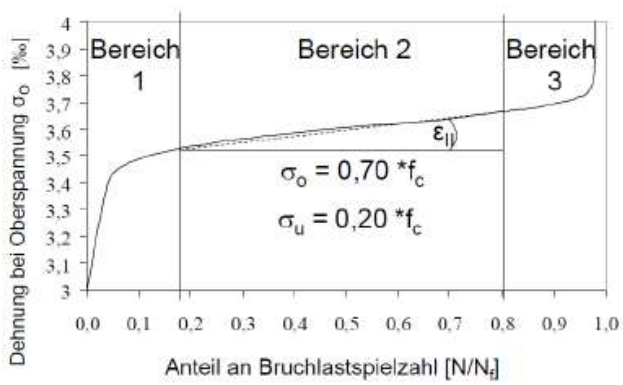

Fig. 6: Strain increase as number of cycles increases (Fehling et al., 2013)

It was found in experiments (Fehling et al., 2013) that the strain in the second stage (Fig. 6), ε_{II}, can hint at the *S-N* curve for more than 10^8 cycles. The value of logε_{II} describes the increase of the strains with the number of cycles in the second branch of the relation between the strains and the number of cycles, and can possibly be used as a good predictor for $N_f > 10^8$, the range for which experimental results are scarce, Fig. 7 (Fehling et al., 2013). When considering the strains and stresses, envelope curves can also be developed, as given in Fig. 8.

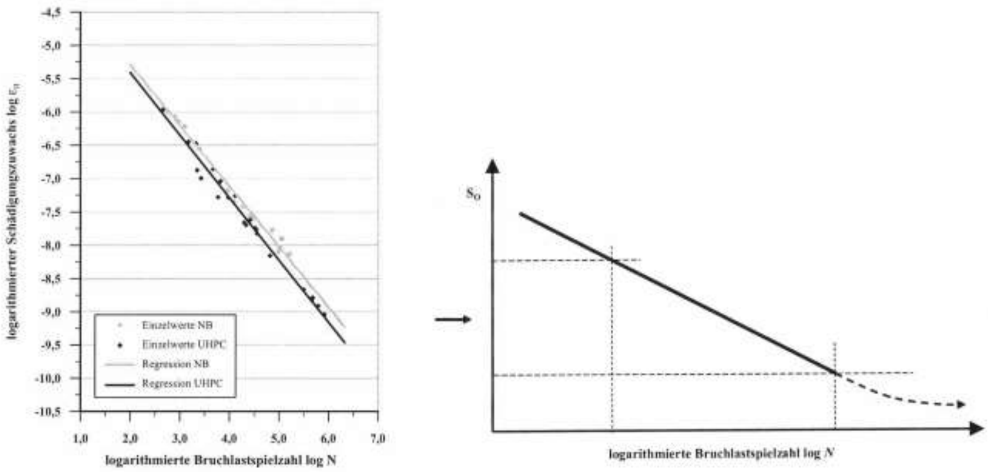

a) **b)**

Fig. 7: Interpretation of the relation between logε_{II} and logN and its impact on the course of the S-N curve. (Fehling et al., 2013).

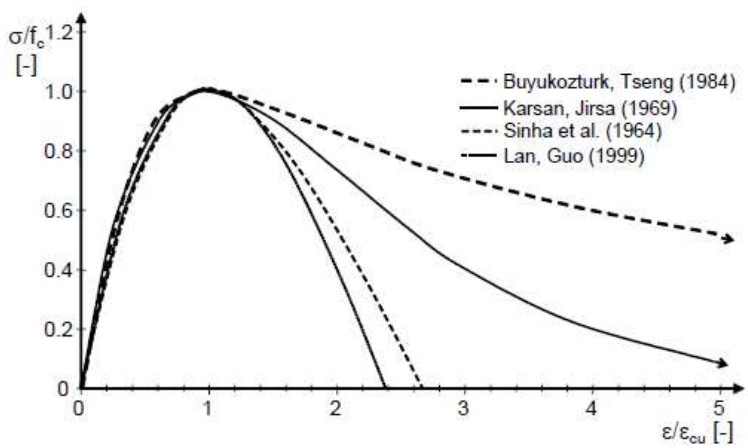

Fig. 8: Stress-strain relations of the envelope curves for concrete under compressive cyclic loading.

The relationship between stresses and strains in the concrete is also influenced by the number of cycles. As the number of load repetitions are increased, the curve changes from concave towards the strain axis to a straight line to convex, Fig. 9. The degree of convexity is an indication of how near the concrete specimen is to fatigue failure.

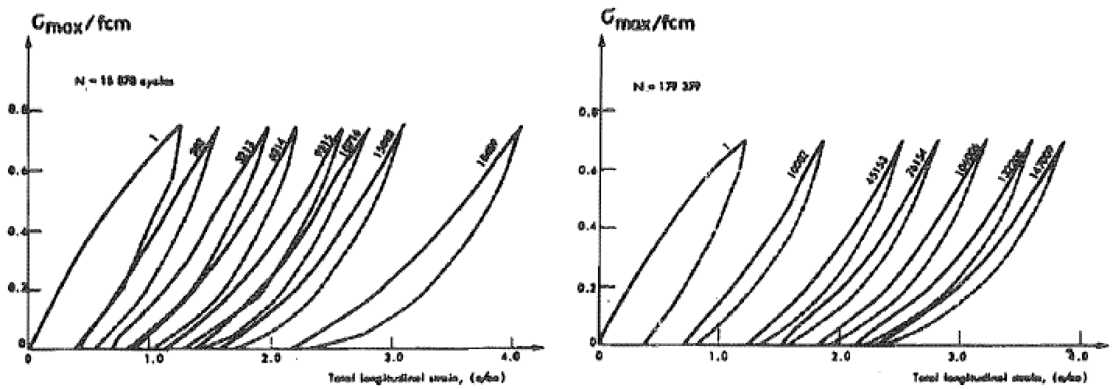

Fig. 9: Cyclic stress-strain curves for concrete in compression (CEB Committee GTG 15, 1988).

Most fatigue experiments are tested by alternating stresses continuously until failure. Some research studied the effect of rest periods. The results of this research, in which repeated rest periods up to 5 minutes after each set of 4500 cycles are used, indicate that rest periods increase the fatigue strength, and that some recovery occurs during the rest periods.

A last parameter that has an influence on the fatigue life is the frequency of loading that is used in experiments. A common conclusion is that a frequency between 1 and 15 Hz has little effect on the fatigue strength, provided that the maximum stress level is less than about 75% of the static strength. At higher stress levels the fatigue strength decreases with decreasing frequency (CEB Committee GTG 15, 1988). As can be seen in Fig. 10, an increase in the loading frequency of about 10 times results in more cycles to failure. It was also found that compressive fatigue tests on concrete prisms varying the loading rate from 0,5 to 50 MPa/s resulted in a tenfold increase in the mean fatigue life expressed as cycles for S_{max} > 0,75. This suggests that accelerated fatigue tests on concrete structures may give an overestimate of their true fatigue life under loading rates that occur in service (CEB Committee GTG 15, 1988). Expressions linking the loading speed to log*N* are available in the literature for normal strength concrete (CEB Committee GTG 15, 1988).

In practice, concrete elements are subjected to cycles of loading of random and varying amplitudes. Typically, the Palmgren-Miner hypothesis, which states that damage accumulates linearly with the number of cycles applied at a certain level, is used. In experiments, random loadings can be used, and then a cycle is only counted after the stress has passed through the mean stress of the total stationary loading histogram, Fig. 11 (CEB Committee GTG 15, 1988).

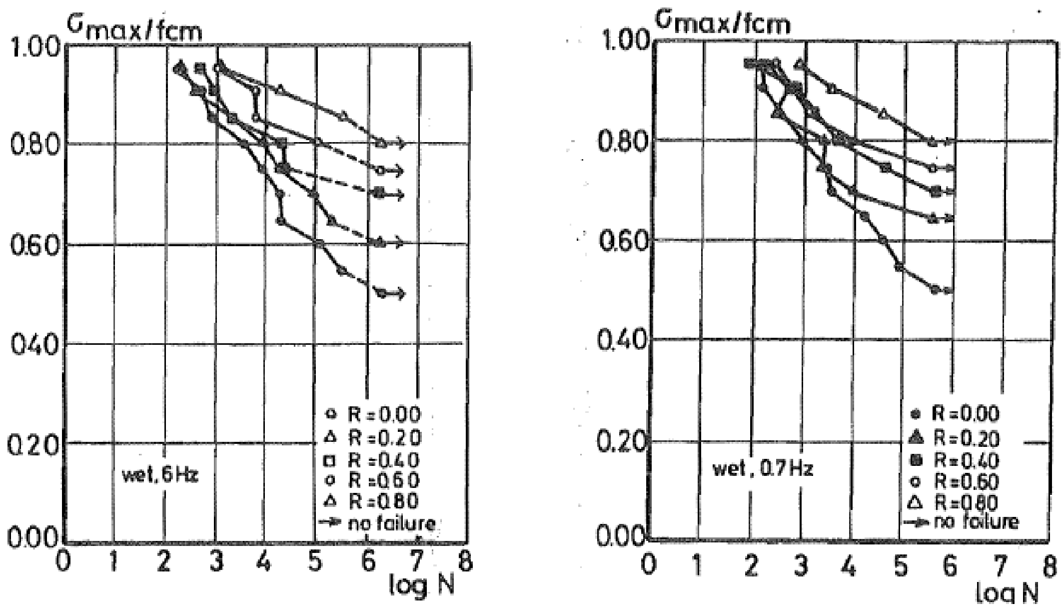

Fig. 10: S-N diagrams for concrete in compression: a) at 6 Hz and b) at 0,7 Hz (CEB Committee GTG 15, 1988).

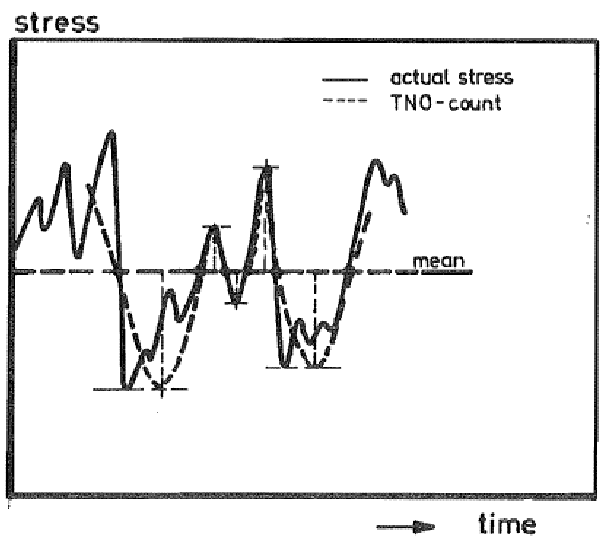

Fig. 11: Counting method for random load signals (CEB Committee GTG 15, 1988).

2.3 Fatigue life of high strength concrete

Currently, there seems to be a disagreement in the literature on whether or not the fatigue strength of concrete under compression decreases as the compressive strength of the concrete increases, or, in other words, if the *S-N* curve should be steeper and reducing more quickly for higher strength concrete.

Some of the first results in this debate come from experiments done in Norway (Petkovic et al., 1990). In this research, three different concrete mixes were used:

"ND65" (f_{ck} = 65 MPa), "ND95" (f_{ck} = 95 MPa) and "LWA75" (light weight aggregate concrete with f_{ck} = 75 MPa). The conclusions of the experiments was as follows: "The results of the constant amplitude tests showed no reason for distinguishing between the fatigue properties of ND65, ND95 and LWA75 in design rules, when the load levels are expressed relatively to the static strength of the concrete. Regression lines through S_{max} = 1,0 of the *S-N* diagram indicated an almost linear relationship between the minimum stress level and the logarithm of the number of cycles to failure for the tested range of S_{min} between 0,05 and 0,6." (Petkovic et al., 1990).

An overview of previous research (Kim and Kim, 1996) mentions that "Kleiber and Lee reported that the fatigue behavior of plain concrete in flexure was somewhat affected by the water-cement ratio of concrete, and the fatigue strength was decreased for a low water-cement ratio concrete, and that Bazant and Schell reported that high strength concrete was more brittle than normal strength concrete under fatigue loading." Their own test results show that the fatigue life decreased with increasing the concrete strength, and they proposed a model for the *S-N* relationship considering the effect of the concrete strength. The strength level in the experiments was varied from 26 MPa to 103 MPa, the maximum stress applied from 75 % to 95 % of the static compressive strength determined before the fatigue tests. They also found that the rate of the fatigue strain increment of HPC is greater than that of lower strength concrete.

When comparing the results of tested specimens of high strength concrete in compressive fatigue to an *S-N* curve that was developed based on experiments on normal strength concrete (with a cube compressive strength of 45 MPa), it was found that the datapoints corresponding to the investigated high strength concrete did not differ much from the Wöhler-curve for normal strength concrete used for the comparison (Hordijk et al., 1995), Fig. 12. In Fig. 13, the *S-N* curve determined by linear regression of the experimental results of the investigated high strength concrete is compared to the results of experiments on normal strength concrete by Holmen and the results for high strength concrete from Norway (Petkovic et al., 1990). The final conclusion of this research was that no significant differences were found between the fatigue behavior of gravel concrete and limestone concrete, and that it appeared that the existing *S-N* relationships derived from experiments on normal strength concrete apply reasonably well for high strength concrete (Hordijk et al., 1995).

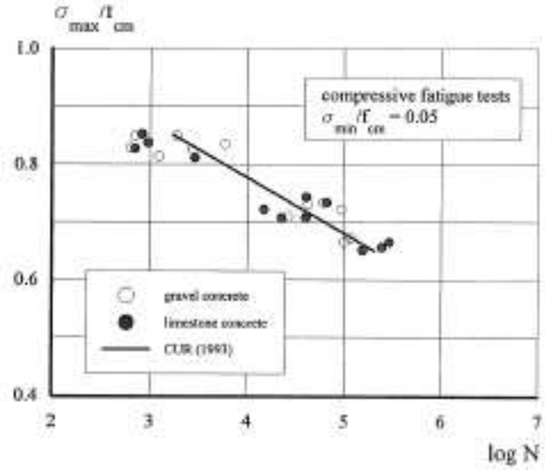

Fig. 12: S-N curve for the investigated high strength concrete compared to an existing relationship for normal strength concrete, (Hordijk et al., 1995)

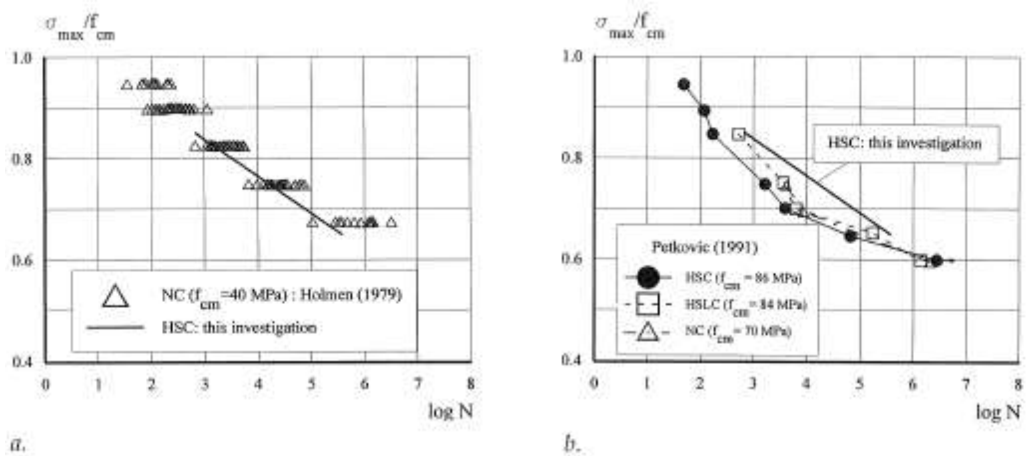

Fig. 13. Comparison between the average S-N curve for the investigated high strength concrete as compared to: (a) normal strength concrete experiments by Holmen, and (b) high strength concrete experiments by Petkovic, (Hordijk et al., 1995)

Experiments on UHPC showed that for all the investigated lower stresses S_{min} larger stress ranges could be attained than in similar experimental investigations that were used to develop the Model Code 1990 (Lohaus et al., 2011). In other experiments on UHPC it was found that heat treated concrete had a better fatigue resistance (Lohaus and Anders, 2006). An explanation for this observation was not given yet, but it could have been related to the large rise in temperature during testing, resulting from the high testing frequency and the dense matrix of the UHPC. The influence of the testing frequency is disputed: some authors argue that the number of cycles to failure increases when the frequency is increased for a constant stress-level (Hsu, 1981), while this effect was reversely observed for UHPC (Lohaus and Anders, 2006). However, the large temperatures that result in testing UHPC at a high frequency can be a cause for concern.

The temperature was measured to rise up to 140°C in an experiment, resulting in a surface temperature of about 133°C, Fig. 14. This figure also shows the evolution of the resonance frequency: the specimen seems to restiffen after having reached the maximum temperature, which might be attributed to an increase in strength and stiffness as a result of the further hydration from elevated temperatures. In the experiments, plain UHPC, AR-glass fiber modified UHPC and steel-fiber reinforced UHPC were subjected to fatigue loading. It was found that the fiber reinforcement does not affect the fatigue strength, and the authors mentioned that UHPC might be more sensible to fatigue loading compared to normal strength concrete (Lohaus and Anders, 2006).

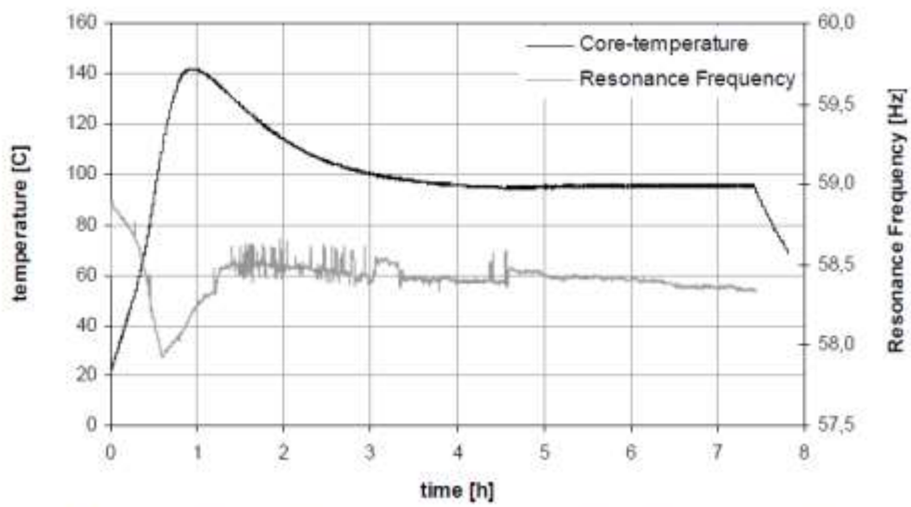

*Fig. 14: Development of the temperature and resonance frequency during a fatigue test to 1,5 * 10^6 cycles (Lohaus and Anders, 2006).*

For the larger upper stress limit S_{max}, the fatigue strength of higher strength concrete is smaller than of normal strength concrete. For $S_{max} > 0{,}6$; the *S-N* curve has a steeper tangent than normal strength concrete (Tue and Mucha, 2006). The researchers also found that the influence of S_{max} on the fatigue behavior is larger for high strength concrete than for normal strength concrete, which could be explained by the larger brittleness of high strength concrete. The larger brittleness and the smaller creep result in a smaller decrease of the stresses around S_{max}, so that the crack progression becomes more intensive and more damage per load cycle results. The fatigue damage is significantly connected with microcracking that can be observed with a high solution light microscopy system (Tue and Mucha, 2006).

When specimens had not reached failure after 2×10^6 or 5×10^6 cycles (the so-called "run-out specimens"), they were tested in static compression to determine their residual strength. For these experiments, only a small decrease in the compressive strength as compared to a single static compression test was found (Fehling et al., 2005). Similar static tests on so-called run-out specimens have shown that the modulus of elasticity was about 6% lower after the fatigue test, and that the strength increased between 0 and 6%, which could as well be contributed to the previously discussed effect of rising temperatures in the specimens during fatigue testing, which then leads to further hydration and hardening of the UHPC (Lohaus and Anders, 2006).

Other research on high strength concrete aimed at investigating the effect of dry and wet moisture conditions on the fatigue behavior of HPC with normal density and with lightweight aggregates. The specimens were tested in air and with a proper curing in water during fatigue tests. As a main result it could be concluded that the specimens that were dried out and tested in air achieved a longer lifetime for the same relative stress situation. The effect was found to be most evident for the concrete with normal density. This observation is even more remarkable since the increase in lifetime occurred despite the fact that the stress range of the dried-out specimens was larger than for the submerged ones. Since thick concrete sections dry out at a much slower rate than thin sections and, therefore, may have a much higher moisture content, there is a size effect on the fatigue resistance of concrete so that thin sections tend to have a higher fatigue strength than very large sections (fib Task Group 8.2, 2008).

Table 1: Comparison between different authors

Source	$f_{c,mean,max}$ **(MPa)**	**Influence** f_c**?**
Petkovic et al., 1990	95 MPa	No
Kim & Kim, 1996	103 MPa	Yes
Hordijk et al., 1995	78,2 MPa	No
Lohaus et al., 2011 Lohaus & Anders, 2006	170 MPa (fibers)	MC 90 too conservative
Tue & Mucha, 2006	65 MPa	Yes

After reviewing the currently existing literature, *fib* task group 8.2 concluded that HPC has a lower fatigue limit compared to normal strength concrete mainly due to a lower water-cement ratio. The final conclusions with regard to the fatigue life of HPC of this task group was the following: “In spite of enhanced research activity in the field of high performance concrete one has not yet succeeded in finding adequate design rules for fatigue behavior taking into consideration the special properties of HPC. On the experimental level further progress has taken place especially concerning the fracture mechanical behavior and the underlying phenomenological mechanisms. Unfortunately it is not possible to convert these results reciprocally by just a simple transformation formula in design rules based on the classical Wöhler approach. For that reason the existing design rules can be applied to HPC as well due to its unnecessarily conservative formulation." (fib Task Group 8.2, 2008).

As can be seen from the previous paragraphs, there is no consensus on whether or not increasing concrete compressive strengths reduce the fatigue life for compression. A brief overview of the different sources and their stated influence of the concrete compressive strength on the fatigue life is given in Table 1.

3 Current code provisions and methods

3.1 NEN 6723:2009

The fatigue reference strength in the Dutch national code NEN 6723:2009 is the following for concrete classes above C25/30:

$$f'_{b,v} = \frac{f'_{b,rep,v}}{\gamma_m} \tag{1}$$

$$f'_{b,rep,v} = 0,5\left(f'_{b,rep,k} - 0,85 \times 30\right) + 0,85 \times 30 \tag{2}$$

with:

γ_m = 1,2

$f'_{b,rep,k}$ the characteristic value of the uniaxial short term concrete compressive strength $0,85f'_{ck}$, in [MPa]

$f'_{b,rep,v}$ the characteristic value of the concrete compressive strength in the limit state of fatigue, in [MPa].

An overview of the fatigue reference strength for different concrete classes (up to C53/65) is given in Table 2.

Table 2: Fatigue reference strength according to NEN 6723:2009

Sterkteklasse	$f'_{b;rep;k}$ N/mm²	$f'_{b;v}$ N/mm²
C12/15	12,75	10,6
C20/25	21,25	17,7
C28/35[a]	29,75	23,0
C35/45	38,25	26,5
C45/55	46,75	30,1
C53/65[a]	55,25	33,6

[a] Deze aanduidingen zijn volgens de sterkteklassen in tabel B van NEN 8005.
Deze aanduidingen wijken af van de in tabel 7 van NEN-EN 206-1 gebruikte aanduidingen C30/37 en C55/67.

According to NEN 6723:2009 §9.6.2.1, the number of cycles to failure N_i for compressive stresses can be determined as:

$$Log\left(N_i\right) = \frac{10}{\sqrt{1-R}}\left(1 - \frac{\sigma'_{b,d,max}}{f'_{b,v}}\right) \text{ for } \frac{\sigma'_{b,d,max}}{f'_{b,v}} > 0,25 \tag{3}$$

For $\frac{\sigma'_{b,d,max}}{f'_{b,v}} \leq 0,25$, the number of cycles to failure N_i is infinite. In Eq. (3), the following parameters are used:

R	the stress rate $R = \frac{\sigma'_{b,d,min}}{\sigma'_{b,d,max}}$, this value is of course the same as $R = \frac{S_{min}}{S_{max}}$
$\sigma'_{b,d,min}$	the design value of the minimum compressive stress in the concrete, in [MPa]
$\sigma'_{b,d,max}$	the design value of the maximum compressive stress in the concrete, in [MPa].

In Fig. 15 the *S-N* curves based on Eq. (3) are shown for concrete classes C40 to C120, for S_{min} = 0,05. Note that these curves are non-dimensional with regard to the stresses: the value of $S_{max} = \sigma_{max}/f_{cd}$ so that the ratio might appear higher, while the design stress that needs to be verified is much smaller. For the higher strength concrete classes, this effect takes place.

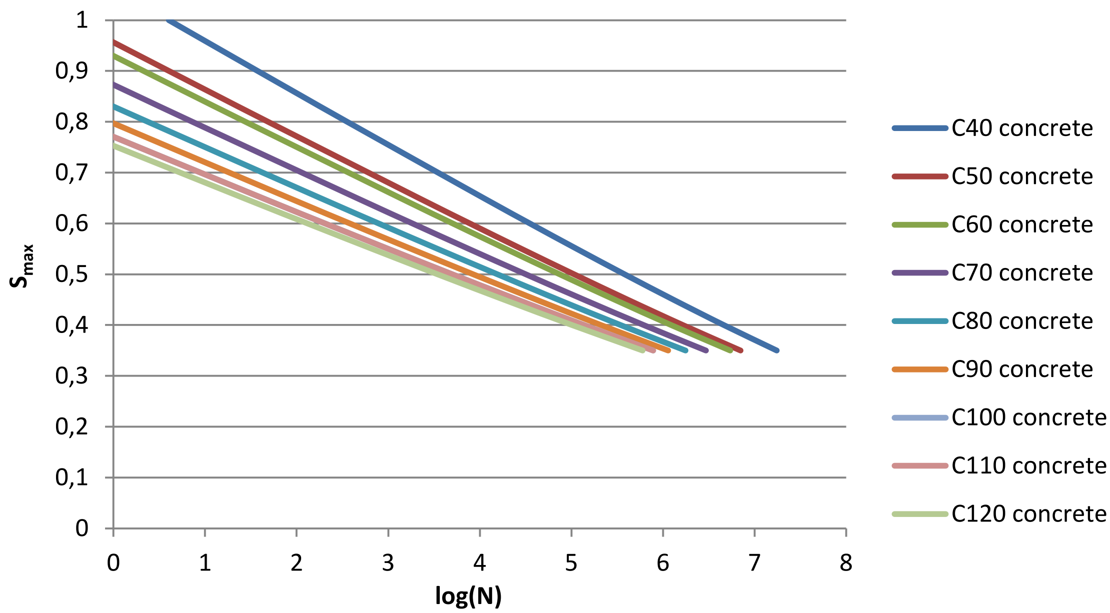

Fig. 15: S-N relations based on NEN 6723:2009 for S_{min} = 0,05.

3.2 NEN-EN 1992-1-1+C2:2011 and Dutch National Annex

The design fatigue strength according to NEN-EN 1992-1-+C2:2011 §6.8.7 is prescribed as:

$$f_{cd,fat} = k_1 \beta_{cc}(t_0) f_{cd} \left(1 - \frac{f_{ck}}{250}\right) \quad (4)$$

$$\beta_{cc}(t_0) = \exp\left\{ s\left[1-\left(\frac{28}{t}\right)^{0,5}\right]\right\}\alpha_{cc} \tag{5}$$

with

$\beta_{cc}(t_0)$	coefficient for concrete strength at first load application, as given in §3.1.2(6)
t_0	the time of the start of the cyclic loading on concrete in days
s	depends on the strength class of the cement, eq. for 42,5N, s = 0,25
t	concrete age in days

$$f_{cd} = \frac{f_{ck}}{\gamma_{c,fat}}$$

$\gamma_{c,fat}$ 1,35 for fatigue

The value for k_1 can be found in the National Annex. The recommended value for $N = 10^6$ cycles is 0,85.

According to NEN-EN 1992-1-1+C2:2011 §6.8.7(1), Eq. 6.72, a satisfactory fatigue resistance may be assumed for concrete under compression, if the following condition is fulfilled:

$$E_{cd,max,equ} + 0,43\sqrt{1-R_{equ}} \leq 1 \tag{6}$$

for which:

$R_{equ} = \frac{E_{cd,min,equ}}{E_{cd,max,equ}}$ the stress ratio

$E_{cd,max,equ} = \frac{\sigma_{cd,max,equ}}{f_{cd,fat}}$ the maximum compressive stress level

$E_{cd,min,equ} = \frac{\sigma_{cd,min,equ}}{f_{cd,fat}}$ the minimum compressive stress level

$f_{cd,fat}$	the design fatigue strength
$\sigma_{cd,max,equ}$	the upper stress of the ultimate amplitude for N cycles
$\sigma_{cd,min,equ}$	the lower stress of the ultimate amplitude for N cycles.

The number of cycles N can be found in the National Annex. The recommended value, also used in The Netherlands, is $N = 10^6$ cycles. In other words, NEN-EN 1992-1-1+C2:2011 uses a damage-equivalent check for fatigue and does not describe a Wöhler diagram.

3.3 NEN-EN 1992-2+C1:2011

According to NEN-EN 1992-2+C1:2011 §6.8.7 (101), the number of cycles to failure can be determined based on nationally prescribed *S-N* diagrams, or based on Eq. 6.72 of NEN-EN 1992-2+C2:2011, here Eq. (6), in which the coefficient 0,43 is replaced by

$\log N_i/14$ and the inequality in the expression is omitted. Sufficient resistance against fatigue for concrete under compression can then be assumed when (Eqs. 6.105 – 6.109):

$$\sum_{i=1}^{m} \frac{n_i}{N_i} \leq 1 \tag{7}$$

with

m	the number of cycles of constant amplitude
n_i	the number of cycles with a constant amplitude at interval i
N_i	the number of cycles to failure with a constant amplitude at interval i

for which:

$$N_i = 10^{\left(14 \frac{1-E_{cd,max,i}}{\sqrt{1-R_i}}\right)} \tag{8}$$

$$R_i = \frac{E_{cd,min,i}}{E_{cd,max,i}} \tag{9}$$

$$E_{cd,min,i} = \frac{\sigma_{cd,min,i}}{f_{cd,fat}} \tag{10}$$

$$E_{cd,max,i} = \frac{\sigma_{cd,max,i}}{f_{cd,fat}} \tag{11}$$

for which:

R_i	the stress ratio
$E_{cd,min,i}$	the minimum stress level
$E_{cd,max,i}$	the maximum stress level
$\sigma_{cd,max,i}$	the largest stress in a cycle
$\sigma_{cd,min,i}$	the smallest stress in a cycle
$f_{cd,fat}$	the design value of the fatigue capacity of concrete according to Eq. (6.76) from NEN-EN 1992-1-1+C2:2011, here given as Eq. (4)

The bridge code NEN-EN 1992-2+C1:2011 thus requires a more elaborate study of fatigue and describes the Wöhler diagram, which the general code NEN-EN 1991-2-2+C2:2011 does not consider. For concrete classes C40 to C120, the resulting *S-N* curves based on the expressions from NEN-EN 1992-2+C1:2011 are given in Fig. 16, for the case of S_{min} = 0,05. As can be seen in Fig. 16, the *S-N* curves as described by NEN-EN 1992-2+C1:2011 are very conservative, because the capacity at 1 cycle is only a fraction of the static design capacity f_{cd}. This reduction is the largest for the highest strength concrete classes, which is a clear disadvantage of this method. In the range of applicability of the *S-N* curves ($\log N > 2$), the capacity seems to be very conservative as well.

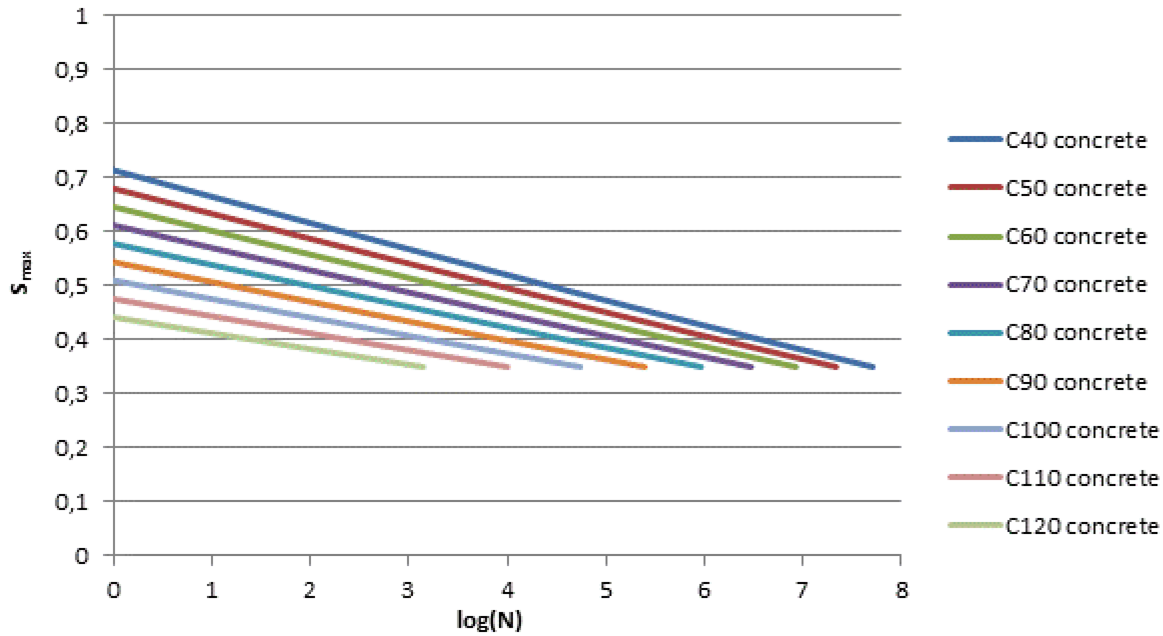

Fig. 16: S-N relations based on NEN-EN 1992-2+C1:2011 for S_{min} = 0,05.

3.4 NEN-EN 1992-2+C1:2011/NB:2011

In the Dutch National annex NEN-EN 1992-2+C1:2011/NB:2011, separate equations for the *S-N* curve are given. Sufficient capacity against fatigue is assumed when Miner's rule is fulfilled

$$\sum_{i=1}^{m} \frac{n_i}{N_i} \leq 1 \tag{12}$$

with

m	the number of cycles of constant amplitude
n_i	the number of cycles with a constant amplitude at interval i
N_i	the number of cycles to failure with a constant amplitude at interval i

for which:

$$N_i = 10^{\left(\frac{6}{1-0,57k_1\left(1-\frac{f_{ck}}{250}\right)} \left(\frac{1-E_{cd,max,i}}{\sqrt{1-R_i}} \right) \right)} \text{ for } N_i \leq 10^6 \tag{13}$$

$$N_i = 10^{\left(14\frac{1-E_{cd,max,i}}{\sqrt{1-R_i}}\right)} \text{ for } N_i > 10^6 \tag{14}$$

$$R_i = \frac{E_{cd,min,i}}{E_{cd,max,i}} \tag{15}$$

$$E_{cd,min,i} = \frac{\sigma_{cd,min,i}}{f_{cd}\left(0,9+\frac{\log N_i}{60}\right)} \text{ for } N_i \le 10^6 \tag{16}$$

$$E_{cd,min,i} = \frac{\sigma_{cd,min,i}}{f_{cd,fat}} \text{ for } N_i > 10^6 \tag{17}$$

$$E_{cd,max,i} = \frac{\sigma_{cd,max,i}}{f_{cd}\left(0,9+\frac{\log N_i}{60}\right)} \text{ for } N_i \le 10^6 \tag{18}$$

$$E_{cd,max,i} = \frac{\sigma_{cd,max,i}}{f_{cd,fat}} \text{ for } N_i > 10^6 \tag{19}$$

for which:

R_i the stress ratio
$E_{cd,min,i}$ the minimum stress level
$E_{cd,max,i}$ the maximum stress level
$\sigma_{cd,max,i}$ the largest stress in a cycle
$\sigma_{cd,min,i}$ the smallest stress in a cycle
$f_{cd,fat}$ the design value of the fatigue capacity of concrete according to Eq. (6.76) from NEN-EN 1992-1-1+C2:2011, here given as Eq. (4)

The value of k_1 in Eq. (4) should be taken as 1 according to the Dutch National Annex, which deviates from the recommended value of k_1 = 0,85. The stress f_{cd} is determined from $\gamma_{c,fat}$ = 1,35 instead of γ_c = 1,5.

To find the compressive capacity at 1 cycle, log$N$ = 0, Equations (13) and (16) are used:

$$0 = \frac{6}{1-0,57\left(1-\frac{f_{ck}}{250}\right)}\left(\frac{1-\frac{S_{max} f_{cd}}{f_{cd}\left(0,9+\frac{0}{60}\right)}}{\sqrt{1-\frac{S_{min}}{S_{max}}}}\right)$$

$$0 = 1-\frac{S_{max}}{0,9}$$

$$S_{max} = 0,9$$

As can be seen from this derivation, the compressive strength at 1 cycle is taken as $0,9f_{cd}$ according to the Dutch National Annex. This value of $f_{cd} = f_{ck}/\gamma_{c,fat}$ instead of $f_{cd} = f_{ck}/\gamma_c$.
As compared to NEN-EN 1992-2+C1:2011 with its reduced capacity at 1 cycle, Fig. 16, this assumption seems to be more realistic.

NEN-EN 1992-2+C1:2011/NB:2011 uses an expression that is different before and after 10^6 cycles. However, the results as determined from Eq. (13) is not the same as from Eq. (14) at the intersection of these curves for 10^6 cycles. Eq. (13) for 10^6 cycles becomes:

$$\log N_i = \frac{6}{1-0,57k_1\left(1-\dfrac{f_{ck}}{250}\right)}\left(\frac{1-\dfrac{S_{max}\,f_{cd}}{f_{cd}\left(0,9+\dfrac{\log N_i}{60}\right)}}{\sqrt{1-R_i}}\right) \tag{20}$$

$$6 = \frac{6}{1-0,57\times 1\left(1-\dfrac{f_{ck}}{250}\right)}\left(\frac{1-\dfrac{S_{max}\,f_{cd}}{f_{cd}\left(0,9+\dfrac{6}{60}\right)}}{\sqrt{1-\dfrac{S_{min}}{S_{max}}}}\right)$$

$$6 = \frac{6\left(1-S_{max}\right)}{\left[1-0,57\times 1\left(1-\dfrac{f_{ck}}{250}\right)\right]\sqrt{1-\dfrac{S_{min}}{S_{max}}}}$$

For 10^6 cycles, Eq. (14) becomes:

$$\log N_i = 14\frac{1-\dfrac{\sigma_{cd,max,i}}{f_{cd,fat}}}{\sqrt{1-R_i}} = 14\frac{1-\dfrac{S_{max}\,f_{cd}}{k_1\beta_{cc}(t_0)\,f_{cd}\left(1-\dfrac{f_{ck}}{250}\right)}}{\sqrt{1-\dfrac{S_{min}}{S_{max}}}}$$

$$6 = 14\frac{1-\dfrac{S_{max}\,f_{cd}}{f_{cd}\left(1-\dfrac{f_{ck}}{250}\right)}}{\sqrt{1-\dfrac{S_{min}}{S_{max}}}}$$

$$6 = 14\frac{\dfrac{f_{cd}\left(1-\dfrac{f_{ck}}{250}\right)-S_{max}f_{cd}}{f_{cd}\left(1-\dfrac{f_{ck}}{250}\right)}}{\sqrt{1-\dfrac{S_{min}}{S_{max}}}}$$

$$6 = 14\frac{\left(1-\dfrac{f_{ck}}{250}\right)-S_{max}}{\left(1-\dfrac{f_{ck}}{250}\right)\sqrt{1-\dfrac{S_{min}}{S_{max}}}}$$

From the comparison between these expressions, it can be seen that there would be no gap between the two expressions, if the first expression, Eq. (20), derived from Eq. (13), would be written as:

$$\log N_i = \frac{6}{\left(1-0,57k_1\right)\left(1-\dfrac{f_{ck}}{250}\right)}\left(\frac{\left(1-\dfrac{f_{ck}}{250}\right)-E_{cd,\max,i}}{\sqrt{1-R_i}}\right) \tag{21}$$

The differences between Eq. (20) and Eq. (21) are the following two elements:

- adding the brackets around 1-0,57k_1, so that $\dfrac{6}{1-0,57k_1}$ = 14 results, and
- replacing 1 in the numerator by $\left(1-\dfrac{f_{ck}}{250}\right)$.

The *S*-*N* curves as prescribed by NEN-EN 1992-2+C1:2011/NB:2011 are shown in Fig. 17. It is clear from this figure that for 1 cycle, a compressive strength of 0,9 times the static strength is used, regardless of the concrete class, and as calculated previously as well. It can also be seen that the connection between the two equations that describe the *S*-*N* curve results in a jump at 10^6 cycles, because these equations do not result in the same solution for 10^6 cycles.

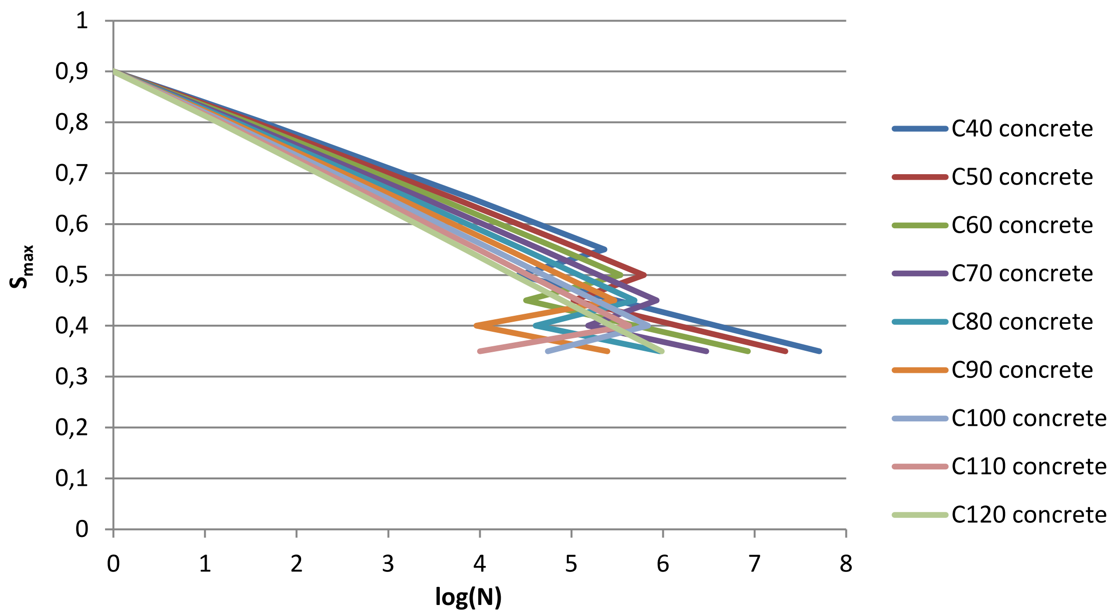

Fig. 17: S-N relations based on NEN-EN 1992-2+C1:2011/NB:2011 for S_{min} = 0,05.

3.5 fib Model Code 2010

In the *fib* Model Code 2010 (fib, 2012), the fatigue reference compressive strength is calculated as (Eq. 5.1-110 in §5.1.11.1.1):

$$f_{ck,fat} = \beta_{cc}(t)\beta_{c,sus}(t,t_0)\, f_{ck}\left(1-\frac{f_{ck}}{400}\right) \tag{22}$$

for which:

f_{ck} the characteristic concrete compressive strength

$\beta_{cc}(t) = \exp\left\{ s\left[1-\left(\frac{28}{t}\right)^{0,5}\right]\right\}$ from Eq. 5.1-51 describes the strength development with time, with

s depends on the strength class of the cement, eq. for 42,5N, s = 0,25

t concrete age in days, corrected for temperature:

$$t_T = \sum_{i=1}^{n} \Delta t_i \exp\left(13,65 - \frac{4000}{273+T(\Delta t_i)}\right), \text{ in which}$$

Δt_i number of days with temperature T

$T(\Delta t_i)$ temperature during time period Δt_i

$\beta_{c,sus}(t,t_0)$ = 0,85 for fatigue

The factor 400 in Eq. (22) is changed with respect to the Model Code 1990, in which 250 was used for this factor. This change was necessary to accommodate compressive strengths larger than 125MPa and corresponds better to experimental results on higher strength concrete specimens (Fehling et al., 2013). The difference in $f_{cd,fat}$ between Model Code 1990 and Model Code 2010 is shown in Fig. 18.

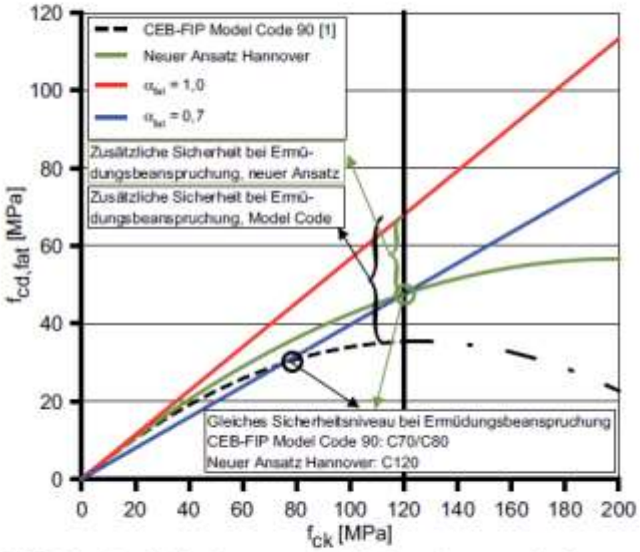

Fig. 18: Comparison of the fib Model Code 2010 and Model Code 90 for $f_{cd,fat}$ (Lohaus et al., 2011).

The *S-N* relations are then graphically represented in Fig. 19 and given as (Eq. 5.1-107 – 5.1-109, for $0 \leq S_{c,min} \leq 0{,}8$):

$$\log N_1 = \frac{8}{Y-1}\left(S_{c,max} - 1\right) \tag{23}$$

$$\log N_2 = 8 + \frac{8\ln(10)}{Y-1}\left(Y - S_{c,min}\right)\log\left(\frac{S_{c,max} - S_{c,min}}{Y - S_{c,min}}\right) \tag{24}$$

with

$$Y = \frac{0{,}45 + 1{,}8S_{c,min}}{1 + 1{,}8S_{c,min} - 0{,}3S_{c,min}^{2}} \tag{25}$$

and

$$S_{c,max} = \frac{\left|\sigma_{c,max}\right|}{f_{ck,fat}} \tag{26}$$

$$S_{c,min} = \frac{\left|\sigma_{c,min}\right|}{f_{ck,fat}} \tag{27}$$

$$\Delta S_c = \left|S_{c,max}\right| - \left|S_{c,min}\right| \tag{28}$$

If $\log N_1 \leq 8$, then $\log N = \log N_1$ and if $\log N_1 > 8$, then $\log N = \log N_2$. If $S_{c,min} > 0{,}8$ the *S-N* relations for $S_{c,min} = 0{,}8$ are valid. These expressions are valid for concrete stored in a constant environment of approximately 20°C, 65% RH. The *S-N* relationships were developed based on experiments with ultra-high strength concrete (up to C200) and validated for high strength and normal strength concrete. The curves have been verified with experiments upp to 10^7 load cycles to failure. For $\log N > 8$ the curves asymptotically approach the minimum stress level of the respective curve.

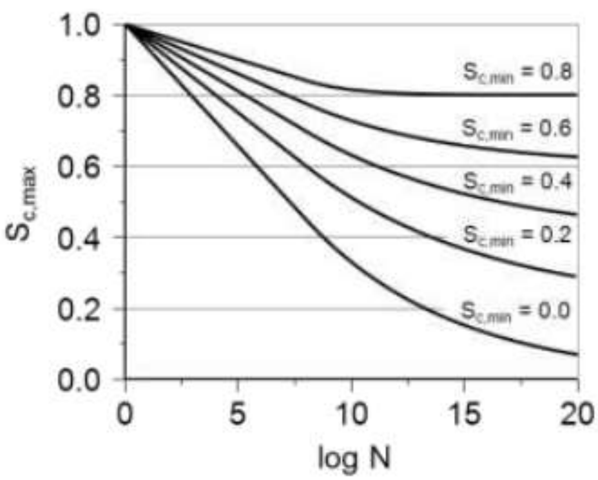

Fig. 19: S-N relations from fib Model Code 2010 (fib, 2012).

The resulting differences in the *S-N* curves based on Model Code 1990 and Model Code 2010 can be seen in Fig. 20. For high strength concrete, Model Code 2010 allows higher strengths for a given number of cycles than Model Code 1990.

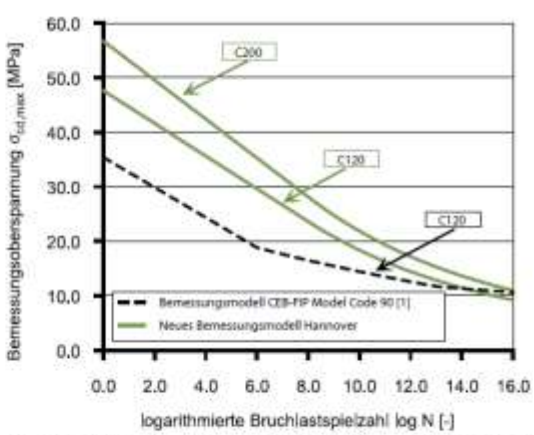

Fig. 20: Comparison between design model of Model Code 1990 and Model Code 2010 for $S_{cd,min} = 0{,}05$ (Lohaus et al., 2011).

For concrete classes C40 to C120, the *S*-*N* curves for S_{min} (with respect to f_{cd}, not the same as $S_{c,min}$ with respect to $f_{ck,fat}$) = 0,05 are shown in Fig. 21. In this graph, S_{max} is used (with respect to f_{cd}) and not $S_{c,max}$ as shown in Fig. 19. It can be seen from Fig. 21 that using $f_{ck,fat}$ from Eq. (22) leads to strengths larger than the design static strength f_{cd} at 1 loading cycle (a static test). Even though the *fib* Model Code 2010 expressions are all function of $S_{c,max}$ and $S_{c,min}$, it is necessary to compare to other codes, which are based on S_{max} and S_{min}. In this perspective it can be said that the large value for S_{max} for a small number of cycles ($0 \leq \log N \leq 2$) is a clear disadvantage of the expression in the *fib* Model Code 2010.

It can be noted that the reduction of the fatigue life for higher strength concrete classes is smaller than as recommended by the other codes. The *fib* Model Code 2010 is the most recent code, and is the first code to be based on experiments on high strength concrete specimens. As such, a more realistic impression of the influence on the concrete compressive strength on the reduction of the fatigue life can be expected from this code.

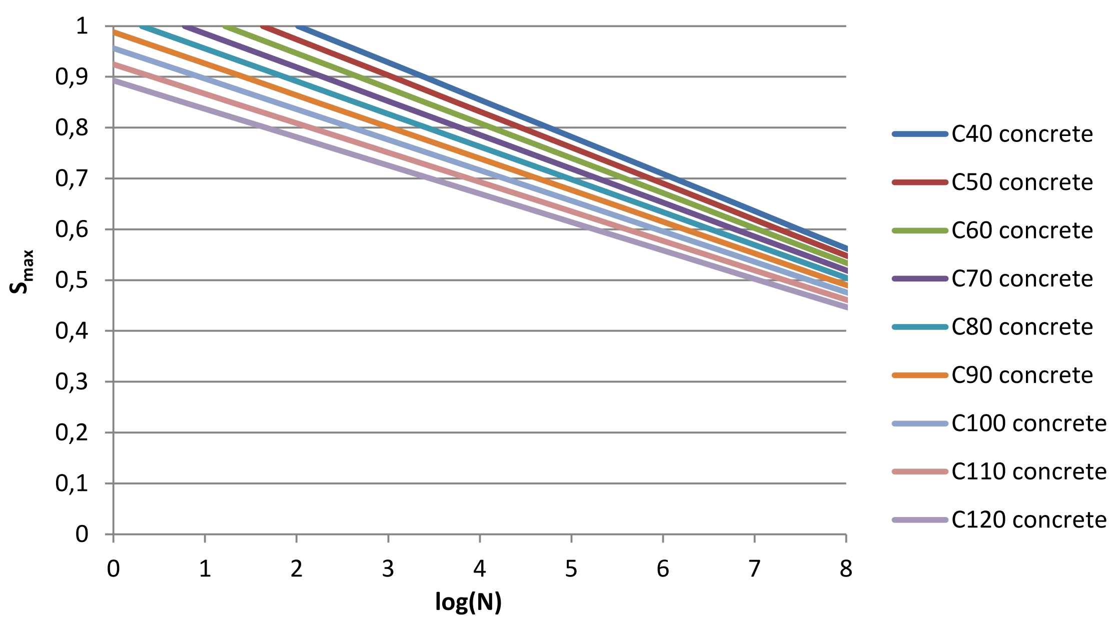

Fig. 21: S-N relations based on fib Model Code.

3.6 Proposal by Hans Bongers

Because of the jump in the *S*-*N* curve from NEN-EN 1992-2+C1:2011/NB:2011 at 10^6 cycles, a proposal was developed by Hans Bongers (Snijders, 2013) for which a capacity of $0{,}9 f_{cd}$ is found for 1 cycle and for which the 2 parts of the expression result in the same value at 10^6 cycles. The expression is based on the formula from NEN-EN 1992-2+C1:2011:

.

$$Log(N_i) = 14\frac{1 - E_{cd,max,i}}{\sqrt{1 - R_i}}$$

with

$$E_{cd,\max,i} = \frac{\sigma_{cd,max,i}}{0,9 f_{cd} - \left(0,9 f_{cd} - f_{cd,fat}\right)\frac{1}{6} Log\left(N_i\right)} \text{ for } N_i \leq 10^6 \qquad (29)$$

$$E_{cd,\max,i} = \frac{\sigma_{cd,max,i}}{f_{cd,fat}} \text{ for } N_i > 10^6 \qquad (30)$$

When plotting the *S-N* curves based on these equations, however, it can be seen that convergence is difficult to reach, Fig. 22. Therefore, this proposal might not be very suitable for use in practice.

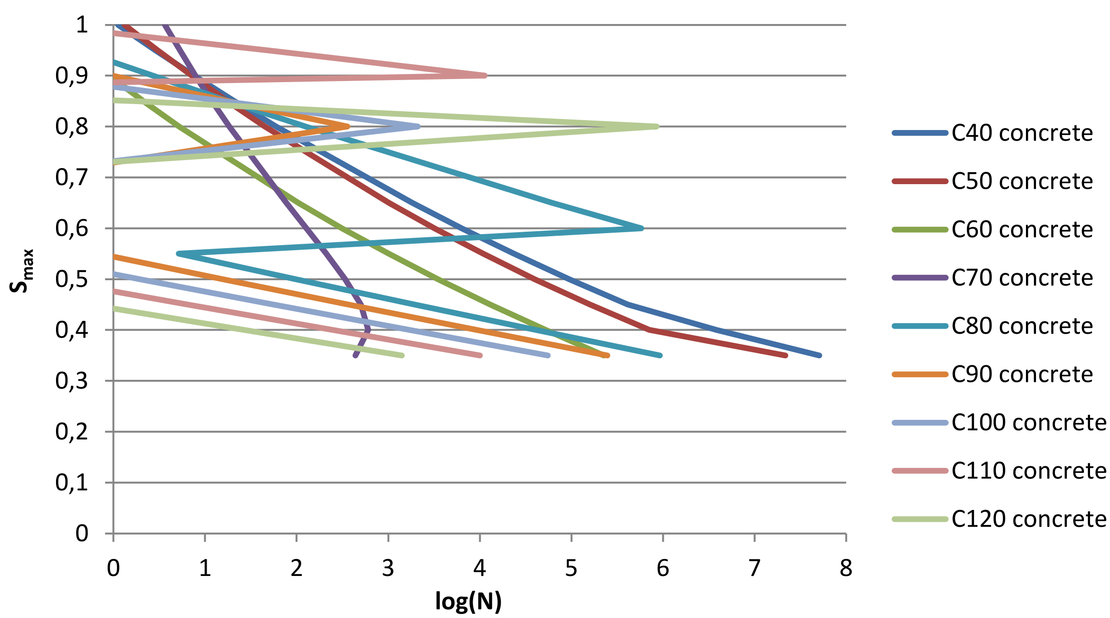

Fig. 22: S-N relations based on the proposal by Hans Bongers.

3.7 Proposal by Kim & Kim

Kim and Kim (1996) studied the influence of the concrete compressive strength on the fatigue life through a series of experiments. They proposed an *S-N* relationship that would take the concrete compressive strength into account as well. Based on their experiments (fatigue and strain rate tests), Kim and Kim (1996) proposed the following *S-N* relationship:

$$S_{max} = -7,6\left(\frac{f_c'}{f_1}\right)^{0,066}\log N_f + 126\left(\frac{f_c'}{f_1}\right)^{-0,025} \quad (31)$$

The result of Eq. (31) is a percentage, not a fraction. In Eq. (31), the value of f_1 = 1 MPa (Kim and Kim, 1996) and for f_c' the design compressive strength f_{cd} can be used.

The *S-N* curves for C40 to C120 concrete and S_{min} = 0,05 are shown in Fig. 23. In this graph, the difference between the concrete classes is rather small. Note that the specimens studied by Kim and Kim had concrete compressive strengths limited to 103MPa, and that the number of specimens and configurations under study was rather small, so that extrapolating these results by means of Eq. (31) might not be advisable.

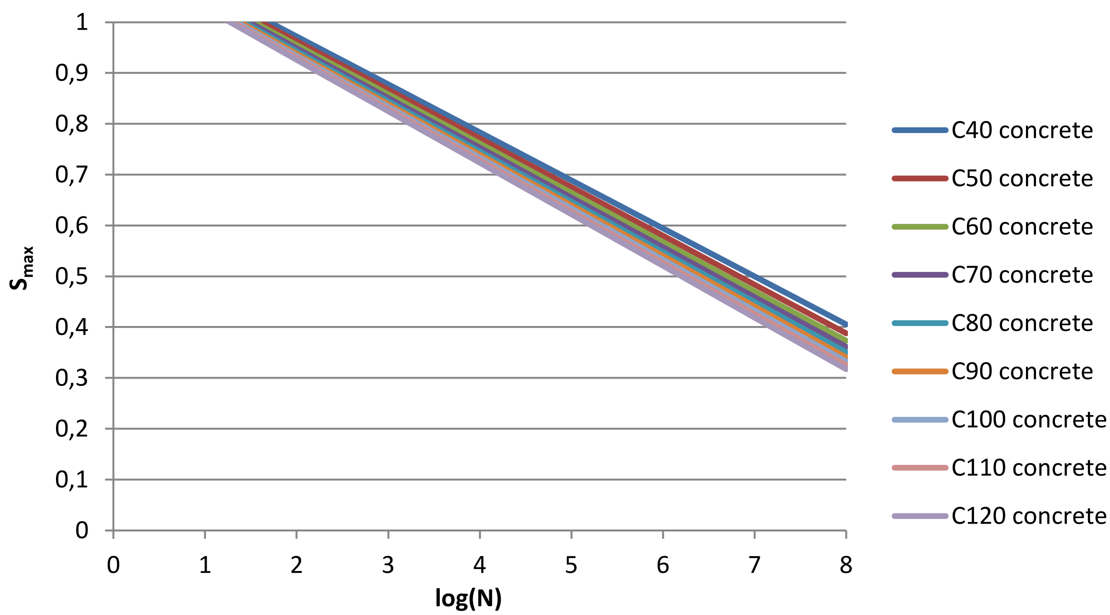

Fig. 23: S-N relations based on expression from Kim and Kim (1996).

3.8 Comparison between different approaches

In the previous paragraphs, the *S-N* curves as described by different codes and calculation methods are studied one by one. As the goal of this report is to find a recommendation for the *S-N* curves that is suitable for the use with higher strength concrete, a few observations with regard to the differences between the codes are given here:

- The former Dutch code NEN 6723:2009 is not aimed at higher concrete classes, but seems not to be overly conservative in its consideration of the influence of the concrete class. However, this code contributes values of S_{max} > 1 for the case of a limited number of cycles (log$N$ = 0 – 2).

- The general Eurocode NEN-EN 1992-1-1+C2:2011 does not prescribe any *S-N* relations for fatigue, but the bridge code NEN-EN 1992-2+C1:2011 does prescribe Wöhler curves for concrete in repeated compression.
- The *S-N* relationship prescribed by NEN-EN 1992-2+C1:2011 seems to be overly conservative. Already at 1 cycle, the strength S_{max} is much smaller than the static compressive strength f_{cd}.
- The *S-N* relationship prescribed by NEN-EN 1992-2+C1:2011/NB:2011 is divided in an expression for $N_i \leq 10^6$ cycles and an expression for $N_i > 10^6$ cycles.
- The *fib* Model Code expression shows smaller decreases in the fatigue life than other codes, and is the first provision that is actually based on the comparison with experimental results on high strength concrete specimens.
- The expression by Kim and Kim (1996) is based on a limited number of specimens, and doesn't seem to catch the influence of the concrete compressive strength in an adequate manner.
- The proposal by Hans Bongers has convergence problems for developing the *S-N* curves.

A comparison between the different codes that have been or are used in the Netherlands is given in Fig. 24. For this case R is used as a fixed value, instead of S_{min}/S_{max}, so that $\log N_i$ as a function of S_{max} can be easily rewritten to have S_{max} as a function of $\log N_i$. As most experimental results are based on a fixed S_{min} and a tested number of cycles N_i for a given S_{max}, it is necessary to keep the expressions based on the relation between S_{max} and N_i for the comparison with experimental results. The difference between results for $R = 0$ and $R = 0{,}5$ is given in Fig. 25 and Fig. 26, showing that only for $R = 0$ the two expressions from NEN-EN 1992-2+C1:2011/NB:2011 meet for 10^6 cycles. A comparison to the proposal by Hans Bongers is given in Fig. 27 and Fig. 28. These figures are developed for a concrete C53/65 assuming $\alpha_{cc} = 1$, $k_1 = 1$, $\gamma_c = \gamma_{c,fat} = 1{,}5$ and $R = 0$ or 0,5.

As Snijders (2013) points out: the main differences between the codes are found in the range between 1 and 10^6 cycles, regardless of the value of R that is assumed. This range is important for heavy trucks (> type 5), which result in less than 10^6 cycles. The result of these differences can be attributed to the slope of the Wöhler diagram, which is altered in some codes so that the static compressive strength is found for a single load cycle.

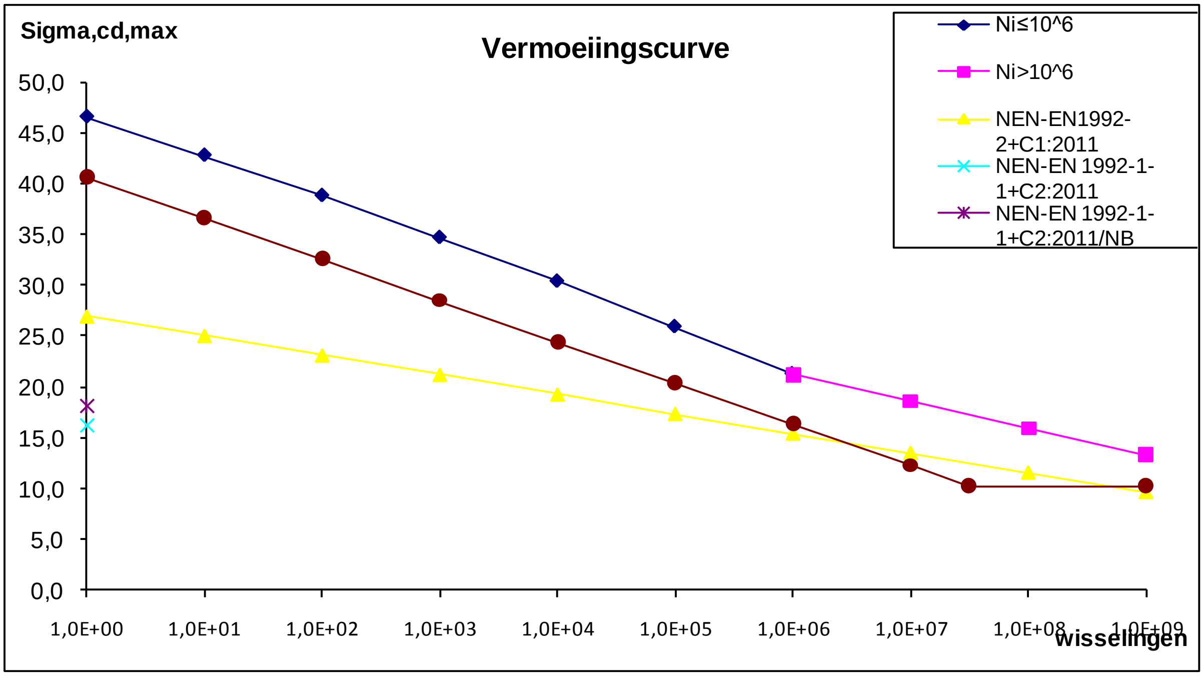

Fig. 24: Comparison between different code method (Snijders, 2013).

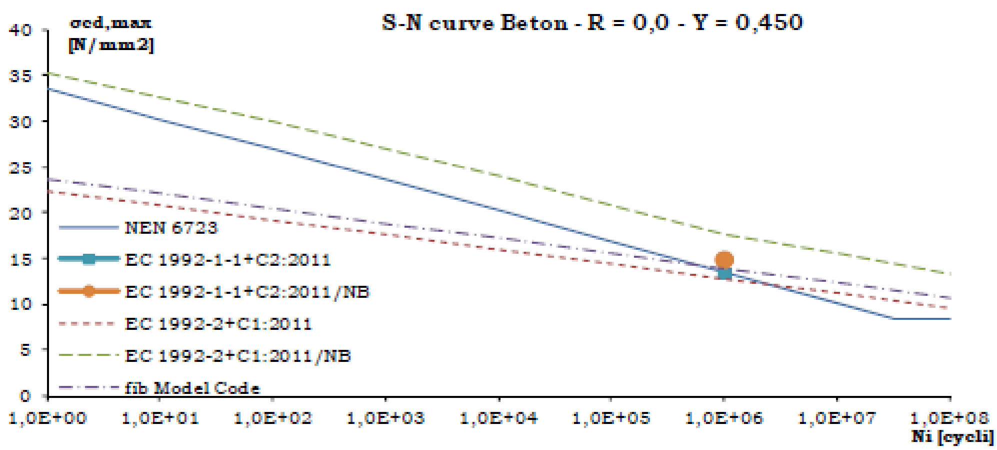

Fig. 25: Comparison between codes for R = 0 (Snijders, 2013)

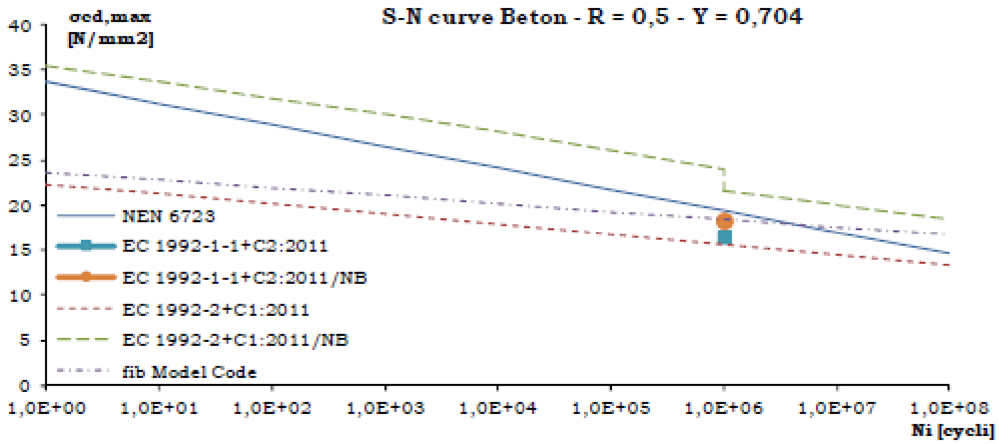

Fig. 26: Comparison between codes for R = 0,5 (Snijders, 2013)

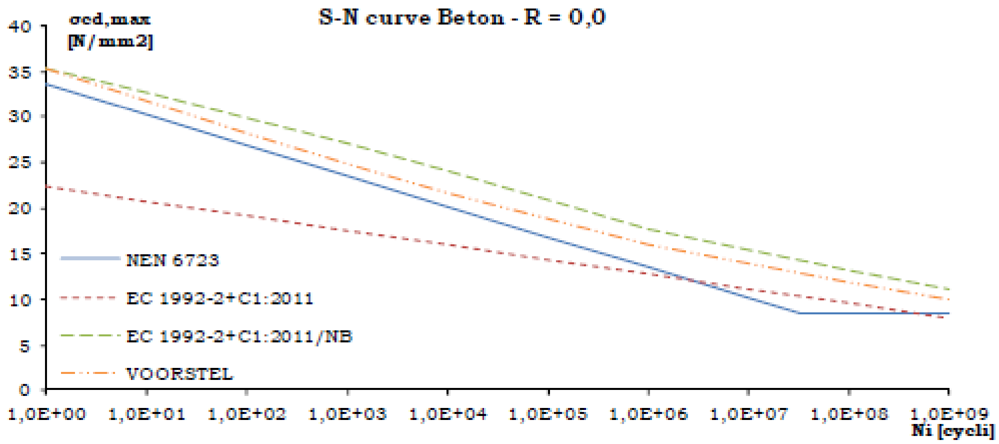

Fig. 27: Comparison between codes and proposal van Hans Bongers for R = 0,0 (Snijders, 2013)

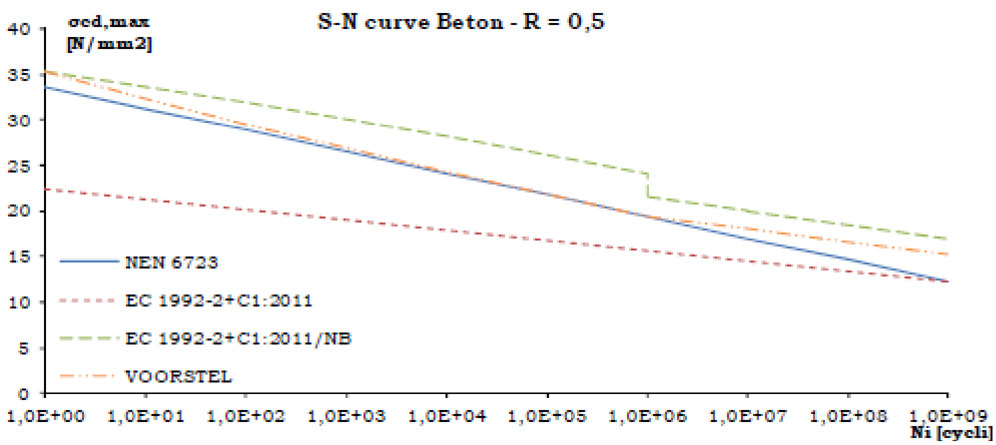

Fig. 28: Comparison between codes and proposal van Hans Bongers for R = 0,5 (Snijders, 2013).

4 Available test results

To develop a new proposal for the fatigue strength of concrete under compression from NEN-EN 1992-2+C1:2011/NB:2011, a database with experimental results on high strength concrete is compiled. The full database is given in Annex 1, the results of the different series are discussed in this part of the report.

The first series of experiments that are of interest are from Norway (Petkovic et al., 1990), Table 3. This table shows that the experimental program consisted of 83 tests in 38 different loading situations. The results are shown graphically in Fig. 29, Fig. 30 and Fig. 31. As compared to the test program outlined in Table 3, some results are not shown in Fig. 29 and Fig. 30, which were used to read the results and put these values into the database from Annex 1. The following results are missing:

- ND65 with S_{max} = 0,75 & S_{min} = 0,05
- LWA75 with S_{max} = 0,75 & S_{min} = 0,20
- ND95 with S_{max} = 0,75 & S_{min} = 0,30
- ND65 with S_{max} = 0,75 & S_{min} = 0,4
- ND65 with S_{max} = 0,70 & S_{min} = 0,4
- ND65 with S_{max} = 0,55 & S_{min} = 0,05

This last case might not have been tested because the fatigue limit was reached for the case of ND65 with S_{max} = 0,60 and S_{min} = 0,05. The results in Fig. 29 and Fig. 30 seem to give the average value of 2 or 3 tests, but not always. In a single case for which the experimental program consists of 3 tests, there are 2 datapoints given in the graph. The missing data could be in Fig. 31, which might be giving individual results, but these values are difficult to distill from the graph because a different legend is used.

Table 3: Overview of test program (Petkovic et al., 1990)

Load levels		ND65	ND95	LWA75
S_{max}	S_{min}			
0.95	0.05		2	
0.90	0.05		2	
0.85	0.05		2	3
0.75	0.05	2	3	2
0.70	0.05	3	2	3
0.65	0.05		3	2
0.60	0.05	1	2	2
0.55	0.05	2		
0.75	0.20	2	2	3
0.70	0.20	3		
0.75	0.30	2	1	4
0.85	0.40	1	2	3
0.80	0.40	1	3	3
0.75	0.40	1	2	2
0.70	0.40	1		
0.95	0.60		1	
0.90	0.60		2	
0.85	0.60		3	2
0.80	0.60		3	

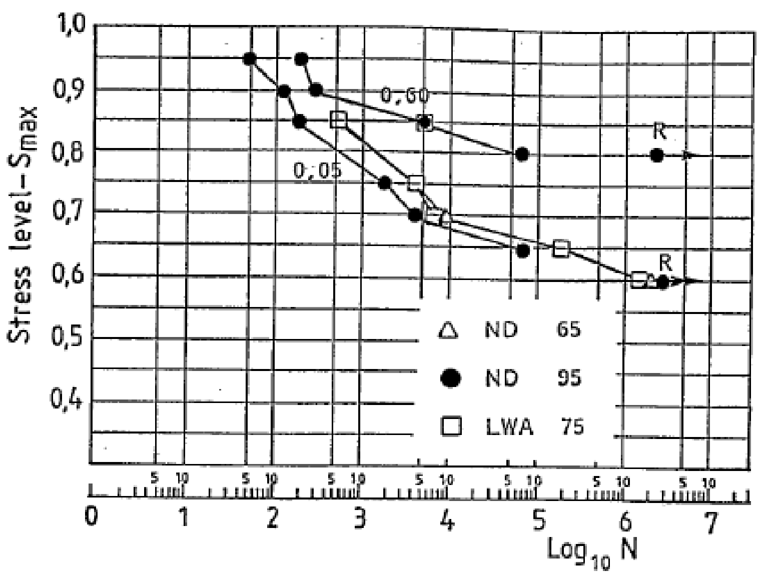

Fig. 29: Results of constant amplitude tests on ND65, ND95 and LWA75 for S_{min} = 0,05 and S_{min} = 0,6. R = run-out specimen. (Petkovic et al., 1990)

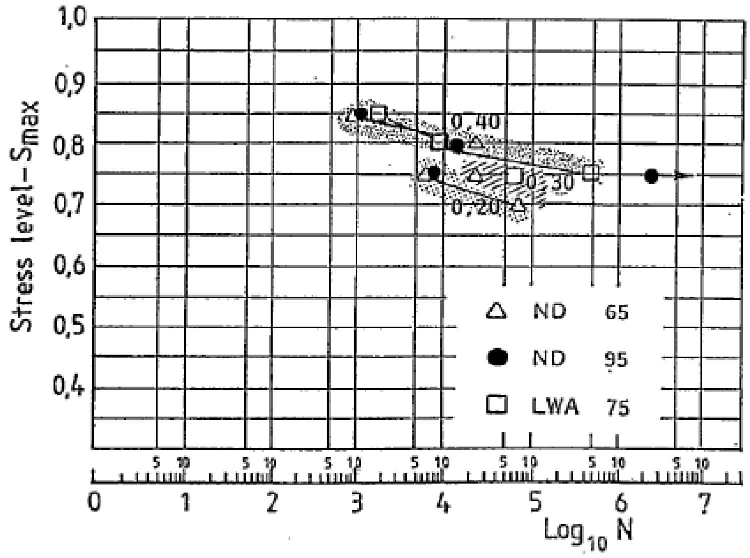

Fig. 30: Results of constant amplitude tests on ND65, ND95 and LWA75 for S_{min} = 0,20; S_{min} = 0,30 and S_{min} = 0,4. R = run-out specimen (Petkovic et al., 1990)

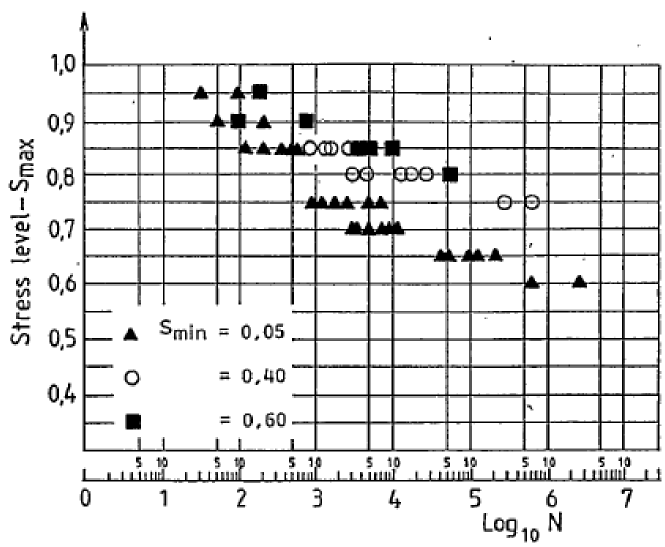

Fig.4-- Results from all three qualities for S_{min}=0.05, 0.40 and 0.60

Fig. 31: Results from all three qualities for S_{min} = 0,05; S_{min} = 0,40 and S_{min} = 0,60. (Petkovic et al., 1990).

A next set of experiments studied the fatigue compressive strength of UHPC (Fehling et al., 2005). The measured static compressive strength of the used mixes is given in Table 4. The behavior of heat-treated UHPC B3Q-90^{o}C with and without 2,5% (by volume) of 9mm steel fibers is studied on cylinders (h = 300mm, d = 150mm). The specimens were heat treated at 90^{o}C and then stored at room temperature (about 20^{o}C and 50% RH) until the day of testing. For this concrete mix, the cylinder compressive strength is 226 MPa or higher, as the maximum capacity of the machine was reached while testing the static strength of these cylinders. The text says that the specimens were with or without steel fibers. The mix design of B3Q however shows that this mixture always contains steel fibers.

Table 4: Measured compressive strength (Fehling et al., 2005).

Prüfkriterium	UHPC – Mischungen					
	M1Q WL	M1Q 90°C	Differenz	B3Q WL	B3Q 90°C	Differenz
Druckfestigkeit [N/mm²]						
f_c nach 7 d	128	200	+72	140	195	+55
f_c nach 28 d	153	208	+55	158	205	+47
f_c nach 56 d	180	222	+42	186	> 226 $^{1)}$	>+40
Rohdichte [kg/dm³]	2,50	2,52		2,51	2,59	

Tabelle 3.5-1: Zeitliche Entwicklung der Zylinderdruckfestigkeit der gefaserten Ultra-Hochfesten Betone M1Q und B3Q, WL-Wasserlagerung 20°C,
90°C – Warmbehandlung für 48h, $^{1)}$ Maximallast der Prüfmaschine erreicht

The results of the fatigue tests are shown in Fig. 32 and compared to the results of normal strength concrete. If failure did not occur for 2 million cycles, the specimen was tested in a static test until failure and considered as a run-out specimen. While usually the results are given as an *S-N* diagram, here the *y*-axis uses $\Delta\sigma = 2\sigma_a = S_{max} - S_{min}$. The lines for normal strength concrete are based on an expression by Weigler and Klausen and by Holmen, respectively. For the database, only the UHPC results are used. After analyzing the test results, Fehling et al. (2005) concluded that a difference with normal strength concrete for the fatigue life of concrete in compression cannot be noticed.

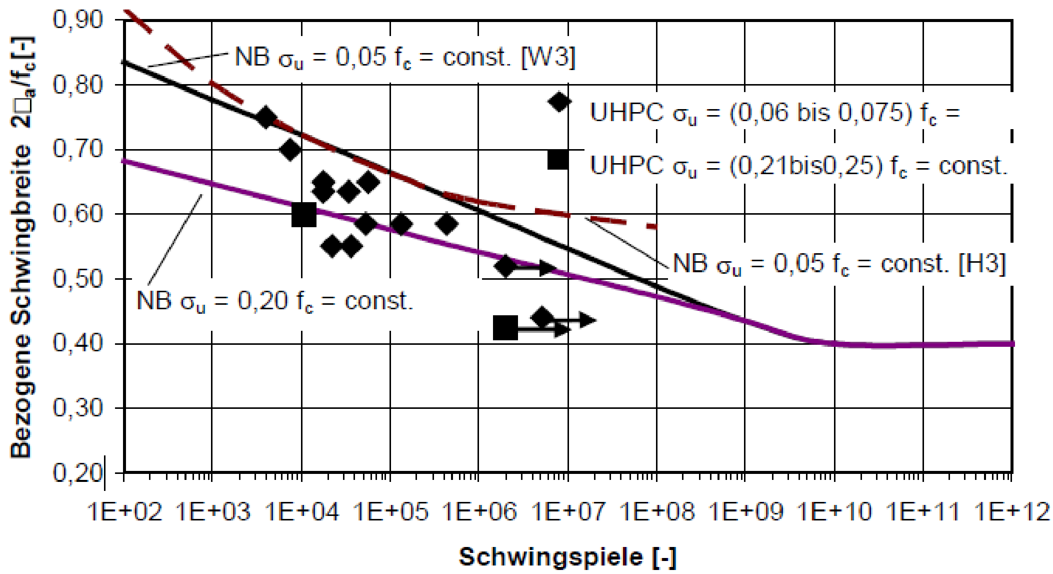

Fig. 32: Experimental results of fatigue strength of UHPC (Fehling et al., 2005).

The next series of experiments compares the fatigue life of different strength concrete mixes (Kim and Kim, 1996). Four different concrete cylinder compressive strengths were used: 26MPa, 52MPa, 84MPa and 103 MPa. An overview of the test program and the results in terms of cycles to failure is given in Table 5. These experiments were tested with a loading history as shown in Fig. 33. The minimum stress level in the experiments was S_{min} = 0,25 and the maximum was varied between S_{max}= 0,95 and S_{max} = 0,75. The frequency of loading was 1Hz, and the loading was applied sinusoidally. In total, 103 specimens were tested for fatigue: 75 specimens were tested for the relationships between stress level, number of cycles to failure and static strength level and 28 specimens were tested for the deformation characteristics of concrete subjected to fatigue loading. The resulting *S-N* diagrams are shown in Fig. 34. Note that the intersection of the *S-N* diagram with the *y*-axis indicates that for 1 cycle a capacity larger than the static strength can be reached.

Table 5: Fatigue test results, (Kim and Kim, 1996)

Mix	Compressive strength (MPa)	Maximum stress level S_{max} (%)	Number of specimen	Average fatigue life $(N_f)_{avg}$
LS	26	95	6 + 2*	123
		85	5 + 2*	1363
		80	5 + 2*	5738
		75	3 + 2*	55739
MS	52	95	5 + 2*	100
		85	6 + 2*	968
		80	6 + 2*	2528
		75	5 + 2*	10117
HS	84	95	4 + 2*	58
		85	6 + 2*	1045
		75	6 + 2*	1644
		70	4 + 2*	3484
VHS	103	95	4 + 1*	46
		85	4 + 1*	481
		75	3 + 1*	1419
		70	4 + 1*	3394

* : number of cylinders used for fatigue deformation tests

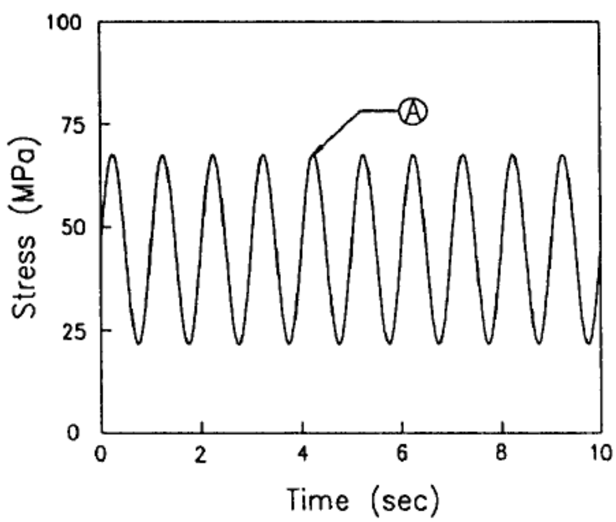

Fig. 33: Typical loading history used for the experiments by Kim and Kim (1996).

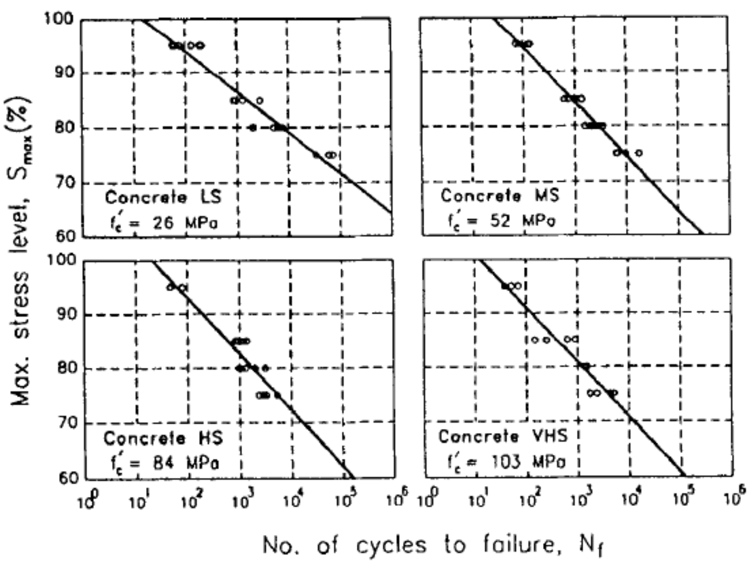

Fig. 34: Resulting S-N relationships based on experiments by Kim and Kim (1996).

The next set of experiments that are used for the database are experiments on high strength concrete in which the difference between gravel and limestone aggregates was studied (Hordijk, 1994; Hordijk et al., 1995). The experiments were not carried out on concrete cylinders, but instead on specimens with the dimensions of 250mm × 100mm × 100mm that were sawn out of concrete piles. The testing frequency was 6Hz. As a result of the execution of the test, in which it was prevented that the first loading would be an impact loading, it took between 20 to 80 cycles before the correct upper and lower load level were reached. Two different concrete mixes were tested: a mix with gravel aggregates with a compressive strength of 78,2 MPa (with a coefficient of variation of 2,9%) and a mix with limestone aggregates with a compressive strength of 73,1MPa (with a coefficient of variation of 3,2%). The compressive strength was also determined based on elements of 250mm x 100mm x 100mm. Failure of the specimens was reported to occur in an explosive way. Pictures of the failed specimens, exhibiting a typical shape as usually found for compressive failure, can be seen in Fig. 35. Differences between the concrete types were reported not to be observed. The resulting Wöhler curves and experimental results are shown in Fig. 36. In the full report (Hordijk, 1994) the measured number of cycles for the different stress levels are given and these values are used for the database.

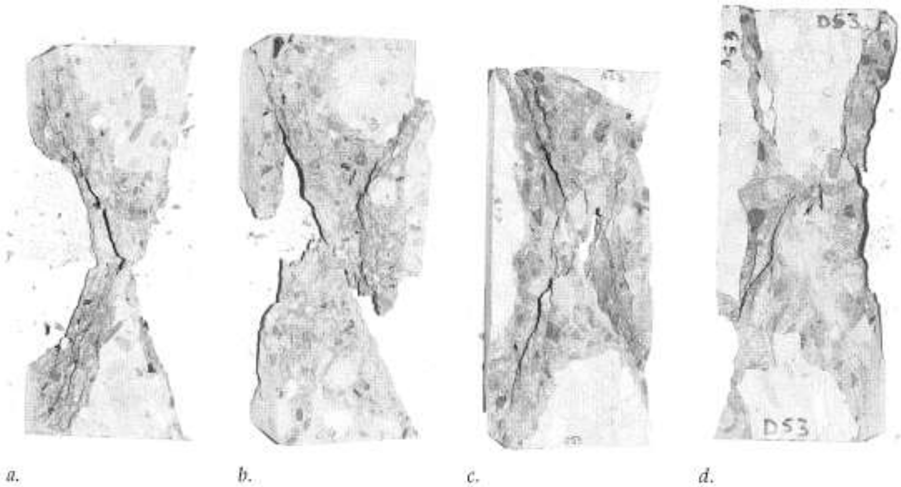

Fig. 35: Specimens after failing in concrete compression: a,b: gravel concrete; c,d: limestone concrete.(Hordijk et al., 1995)

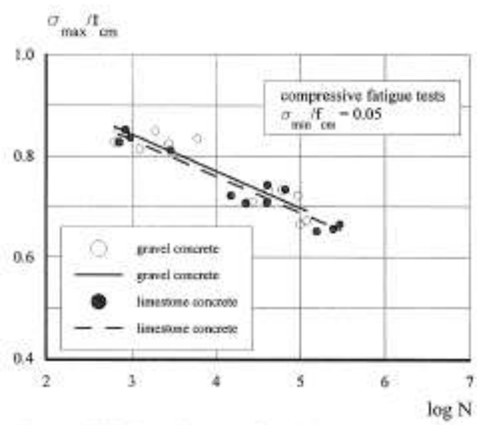

Fig. 36: Wöhler-diagram for the compressive fatigue tests.

The next set of experimental results that is used for the database studies the influence of the stress ratio and loading frequency on the fatigue capacity of high strength concrete (Saucedo et al., 2013). The concrete compressive strength was determined based on cubic specimens. The results of the static tests are shown in Table 6, also including *r*, which here is the Pearson's coefficient of correlation. The value of σ_{min0} is the endurance limit assuming a Weibull distribution. This value appears to be rather low, so that the authors suggest that concrete materials might not have an endurance limit. Part of the research also focused on the relation between the secondary strain rate and the fatigue life based on the observed experimental trend. The measured number of cycles until failure are given in Table 7. These experiments were tested on cubic specimens of concrete C1 with an edge length of 80mm. The maximum stress was σ_{max} = 90MPa and the loading frequency 4 Hz. To study the influence of the loading frequency, fatigue tests on cube specimens with an edge length of 100mm of C2 concrete were carried out at four different frequencies. The results of this series of experiments are shown in Table 8.

Table 6: Statistic results of the static compression tests, (Saucedo et al., 2013).

Material	λ (MPa)	k	σ_{min_0} (MPa)	r
C1	94.7	12.4	3.1	0.98
C2	76.1	19.8	3.1	0.98

Table 7: Results of fatigue tests, (Saucedo et al., 2013).

R	Number of cycles resisted for f = 4 Hz, σ_{max} = 90 MPa							
0.3	150	2927	2149	667	7600	75,378	7839	20,426
	38	73	17,172	11,863	9218	7288	2798	
0.1	2265	4276	2352	222	46	125	731	1106
	7153	3961	1231	1753	302	858	5988	

Table 8:Results of fatigue tests considering different frequencies (Saucedo et al., 2013)

Table 5
Results of the fatigue tests loaded at a stress ratio of 0.3, maximum stress of 66.4 MPa, and four different frequencies on cubic specimens for concrete C2.

f (Hz)	Number of cycles for R = 0.3, σ_{max} = 66.4 MPa						
4	8411	821	2485	1660	13,020	22,570	9521
	4192	170,256	1578	1222	133	7038	
1	282	23	759	1351	85	157	479
	368	833	1571				
0.25	98	1242	535	157	18	30	219
	650	122	400				
0.0625	339	473	102	234	11	142	76
	275	329	38				

A next series of experiments are carried out on ultrahigh strength concrete (Lohaus et al., 2011). The concrete compressive strength at 28 days of mix M2Q was 160MPa and of mix B4Q this was 180MPa. The authors write this as: $f_{c,cube,100}$ = 160 MPa, and thus it can be assumed that this compressive strength is determined based on cube specimens. The measured stress-strain relationship is shown in Fig. 37. The mix design of the M2Q and B4Q concrete is shown in Table 9. Both concrete mixes contained 2,5 volume% of smooth, high strength steel fibers of 9mm length and with an *l/d* ratio of 60. The fatigue tests were carried out on cylinders with *d/h* = 60mm/180mm. These specimens were heat treated at 120°C during two days, after which the specimens were stored at room climate (20°C and 65% RH) until testing. The authors mention two different concrete mixes with two concrete compressive strengths, but the results of the fatigue testing are mixed together. Therefore in the database a cube compressive strength $f_{c,cube}$ = 170MPa is used. The conversion between the cube compressive strength and the cylinder compressive strength is not very clear for high strength concrete. Some results are given in the literature (del Viso et al., 2008), but these values are for compressive strengths of

100MPa. For the results, a cylinder strength of 150MPa is assumed, and this value is used in the database.

Table 9: Mix design of M2Q and B4Q (Wefer, 2010)

	M2Q	B4Q	NB
Ausgangstoffe	[kg/m³]	[kg/m³]	[kg/m³]
Zement CEM I 52,5R HS/NA	832	650	311
Mikrosilika Elkem Grande 983	135	177	-
Feinquarz MILLISIL W3	-	131	-
Feinquarz MILLISIL W12	207	325	51
Sand H 33 0,125/0,5 [mm]	975	354	696
Basalt 2/5 - 5/8 [mm]	-	597	926
Stahlfasern l/d = 9,0/0,15 [mm]	192	194	-
Wasser	166	158	171
PCE-Fließmittel Glenium 51	29,4	30,4	-
Summe	2536,4	2616,4	2455,0
w/z-Wert [-]	0,20	0,24	0,55
w/b-Wert [-]	0,19	0,21	-
28-Tage Druckfestigkeit [N/mm²]	160,0	180,0	40,0

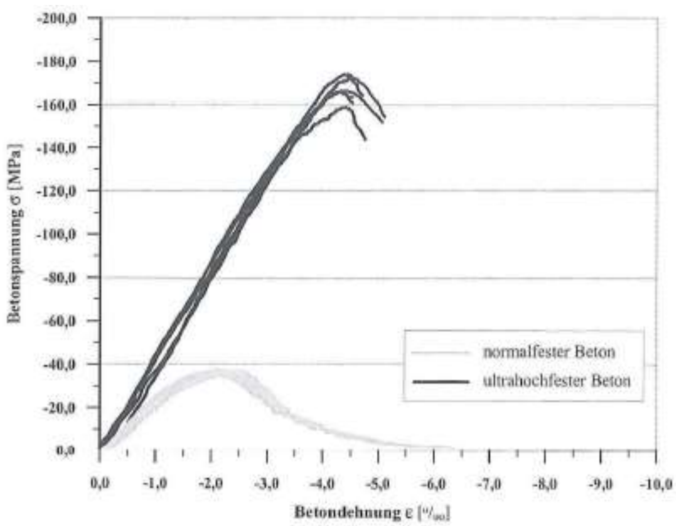

Fig. 37: Stress-strain relationship of ultrahigh strength concrete (Wefer, 2010).

The fatigue experiments were tested with a frequency of 10Hz up to 2×10^6 cycles. If failure did not occur after 2 million cycles, the frequency was increased to 60Hz. If it was expected that the fatigue life would be more than 2 million cycles, 60Hz was used for testing. Two different machines were used, one at 10Hz (universal testing machine) and a different one at 60 Hz (system based on alternating resonances), and the results showed that the 60Hz machine resulted in a smaller number of cycles to failure. The authors then state that as such the experimental results are on the safe side.

The lower stress rate in the experiments was S_{min} = 0,05; S_{min} = 0,20 and S_{min} = 0,40. In total 121 specimens are tested: 88 for S_{min} = 0,05; 21 for S_{min} = 0,20 and 12 for S_{min} = 0,40. An overview of the test program is shown in Table 10. The results are shown in Fig. 38. These results are described in more detail in (Wefer, 2010), in which also the measured number of cycles to failure were given. This reported number of cycles to failure was then used in the database.

Table 10: Overview of the experimental program (Wefer, 2010)

Spannungsniveaus		M2Q	M2Q	M2Q	M2Q	B4Q	B4Q	NB
S_O	S_U	01	02	03	04	05	06	07
0,90	0,05	4	-	-	-	13	-	10
0,85	0,05	-	-	-	-	4	-	-
0,80	0,05	15	-	3	-	16	6	10
0,75	0,05	-	-	-	20	5	-	-
0,70	0,05	2	-	-	-	19	7	5
0,65	0,05	-	-	-	-	5	-	-
0,60	0,05	-	-	-	-	5	-	-
0,90	0,20	-	3	-	Keine Untersuchungen durchgeführt			
0,85	0,20	-	4	-				
0,80	0,20	-	6	4				
0,75	0,20	-	4	-				
0,70	0,20	-	1	-				
0,65	0,20	-	4	-				
0,90	0,40	-	-	3				
0,80	0,40	-	-	9				
0,80	0,50	-	-	2				
Summe		21	22	21	20	67	13	25

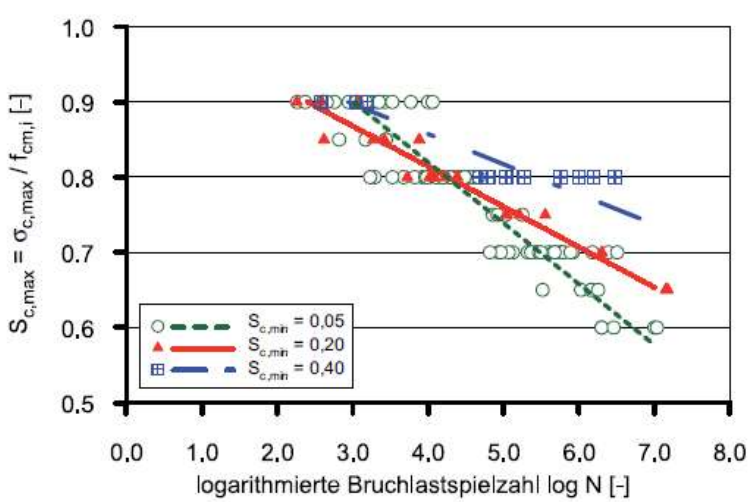

Fig. 38: Fatigue test results of ultrahigh strength concrete (Lohaus et al., 2011)

Another set of experiments from Hannover tested high strength concrete in fatigue with and without fiber reinforcement (Lohaus and Anders, 2006). The concrete mixes were based on a reference mix with a compressive strength of about 140MPa. The mixtures with fibers contain alkali-resistant glass or steel fibers. For the AR-glass fibers, the fiber content was varied between 3kg/m^3 and 6kg/m^3 and both integral and dispersible fibers were studied. The fiber length was kept constant at 13mm. For the steel fibers, smooth fibers with a length of 6mm and an *l/d* ratio of 37,5 were used. Two fiber contents were used: 1,75 volume% (137 kg/m^3) and 0,75 volume% (60 kg/m^3). The measured compressive strength and Young's modulus can be seen in Table 11. The specimens were cylinders with a diameter of 70 mm and a length of 210 mm.

Table 11: Properties of hardened concrete used in fatigue tests (Lohaus and Anders, 2006)

	Fibres			Compressive strength [MPa]	Young's modulus [MPa]
	Material	Type	Content		
Reference	---	---	---	140 MPa	44.100 MPa
Reference (heat treated)	---	---	---	145 MPa	--- MPa
SF 0,75	steel	smooth	0,75 Vol.-%	140 MPa	44.250 MPa
SF 1,75	steel	smooth	1,75 Vol.-%	130 MPa	44.650 MPa
AR S 3,0	AR-glass	dispersible	3,0 kg/m³	120 MPa	41.150 MPa
AR Y 6,0	AR-glass	integral	6,0 kg/m³	130 MPa	42.500 MPa

The specimens were demoulded one day after casting and stored in 20^{o}C at 65% RH. At 7 days, the specimens were sawn to their final length and the surface was smoothed. Then, the specimens were stored again in 20^{o}C at 65% RH until the day of testing, typically at an age between 28 and 36 days. The fatigue tests were carried out at a high testing frequency (60 Hz), which resulted in a high temperature in the specimens during testing, Therefore, the next concrete batches were cast and heat treated after demoulding with a maximum temperature of 200^{o}C for 10 hours. The results of the fatigue tests are summarized in the *S-N* diagram in Fig. 39. The results are read from this graph and then put into the database. The problem with the analysis of these experiments is that the lower bound S_{min} is not given, only the stress range $\Delta\sigma$ is given in Fig. 39. For the database, it is assumed that S_{min} was similar as in the other Hannover tests, with S_{min} = 0,05.

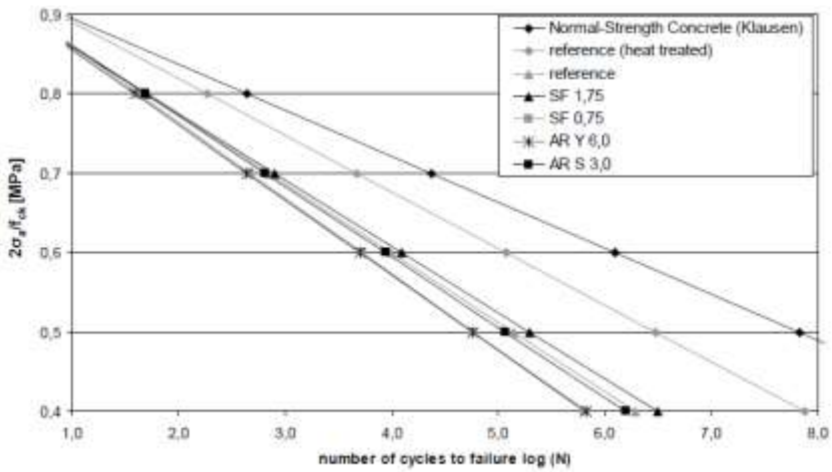

Fig. 39: S-N curves resulting from the fatigue tests (Lohaus and Anders, 2006)

A next series of experiments concentrated on investigating different stress ranges for specimens on high strength concrete (Tue and Mucha, 2006). The precise measured concrete compressive strength is unfortunately not given, the authors only mention that “the compressive strength was always above 65MPa”. In total, 170 specimens were tested in fatigue under compression. An overview of the test program is given in Table 12. The results of the fatigue tests are then given in . Since in these experiments the average measured number of cycles until fatigue failure of the number of specimens tested under the studied condition are given, these values are used in the database.

Table 12: Overview of test program (Tue and Mucha, 2006)

S_u	S_o	Anzahl der Probekörper
0,20	0,60	10
	0,65	10
	0,70	10
	0,75	10
	0,80	10
	0,85	10
0,05	0,60	6
	0,65	6
	0,70	6
	0,75	6
	0,80	6
0,10	0,60	6
	0,65	3
	0,70	6
	0,75	3
	0,80	6
0,30	0,60	6
	065	3
	0,70	6
	0,75	3
	0,80	6
0,40	0,60	6
	0,70	6
	0,80	6

Table 13: Results as the mean values of fatigue cycles (Tue and Mucha, 2006)

S_u	S_o	Anzahl	N_m	Log N_m		$(E_{100}/E_0)_m$	$(f_{c,100}/f_{c,0})_m$
	0,8	6	14.489	4.23			
0,4	0,7	7	1.471.316	6.17	*	0,92	1,06
	0,6	6	2.540.240	6.40	*	0,93	0,98
	0,8	6	2.203	3.34			
	0,75	5	878.830	5.94			
0,3	0,7	6	1.832.482	6.26	*	0,96	1,04
	0,65	3	2.263.330	6.35	*	0,92	1,07
	0,6	7	2.393.031	6.38	*	0,91	1,00
	0,85	8	338	2.53			
	0,8	10	2.229	3.35			
	0,75	12	9.691	3.99			
0,2	0,7	10	33.536	4.53			
	0,65	10	1.808.836	6.26	*	0,88	1,02
	0,6	10	2.316.853	6.36	*	0,89	0,99
	0,55	2	2.495.845	6.40	*	0,90	
	0,8	9	500	2.70			
	0,75	6	4.428	3.65			
0,1	0,7	7	4.871	3.69			
	0,65	4	62.483	4.80			
	0,6	6	2.115.172	6.33	*	0,87	1,01
	0,8	6	1.000	3.00			
	0,75	6	3.847	3.59			
0,05	0,7	7	5.179	3.71			
	0,65	6	46.402	4.67			
	0,6	6	1.908.925	6.28	*	0,83	0,98
Summe		171					

Finally, a number of experiments from the literature are cited by Wefer (2010). These results are also submitted to the database. The first set of experiments were tested by Zhao et al. (1996). The lower stress ratio S_{min} was taken as 0,1. The results are not given separately, only the *S-N* curve is reported, and from there some points are read from this graph and used for the database The cube compressive strength is given, this value is converted to the cylinder compressive strength by using a factor 0,82 (van der Veen and Gijsbers, 2011). The reported *S-N* curve is shown in Fig. 40.

A final series of experiments that was cited by Wefer (2010) are the experiments by Hohberg (2004) in which three different concrete classes (B25, B45 and B95) are studied. Instead of using a lower stress ratio S_{min}, in these experiments the lower bound of the stress was always kept as σ_{min} = 2MPa, so that a different value for S_{min} was obtained for each of the studied concrete classes. The loading sequence in this series of experiments was slightly different as well. A statical loading part was applied after every set of 2500 cycles. The frequency of testing was 10Hz. The results are shown in Fig. 41. These points were read off from the *S-N* curve and used in the database. The concrete compressive strength is only given as the strength class, so the average cylinder compressive strength is read from Table 3.1 from EN 1992-1-1:2005 (CEN, 2005) for use with the database.

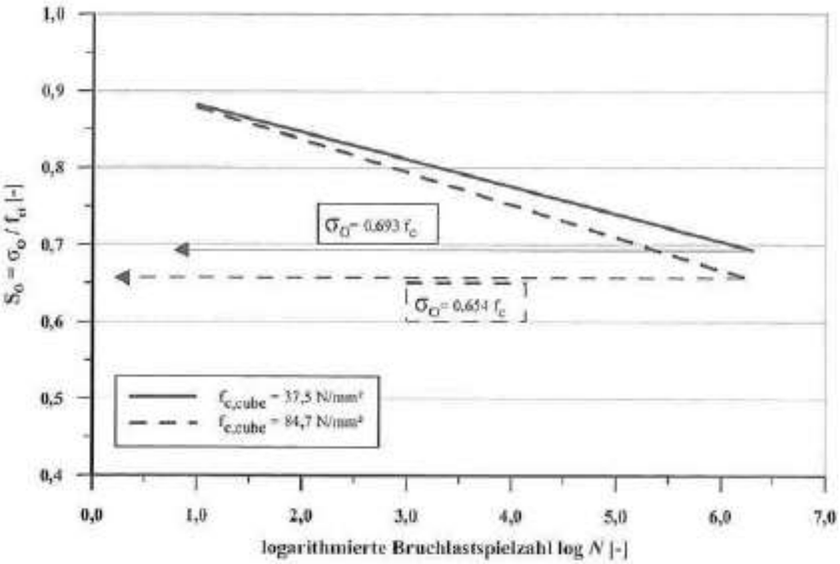

Fig. 40: S-N curve that results from the experiments by Zhao et al., 1996 (Wefer, 2010)

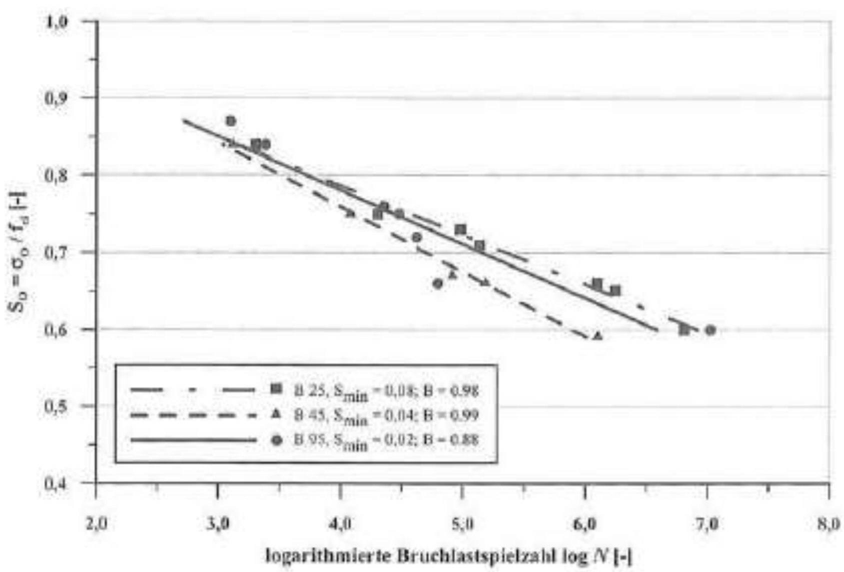

Fig. 41: Results of fatigue experiments on 3 different concrete classes by Hohberg (2004), as reported by Wefer (2010).

All these experimental results are gathered in the database in Annex 1. In total, 429 experiments are in the database, of which 234 experiments do not contain fibers in the concrete mix (maximum compressive strength of 145 MPa) and of which 195 experiments contain fibers and have a maximum compressive strength of 226 MPa. If the experiment contained a run-out specimen, the cell in the table is highlighted in grey.

Special observations from the experiments are added in the column of "comments". As the range of a low number of cycles to failure is interesting, a histogram showing the distribution of the number of cycles to failure in the database is given in Fig. 42. High strength concrete is of interest for this study, and therefore also a histogram showing the distribution of the concrete compressive strengths in the database is given in Fig. 43. The distribution of the compressive strength follows less a typical normal or lognormal distribution, because a large number of experiments with a compressive strength of 170MPa were carried out, which results in this large peak in the histogram. It can be seen, however, from Fig. 43 that a good variety of experiments with high strength concrete was achieved for the database.

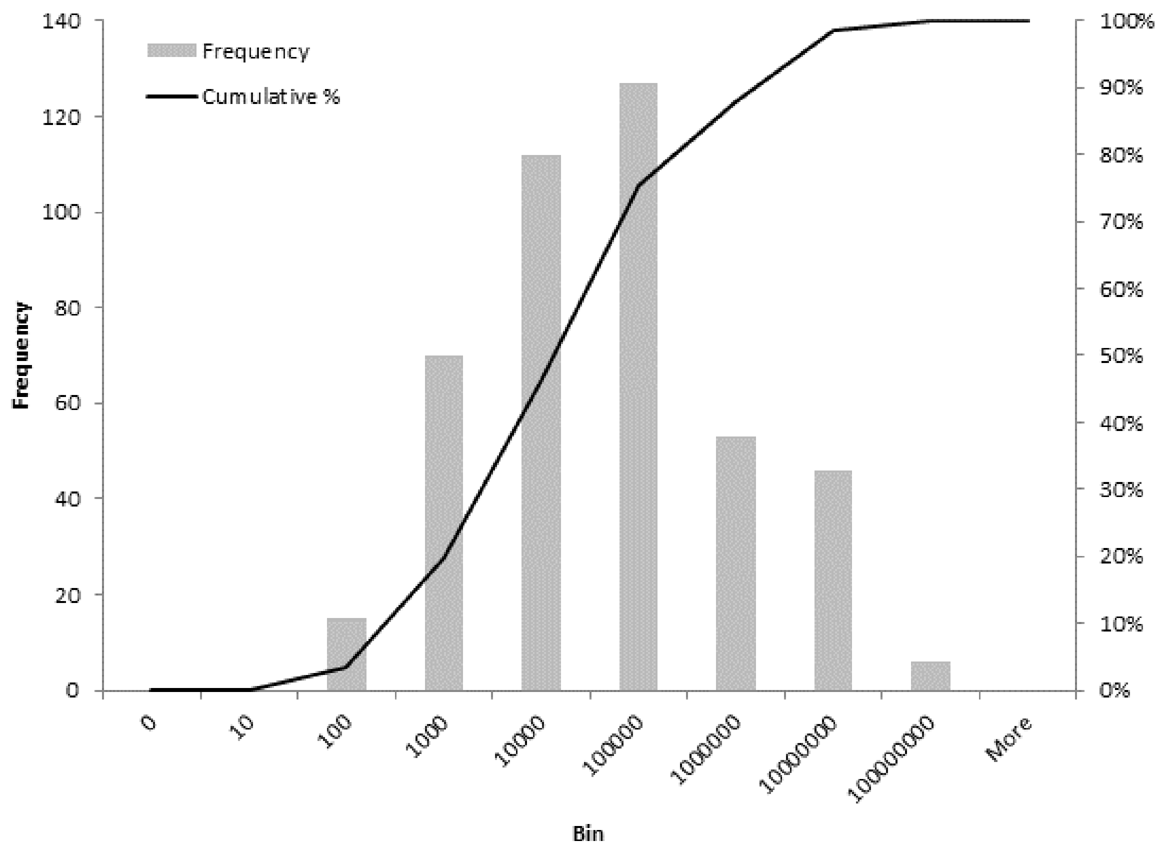

Fig. 42: Distribution of numbers of cycles to failure in the database.

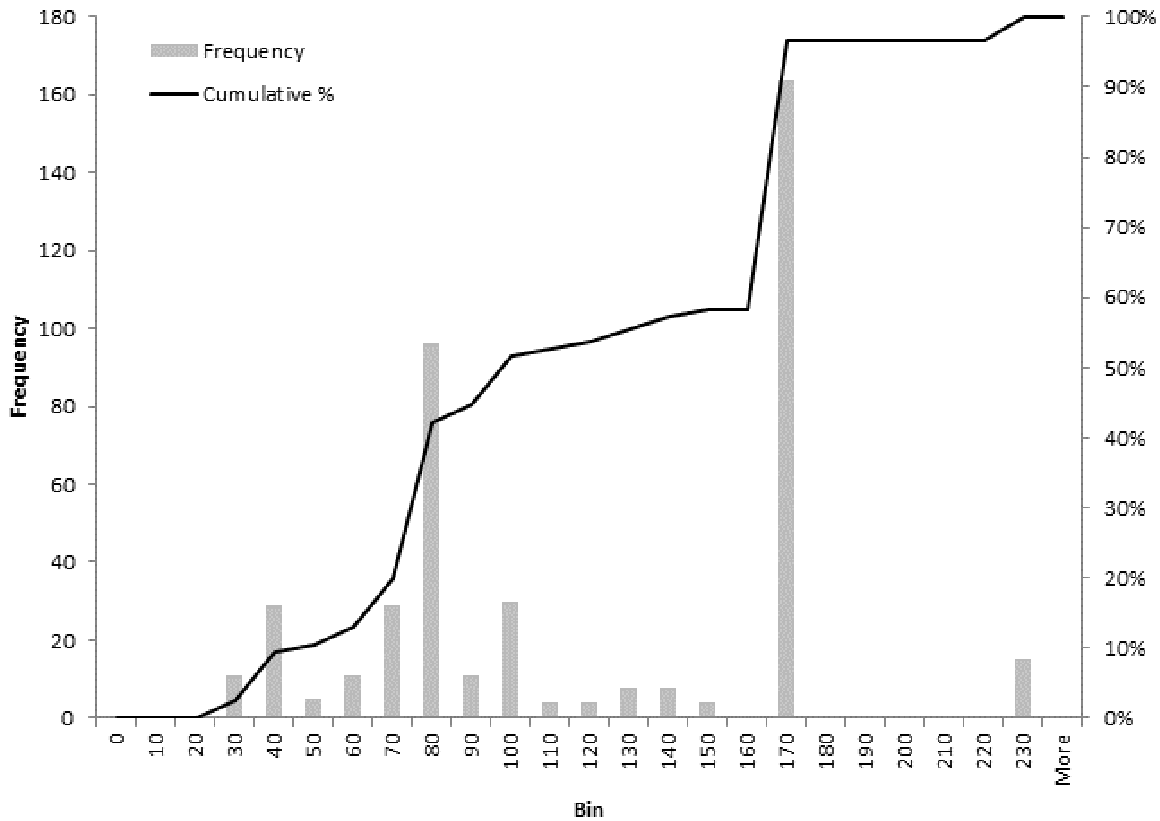

Fig. 43: Distribution of concrete compressive strength in the database.

5 Analysis of test results and proposal

5.1 Proposal based on correction of NEN-EN 1992-2+C1:2011/NB:2011

To make sure that the same value for S_{max} is found for $N_i = 10^6$ cycles, the following method is proposed, which is based on NEN-EN 1992-2+C1:2011/NB:2011:

$$\log N_i = \frac{6}{\left(1-0,57k_1\right)\left(1-\frac{f_{ck}}{250}\right)}\left(\frac{\left(1-\frac{f_{ck}}{250}\right)-E_{cd,max,i}}{\sqrt{1-R_i}}\right) \text{ for } N_i \leq 10^6 \tag{32}$$

$$\log N_i = 14\frac{1-E_{cd,max,i}}{\sqrt{1-R_i}} \text{ for } N_i > 10^6 \tag{33}$$

$$E_{cd,max,i} = \frac{\sigma_{cd,max,i}}{f_{cd}\left(\frac{\gamma_{c,fat}}{\gamma_c}+\frac{\log N_i}{600\left(1-\frac{\gamma_{c,fat}}{\gamma_c}\right)}\right)} \text{ for } N_i \leq 10^6 \tag{34}$$

$$E_{cd,max,i} = \frac{\sigma_{cd,max,i}}{f_{cd,fat}} \text{ for } N_i > 10^6 \tag{35}$$

$$f_{cd,fat} = k_1\beta_{cc}(t_0)\, f_{cd}\left(1-\frac{f_{ck}}{250}\right) \tag{36}$$

$$\beta_{cc}(t_0) = \exp\left\{s\left[1-\left(\frac{28}{t}\right)^{0,5}\right]\right\}\alpha_{cc} \tag{37}$$

According to NEN-EN 1992-2+C1:2011/NB:2011, $\gamma_{c,fat}$ = 1,35; k_1 = 1 and α_{cc} = 1. The proposed expression is now compared to experimental results, in separate graphs for the different values of S_{min} that are tested. The experimental results are first categorized into different concrete classes, and then compared with the *S-N* curves based on the design compressive strength f_{cd} according to the proposed formulas, Eqs. (32) to (37). The categorization into the experimental results is done by finding the characteristic compressive strength f_{ck} as $f_{c,mean}$ – 8 MPa, with $f_{c,mean}$ the compressive strength that was given in the database. The concrete class is then based on this value for f_{ck}. If the value is not exactly the same as a concrete class, it is rounded off down to the nearest concrete class. The comparison between the proposal and the experiments with S_{min} = 0,05 is shown in Fig. 44, with S_{min} =0,02 in Fig. 45, with S_{min} = 0,1 in Fig. 46, with S_{min} = 0,2 in Fig. 47, with S_{min} = 0,3 in Fig. 48, with S_{min} = 0,4 in Fig. 49 and with S_{min} = 0,6 in Fig. 50.

For S_{min} = 0,6 convergence of the method is difficult to reach when using the iterative procedure to determine the corresponding number of cycles N_i.

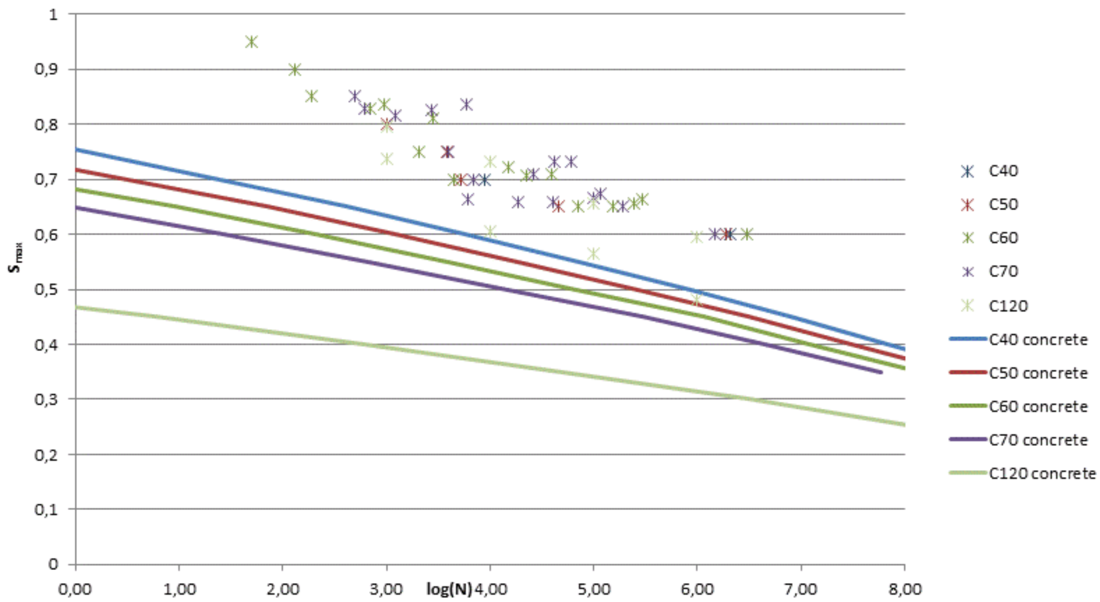

Fig. 44: Comparison between experiments with S_{min} = 0,05 and the proposed correction of NEN-EN 1992-2+C1:2011/NB:2011.

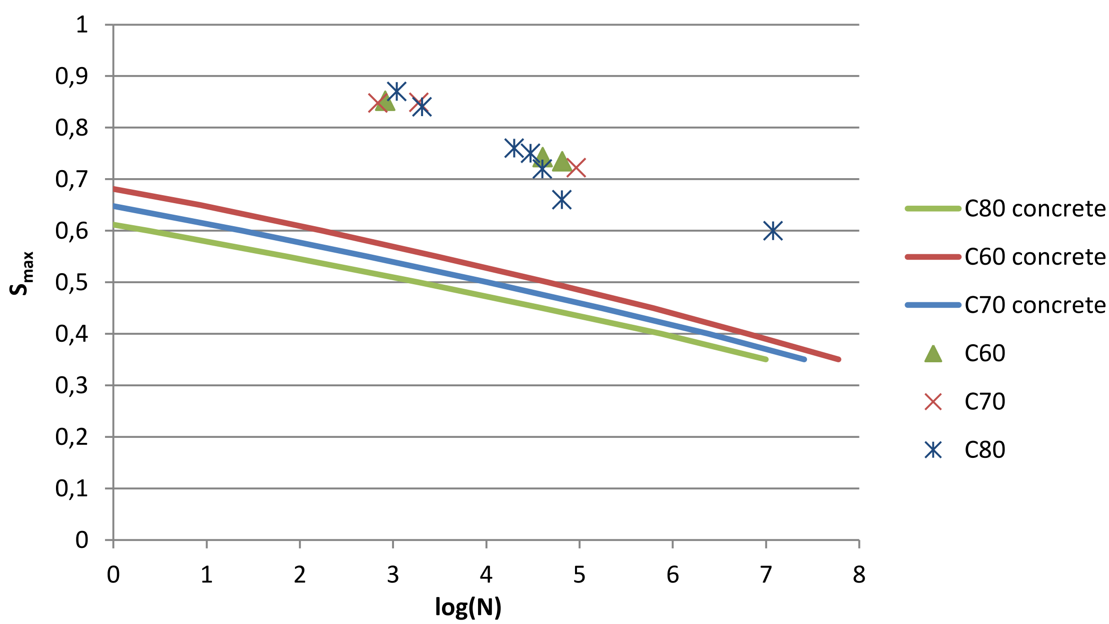

Fig. 45: Comparison between experiments with S_{min} = 0,02 and the proposed correction of NEN-EN 1992-2+C1:2011/NB:2011.

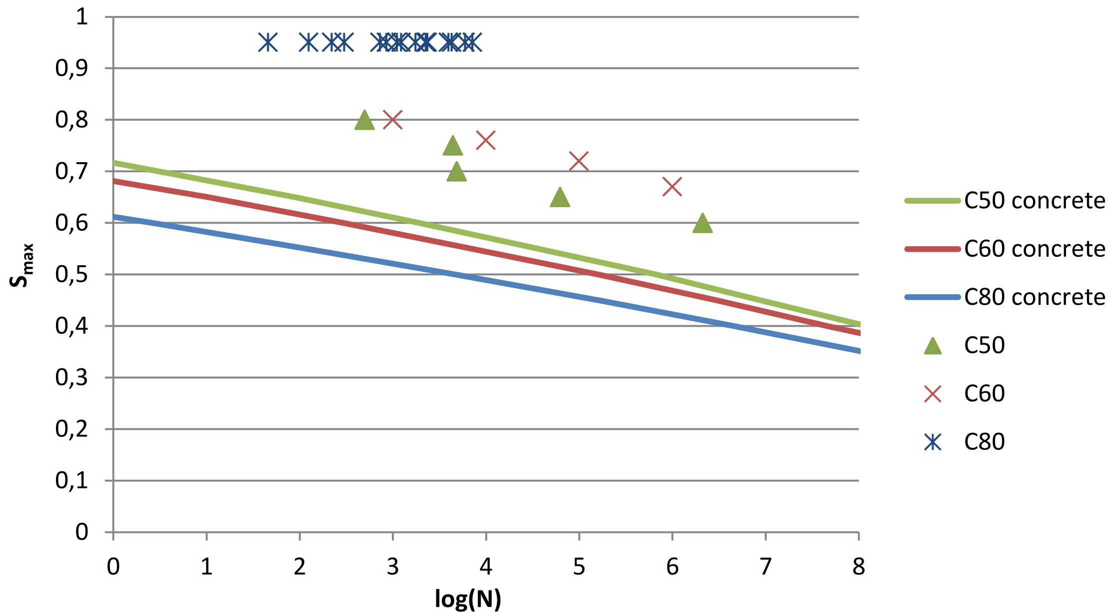

Fig. 46: Comparison between experiments with S_{min} = 0,1 and the proposed correction of NEN-EN 1992-2+C1:2011/NB:2011.

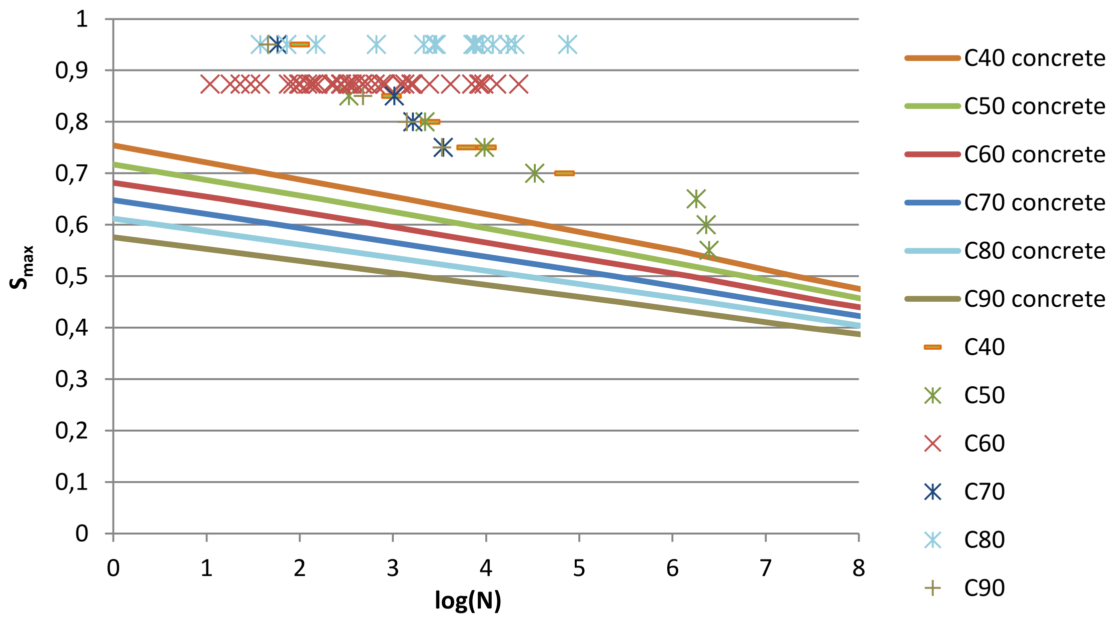

Fig. 47: Comparison between experiments with S_{min} = 0,2 and the proposed correction of NEN-EN 1992-2+C1:2011/NB:2011.

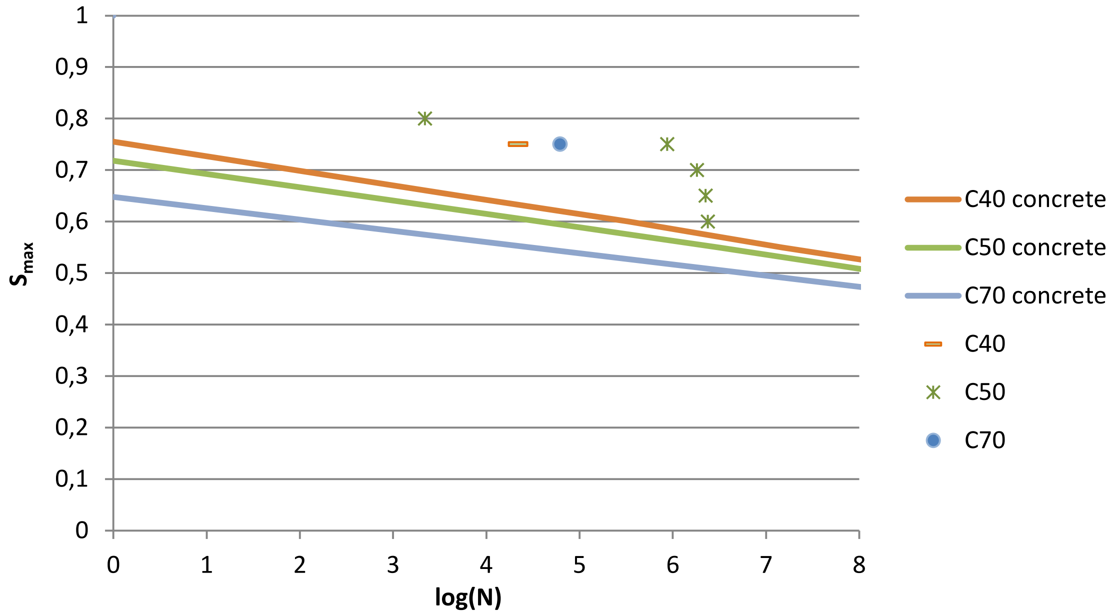

Fig. 48: Comparison between experiments with S_{min} = 0,3 and the proposed correction of NEN-EN 1992-2+C1:2011/NB:2011.

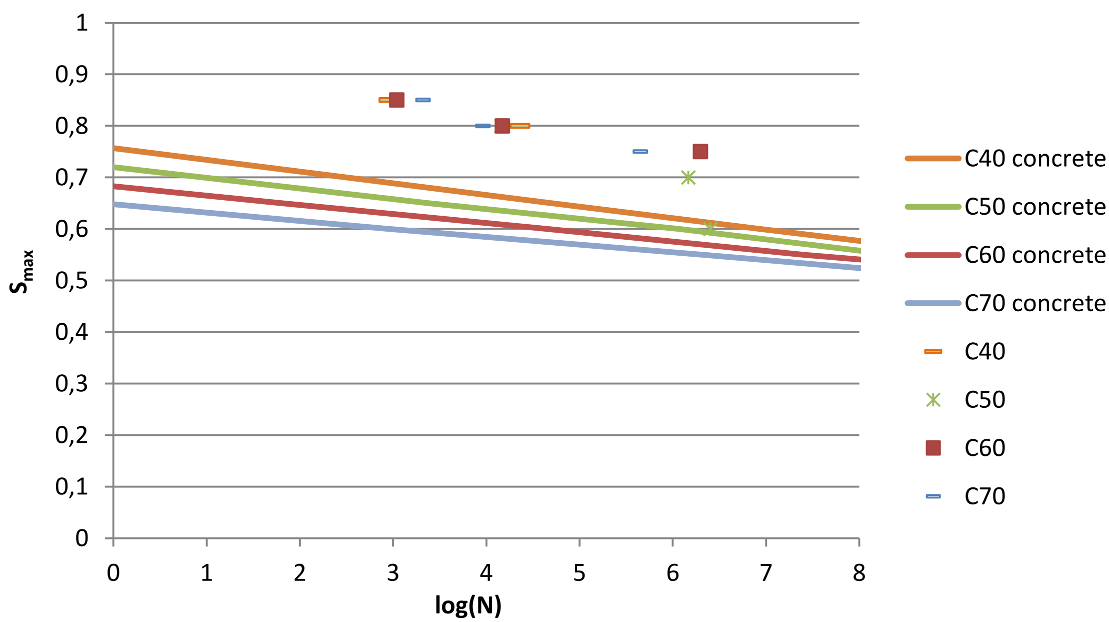

Fig. 49: Comparison between experiments with S_{min} = 0,4 and the proposed correction of NEN-EN 1992-2+C1:2011/NB:2011.

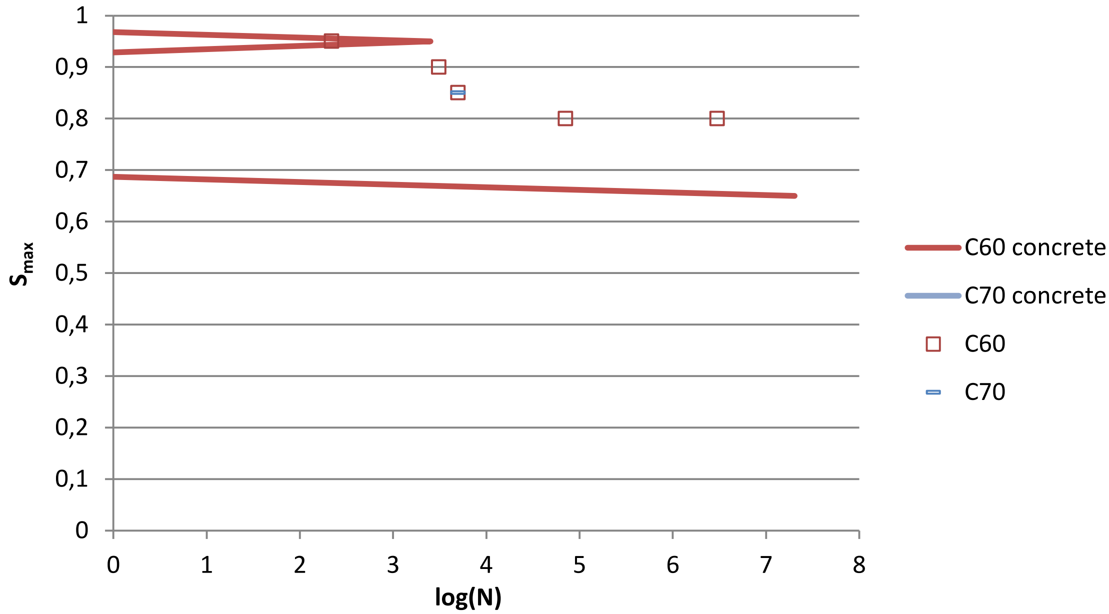

Fig. 50: Comparison between experiments with S_{min} = 0,6 and the proposed correction of NEN-EN 1992-2+C1:2011/NB:2011.

In a next step, a direct comparison between the tested and predicted values is made to see if sufficient safety is built into the method. For this purpose, the calculated value of S_{max} for an experimentally found number of cycles N_i is determined. The value of R as found in the experiment is used, instead of being replaced by S_{max}/S_{min}. The value of S_{max} is then expressed as:

$$S_{max} = \left[\left(1-\frac{f_{ck}}{250}\right)-\frac{1}{6}\log N_i\left(1-0,57k_1\right)\left(1-\frac{f_{ck}}{250}\right)\sqrt{1-R_i}\right]\left[\frac{\gamma_{c,fat}}{\gamma_c}+\frac{\log N_i}{600\left(1-\frac{\gamma_{c,fat}}{\gamma_c}\right)}\right] \quad (38)$$

for $N_i \leq 10^6$

$$S_{max} = \frac{f_{cd,fat}}{f_{cd}}\left(1-\frac{1}{14}\log N_i\sqrt{1-R_i}\right) \text{ for } N_i > 10^6 \quad (39)$$

A total of 234 experiments from the database are used for the comparison. These 234 experiments are all experiments from the database on concrete without fibers. An average value of tested S_{max} over predicted S_{max} of 1,56 is found, with a standard deviation of 0,275 so that the coefficient of variation equals 17,6% and the characteristic value (5% lower bound based on a normal distribution) equals 1,11. Since the 5% lower bound is larger than 1, the method is considered safe and suitable for application in design.

5.2 Proposal for higher strength concrete classes

In the previous section, it can be seen that the proposed method is quite conservative for higher concrete compressive strengths. Therefore, it is proposed to use a smaller reduction for the concrete compressive strength, as is also used for the *fib* Model Code 2010.

$$\log N_i = \frac{6}{\left(1-0,57k_1\right)\left(1-\frac{f_{ck}}{400}\right)}\left(\frac{\left(1-\frac{f_{ck}}{400}\right)-E_{cd,max,i}}{\sqrt{1-R_i}}\right) \text{ for } N_i \leq 10^6 \tag{40}$$

$$\log N_i = 14\frac{1-E_{cd,max,i}}{\sqrt{1-R_i}} \text{ for } N_i > 10^6 \tag{41}$$

$$E_{cd,max,i} = \frac{\sigma_{cd,max,i}}{f_{cd}\left(\frac{\gamma_{c,fat}}{\gamma_c}+\frac{\log N_i}{600\left(1-\frac{\gamma_{c,fat}}{\gamma_c}\right)}\right)} \text{ for } N_i \leq 10^6 \tag{42}$$

$$E_{cd,max,i} = \frac{\sigma_{cd,max,i}}{f_{cd,fat}} \text{ for } N_i > 10^6 \tag{43}$$

$$f_{cd,fat} = k_1\beta_{cc}(t_0)\,f_{cd}\left(1-\frac{f_{ck}}{400}\right) \tag{44}$$

$$\beta_{cc}(t_0) = \exp\left\{s\left[1-\left(\frac{28}{t}\right)^{0,5}\right]\right\}\alpha_{cc} \tag{45}$$

According to NEN-EN 1992-2+C1:2011/NB:2011, $\gamma_{c,fat}$ = 1,35; k_1 = 1 and α_{cc} = 1. The proposed expression is now compared to experimental results, in separate graphs for the different values of S_{min} that are tested. The experimental results are first categorized into different concrete classes, and then compared with the *S-N* curves based on the design compressive strength f_{cd} according to the proposed formulas, Eqs. (40) to (45). The same approach is used as explained in the previous section. The comparison between the proposal and the experiments with S_{min} = 0,05 is shown in Fig. 51, with S_{min} =0,02 in Fig. 52, with S_{min} = 0,1 in Fig. 53, with S_{min} = 0,2 in Fig. 54, with S_{min} = 0,3 in Fig. 55, with S_{min} = 0,4 in Fig. 56 and with S_{min} = 0,6 in Fig. 57.

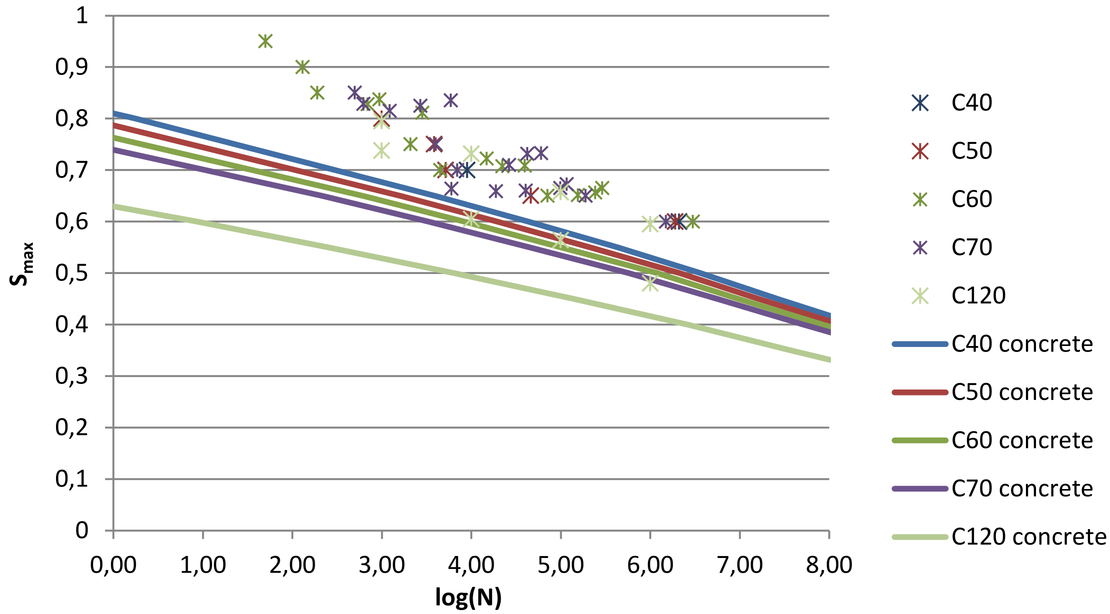

Fig. 51: Comparison between experiments with S_{min} = 0,05 and proposal.

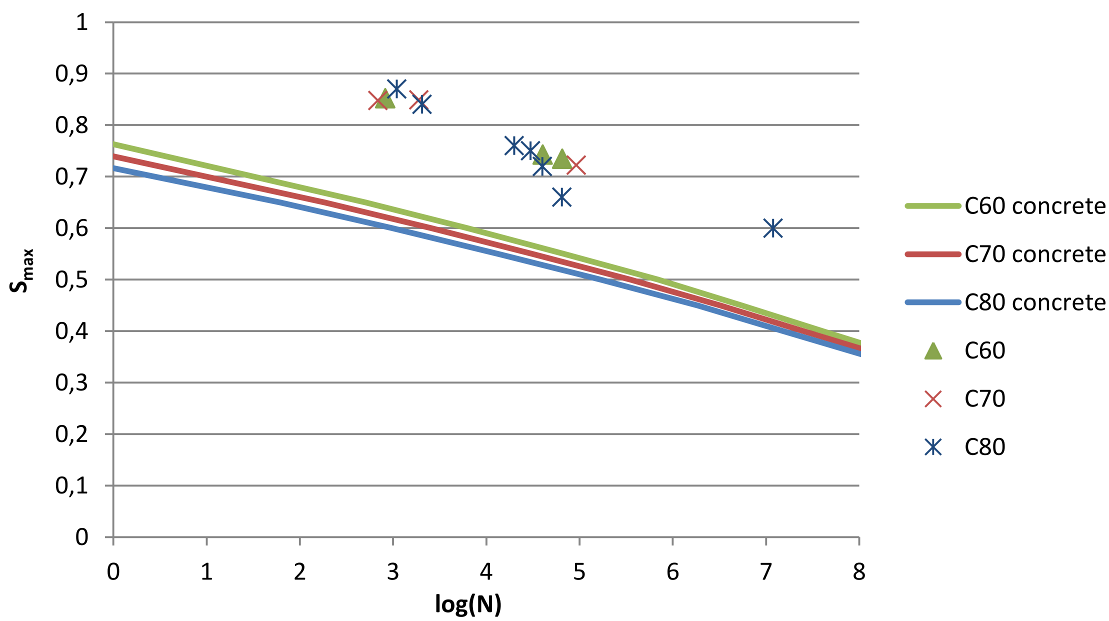

Fig. 52: Comparison between experiments with S_{min} = 0,02 and proposal.

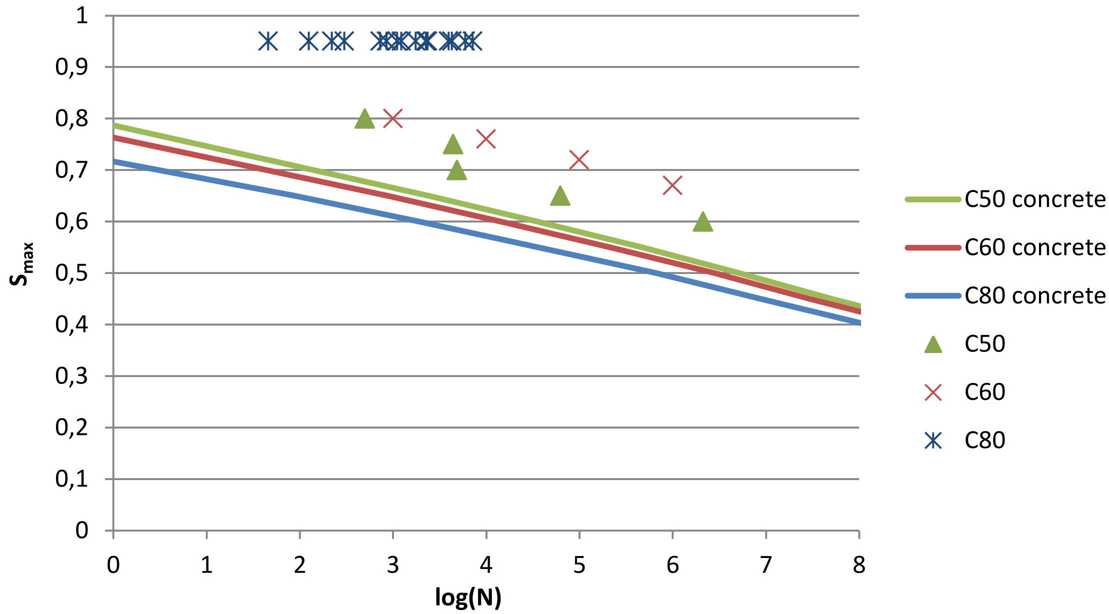

Fig. 53: Comparison between experiments with S_{min} = 0,1 and proposal.

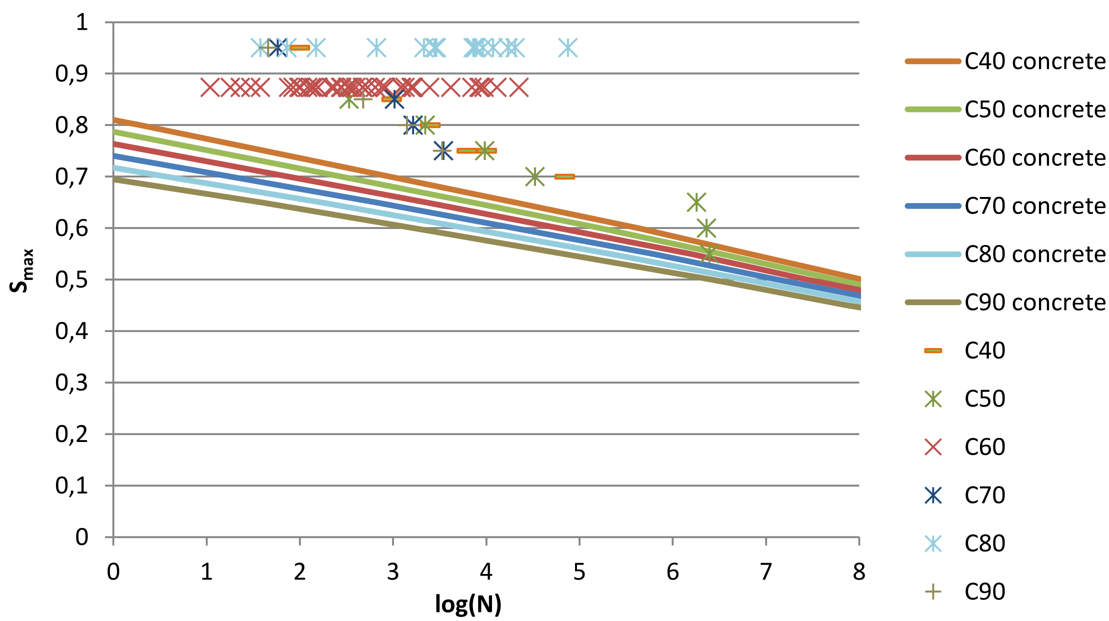

Fig. 54: Comparison between experiments with S_{min} = 0,2 and proposal.

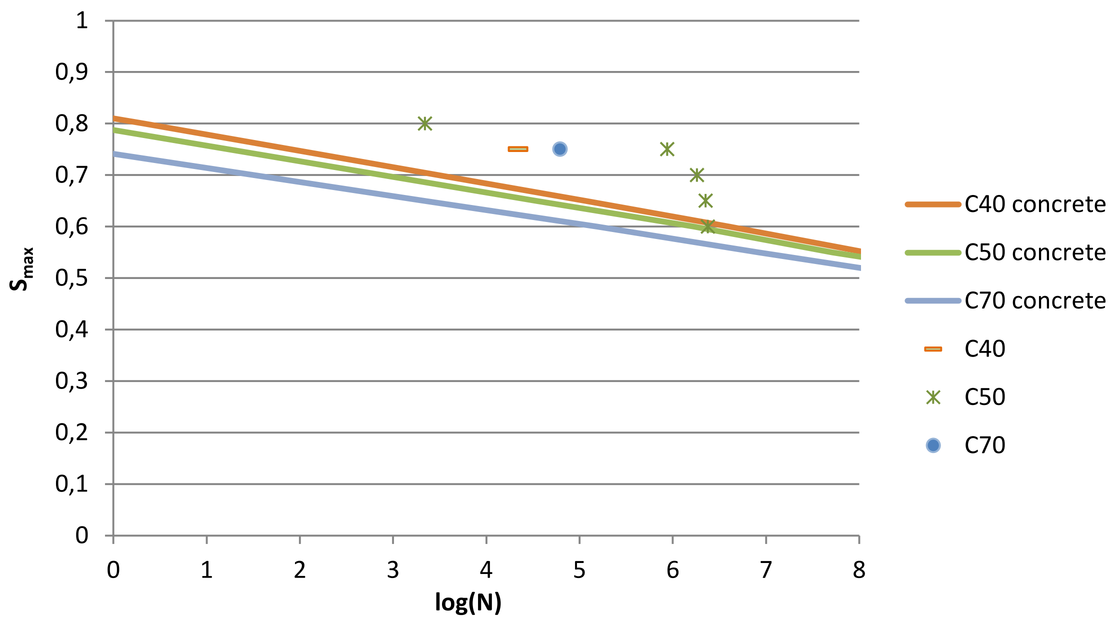

Fig. 55: Comparison between experiments with S_{min} = 0,3 and proposal.

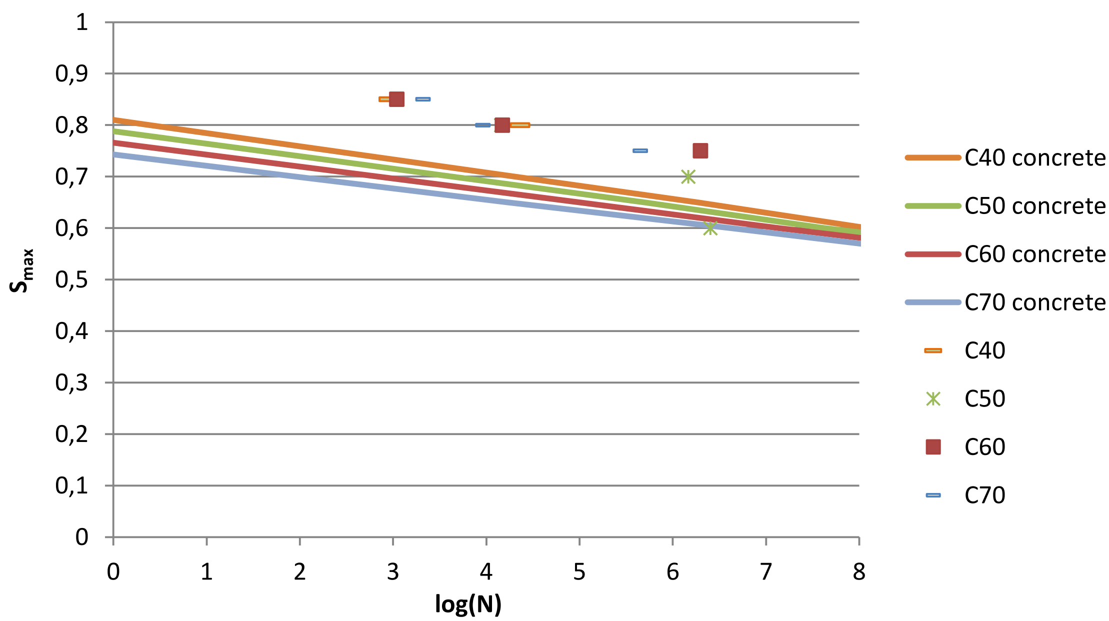

Fig. 56: Comparison between experiments with S_{min} = 0,4 and proposal.

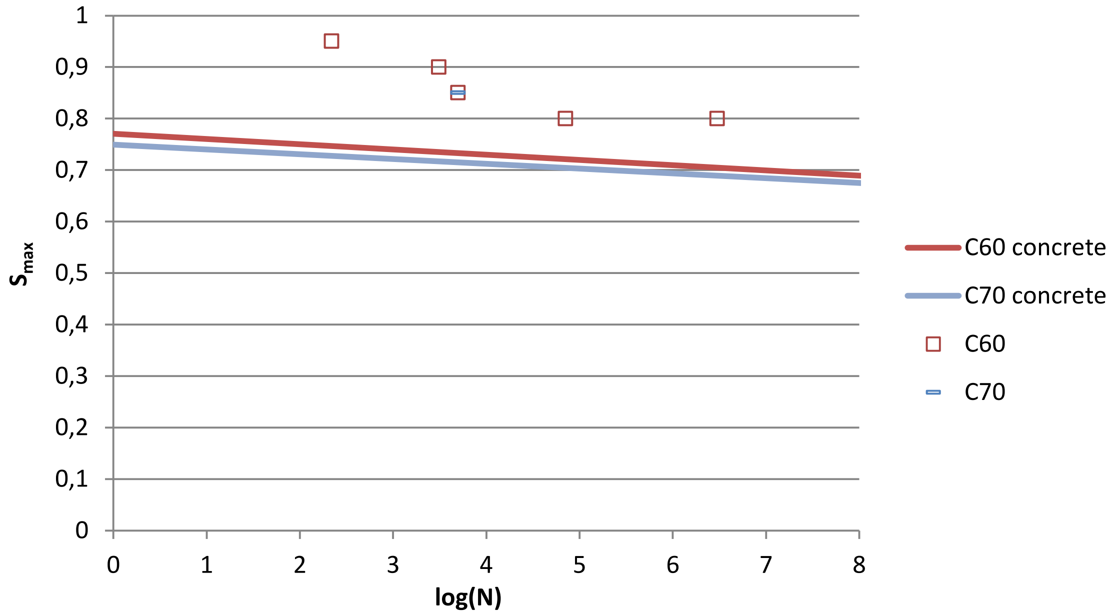

Fig. 57: Comparison between experiments with S_{min} = 0,6 and proposal.

In a next step, a direct comparison between the tested and predicted values is made to see if sufficient safety is built into the method. For this purpose, the calculated value of S_{max} for an experimentally found number of cycles N_i is determined. The value of R as found in the experiment is used, instead of being replaced by S_{max}/S_{min}. The value of S_{max} is then expressed as:

$$S_{max} = \left[\left(1-\frac{f_{ck}}{400}\right)-\frac{1}{6}\log N_i\left(1-0{,}57k_1\right)\left(1-\frac{f_{ck}}{400}\right)\sqrt{1-R_i}\right]\left[\frac{\gamma_{c,fat}}{\gamma_c}+\frac{\log N_i}{600\left(1-\frac{\gamma_{c,fat}}{\gamma_c}\right)}\right] \tag{46}$$

for $N_i \leq 10^6$

$$S_{max} = \frac{f_{cd,fat}}{f_{cd}}\left(1-\frac{1}{14}\log N_i\sqrt{1-R_i}\right) \text{ for } N_i > 10^6 \tag{47}$$

A total of 234 experiments from the database are used for the comparison. These 234 experiments are all experiments from the database on concrete without fibers. An average value of tested S_{max} over predicted S_{max} of 1,37 is found, with a standard deviation of 0,175 so that the coefficient of variation equals 12,8% and the characteristic value (5% lower bound based on a normal distribution) equals 1,081. Since the 5% lower bound is larger than 1, the method is considered safe and suitable for application in design. In comparison with the other proposal, the coefficient of variation is smaller in this proposal as the predicted values for the higher strengths of concrete are not as overly conservative as in the previous proposal. Therefore, this proposal is to be preferred.

5.3 Changing $\gamma_{c,fat}$

In the Dutch National Annex NEN-EN 1992-2+C1:2011/NB:2011, the value of γ_c = 1,5 is replaced by $\gamma_{c,fat}$ = 1,35. To find the static compressive strength for 1 cycle of loading, $S_{max} = f_{cd}/f_{cd}^*$ is the maximum value, with $f_{cd}^* = f_{ck}/\gamma_{c,fat}$ and $f_{cd} = f_{ck}/\gamma_c$. Since the value of $\gamma_{c,fat}$ is prescribed by the Dutch National Annex, the effect of this value is now studied. Moreover, the use of two different values for γ_c can be rather confusing, and therefore it might be advisable to use $\gamma_{c,fat} = \gamma_c$ = 1,5.

Table 14: S_{max} for different values of $\gamma_{c,fat}$

$\gamma_{c,fat}$	S_{max}
1,5	$1-\frac{f_{ck}}{250}$
1,35	$0,9\left(1-\frac{f_{ck}}{250}\right)$
1,2	$0,8\left(1-\frac{f_{ck}}{250}\right)$
1	$0,667\left(1-\frac{f_{ck}}{250}\right)$

When the proposal based on correcting NEN-EN 1992-2+C1:2011/NB:2011 is followed, Eqs. (32) to (37), the value of S_{max} at 1 cycle of loading becomes $S_{max} = \frac{\gamma_{c,fat}}{\gamma_c}$.

Thus, the value of S_{max} for 1 cycle can be calculated for different values of $\gamma_{c,fat}$ as shown in Table 14. After 10^6 cycles, the standard equation of NEN-EN 1992-2+C1:2011 needs to be followed, and for this equation, the influence of $\gamma_{c,fat}$ is only on the value of $f_{cd,fat}$ which depends on f_{cd}, where f_{cd} is $f_{cd}^* = f_{ck}/\gamma_{c,fat}$. The main influence of $\gamma_{c,fat}$ lies in the first branch of the *S-N* curve. The effect of $\gamma_{c,fat}$ can be seen by comparing the *S-N* curves for different values of $\gamma_{c,fat}$: Fig. 58 for $\gamma_{c,fat}$ = 1,35; Fig. 59 for $\gamma_{c,fat}$ = 1,2 and Fig. 60 for $\gamma_{c,fat}$ = 1,0. As can be seen from these figures, the approach becomes more conservative in terms of the relative maximum stress S_{max} for decreasing safety factors, because $\gamma_{c,fat}$ is used in de denominator. The change is most obvious in the first branch of the *S-N* curve, which becomes much flatter as $\gamma_{c,fat}$ decreases. Note that $S_{max} = \frac{\sigma_{max}}{\frac{f_{ck}}{\gamma_{c,fat}}}$, so that the resulting maximum stress (as an absolute value and not relative to f_{cd}) σ_{max} that can be obtained then becomes smaller for larger values of $\gamma_{c,fat}$.

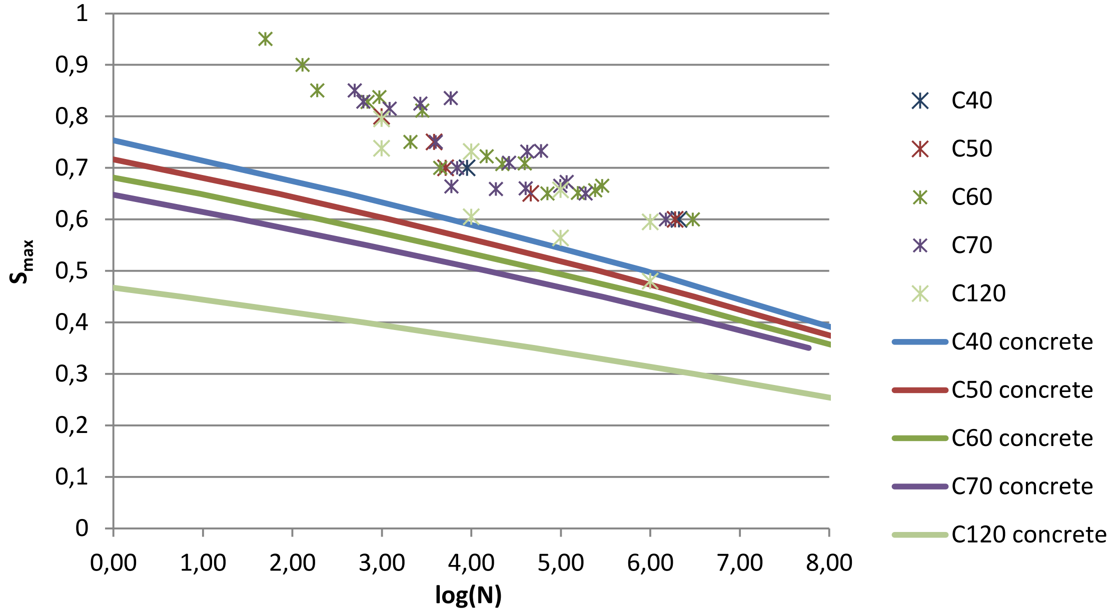

Fig. 58: S-N curves from the proposal from §5.1 with $\gamma_{c,fat}$ = 1,35 and S_{min} = 0,05.

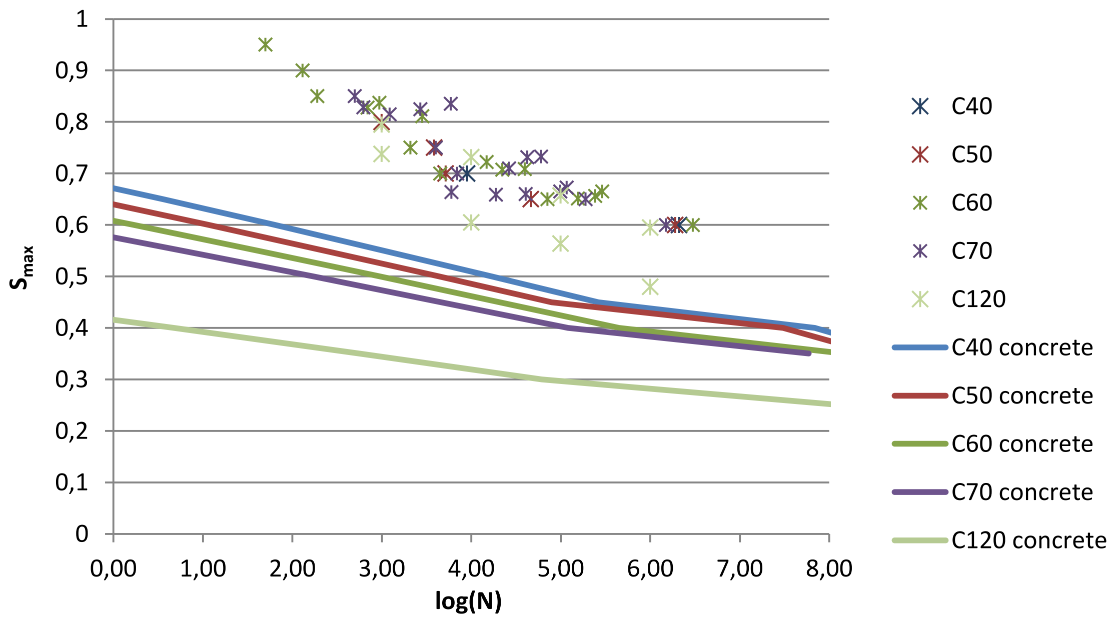

Fig. 59: S-N curves from the proposal from §5.1 with $\gamma_{c,fat}$ = 1,2 and S_{min} = 0,05.

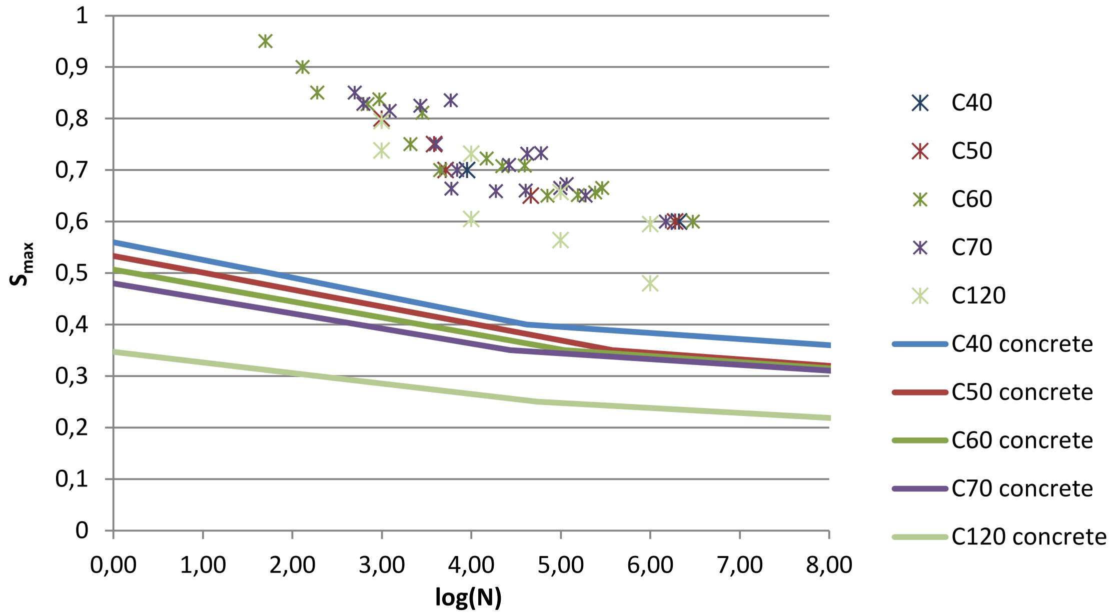

Fig. 60: S-N curves from the proposal from §5.1 with $\gamma_{c,fat}$ = 1,0 and S_{min} = 0,05.

For the case of $\gamma_{c,fat} = \gamma_c = 1{,}5$ the equations from the proposal, Eqs. (32) to (37), cannot be used anymore, as the term in the denominator of $\dfrac{\log N_i}{\left(1-\dfrac{\gamma_{c,fat}}{\gamma_c}\right)600}$ would result in dividing by zero. The expressions then should be replaced by:

$$\log N_i = \frac{6}{(1-0{,}57k_1)\left(1-\dfrac{f_{ck}}{250}\right)}\left(\frac{\left(1-\dfrac{f_{ck}}{250}\right)-E_{cd,max,i}}{\sqrt{1-R_i}}\right) \quad \text{for } N_i \le 10^6 \qquad (48)$$

with

$$E_{cd,max,i} = \frac{\sigma_{cd,max,i}}{f_{cd}} \quad \text{for } N_i \le 10^6 \qquad (49)$$

The expressions for the *S-N* curve for $N > 10^6$ cycles remain unchanged. Simplifying Eq. (48) results in:

$$\log N_i = \frac{14}{\sqrt{1-R_i}}\,\frac{\left(1-\dfrac{f_{ck}}{250}\right)-\dfrac{\sigma_{max}}{f_{cd}}}{1-\dfrac{f_{ck}}{250}} \qquad (50)$$

and this expression is the same as the Eurocode expression for $N_i > 10^6$ (here written for $k_1 = 1$ as prescribed by the Dutch National Annex). As such, it shows that one of the better solutions for the proposal would be to simply adopt the Eurocode expression, with $k_1 = 1$ and $\gamma_{c,fat} = \gamma_c = 1{,}5$. The resulting *S-N* curves can be seen in Fig. 61. The average value of S_{max} as tested to S_{max} as predicted is 1,45 with a standard deviation of 0,23 and a coefficient of variation of 15,8%. The characteristic value is then 1,075 and thus the approach is safe.

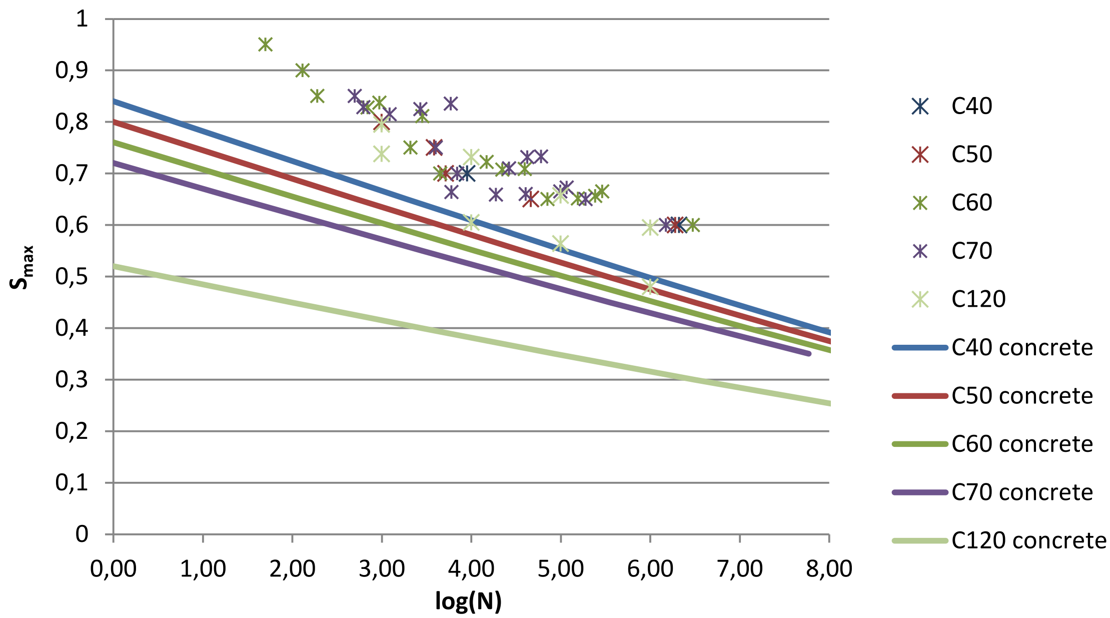

Fig. 61: S-N curves from EN 1992-2+C1:2011 with $\gamma_{c,fat} = 1{,}5$; $k_1 = 1$ and $S_{min} = 0{,}05$.

5.4 EC2-2 for high strength concrete

Since the expression from NEN-EN 1992-2+C1:2011 is easy to use and does not require iterations, it can easily be modified to become suitable for high strength concrete by replacing $f_{ck}/250$ with $f_{ck}/400$:

$$f_{cd,fat} = k_1 \beta_{cc}(t_0) f_{cd} \left(1 - \frac{f_{ck}}{400}\right) \tag{51}$$

$$N_i = 10^{\left(14 \frac{1-E_{cd,max,i}}{\sqrt{1-R_i}}\right)} \tag{52}$$

$$R_i = \frac{E_{cd,min,i}}{E_{cd,max,i}} \tag{53}$$

$$E_{cd,min,i} = \frac{\sigma_{cd,min,i}}{f_{cd,fat}} \tag{54}$$

$$E_{cd,max,i} = \frac{\sigma_{cd,max,i}}{f_{cd,fat}} \tag{55}$$

The comparison between the experiments and the improved recommendation from NEN-EN 1992-2+C1:2011 gives an average value of the tested to predicted S_{max} of 1,27 with a standard deviation of 0,139. The coefficient of variation is then 10,9% and the characteristic value is 1,044. The method is thus suitable for design. The graphical comparison between the experiments and the *S-N* curves is given in Fig. 62 for S_{min} = 0,05 and in Fig. 63, Fig. 64, Fig. 65, Fig. 66, Fig. 67 and Fig. 68 for the other values of S_{min}.

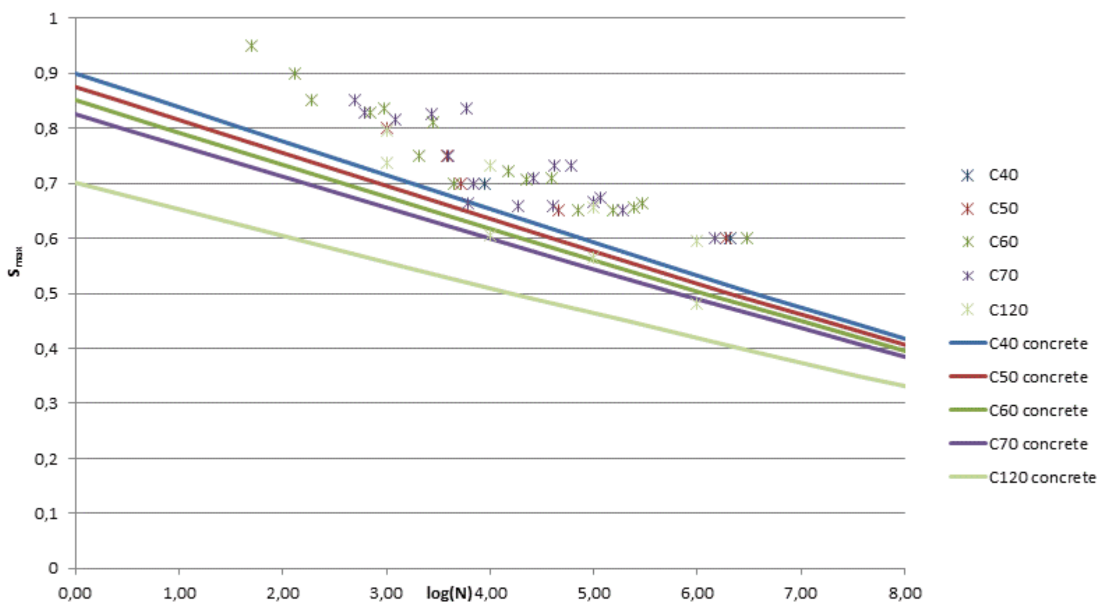

Fig. 62: S-N curves from the altered expression from EN 1992-2+C1:2011 with k_1 = 1 and S_{min} = 0,05.

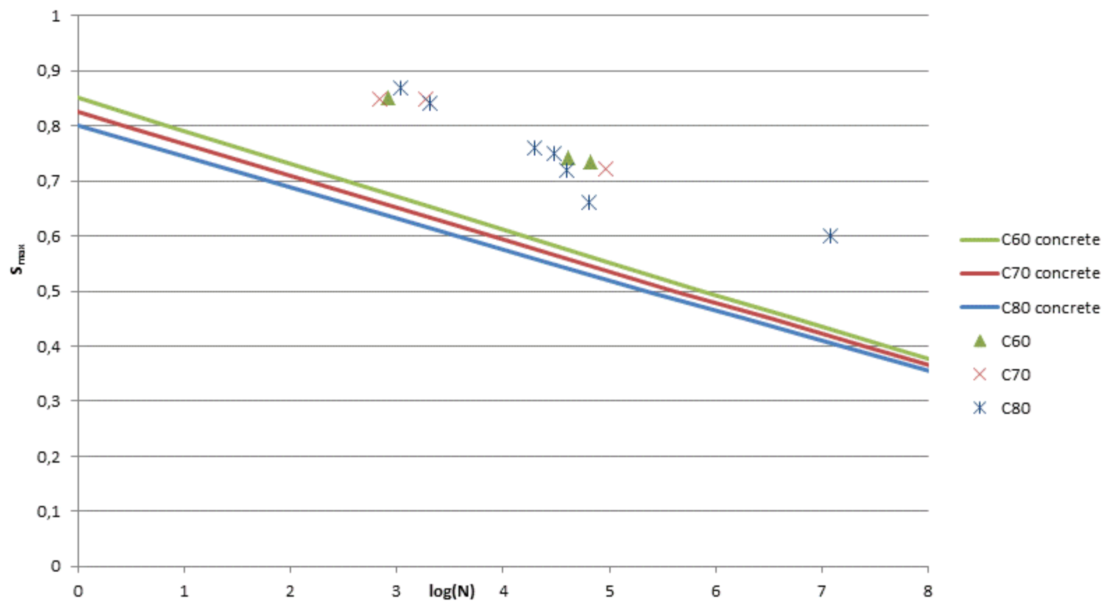

Fig. 63: S-N curves from the altered expression from EN 1992-2+C1:2011 with k_1 = 1 and S_{min} = 0,02.

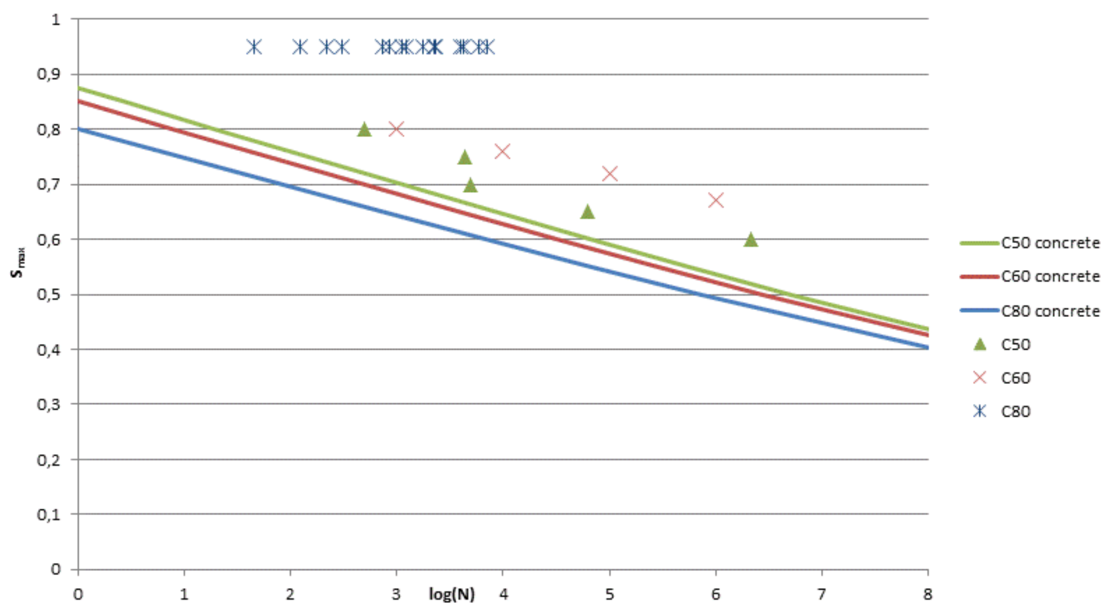

Fig. 64: S-N curves from the altered expression from EN 1992-2+C1:2011 with k_1 = 1 and S_{min} = 0,1.

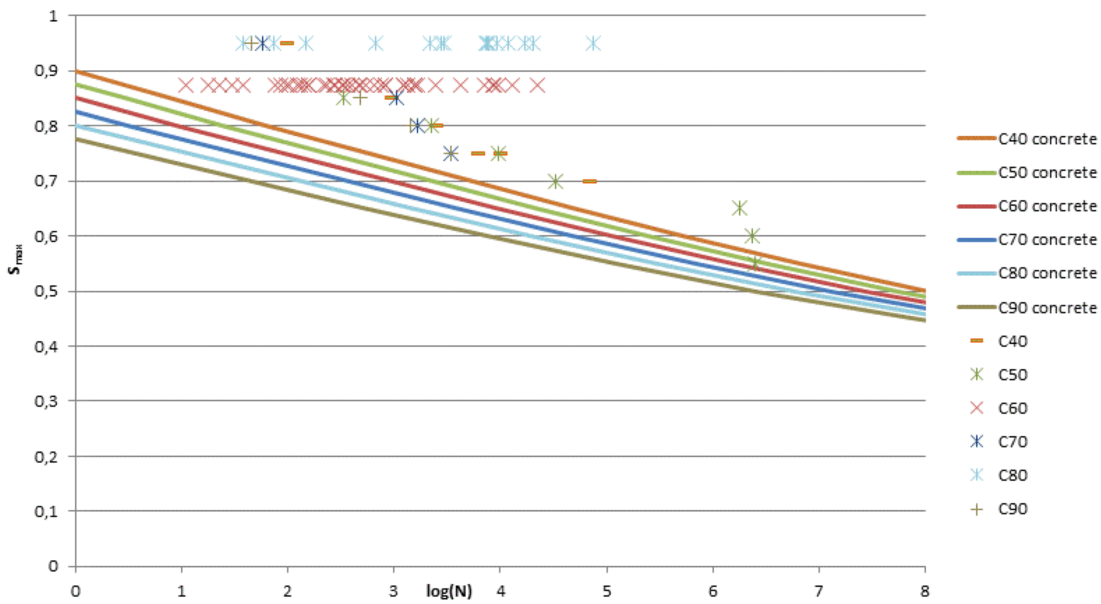

Fig. 65: S-N curves from the altered expression from EN 1992-2+C1:2011 with k_1 = 1 and S_{min} = 0,2.

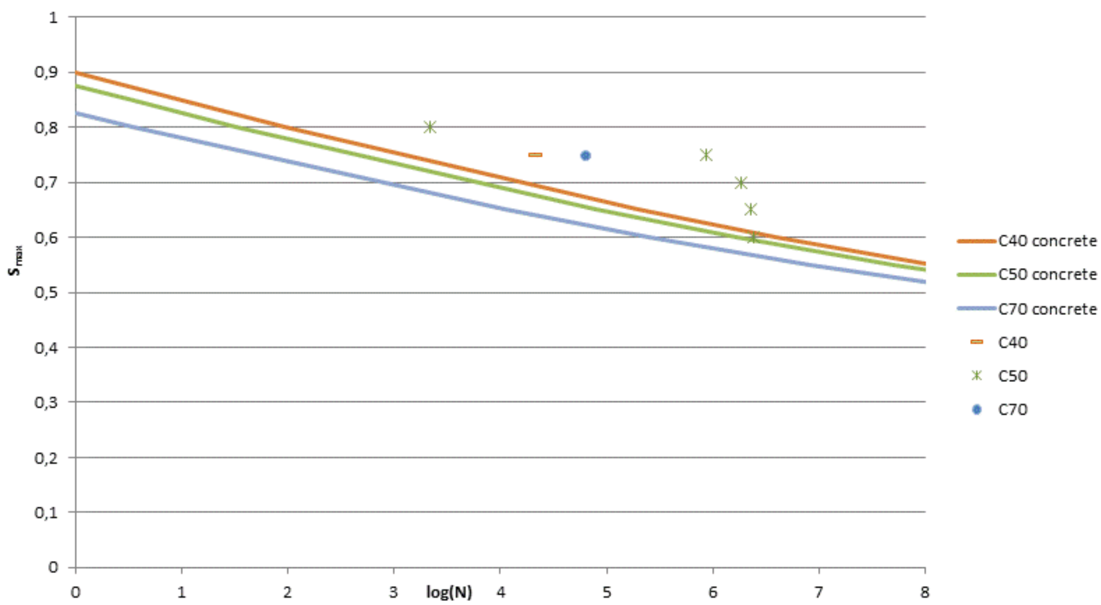

Fig. 66: S-N curves from the altered expression from EN 1992-2+C1:2011 with k_1 = 1 and S_{min} = 0,3.

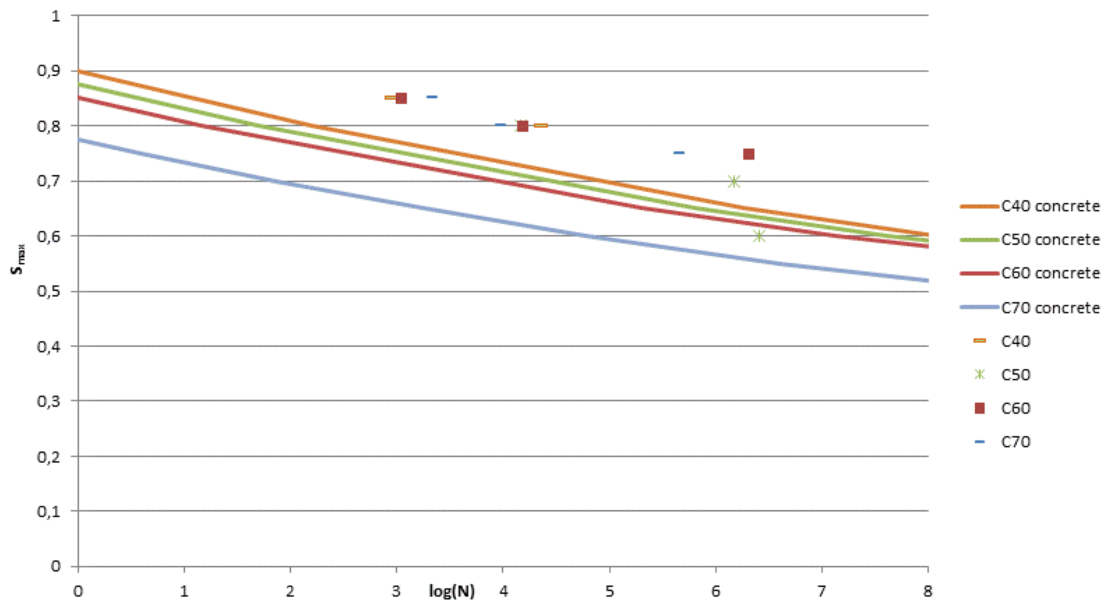

Fig. 67: S-N curves from the altered expression from EN 1992-2+C1:2011 with k_1 = 1 and S_{min} = 0,4.

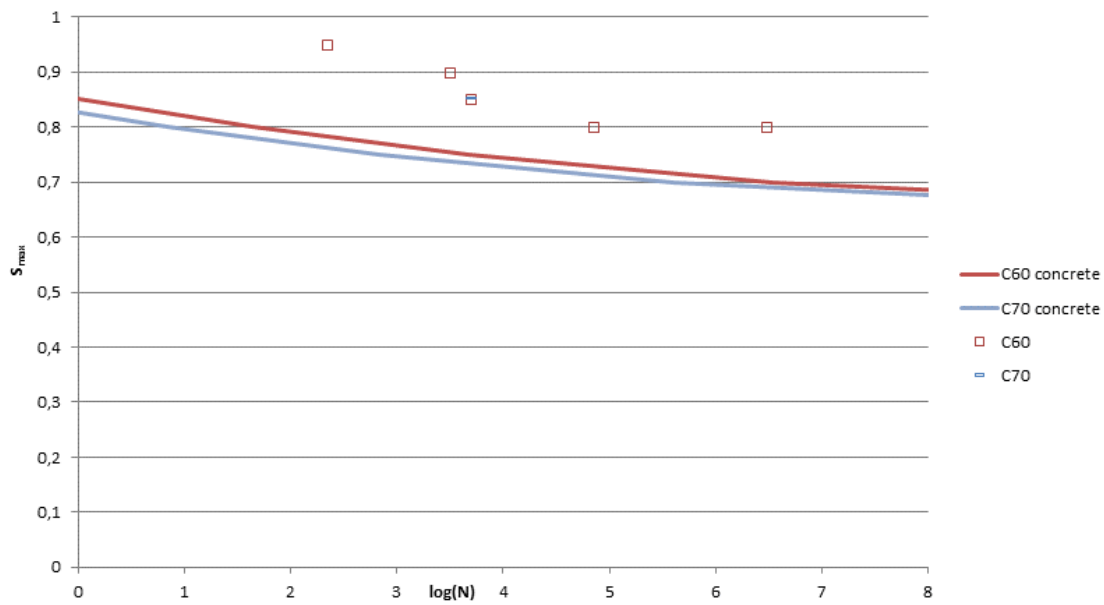

Fig. 68: S-N curves from the altered expression from EN 1992-2+C1:2011 with k_1 = 1 and S_{min} = 0,6.

5.5 Improved proposal for Dutch National Annex

As can be seen from Fig. 61, the first part of the *S*-*N* curve is rather conservative. It would be more logical to develop an expression for which S_{max} for 1 cycle equals 1, or, in other words, that for a single load repetition (ie. a static test), the static compressive strength can be found. However, it should be taken into account that the literature shows that the linear *S*-*N* curves are mostly valid starting for $\log N_i \approx 2$. A new approach is now followed to develop an expression for the first branch of the *S*-*N* curve, for $N_i \leq 10^6$ cycles. At 10^6 cycles, the formula should have a perfect fit with the expression from NEN-EN 1992-2+C1:2011, Eqs. (8) to (11). Using linear interpolation to describe the first branch of the *S*-*N* curve leads to the following expression:

$$\log N_i = \frac{6\left(S_{max} - 1\right)}{S_{max,EC} - 1} \qquad (56)$$

$S_{max,EC}$ is here the value of S_{max} which is found for 10^6 cycles, and can be expressed as:

$$S_{max,EC} = \left(1 - \frac{f_{ck}}{250}\right)\left(1 - \frac{3}{7}\sqrt{1 - R_i *}\right) \qquad (57)$$

with $R_i * = \dfrac{S_{min}}{S_{max,EC}}$. $S_{max,EC}$ can be found through an iterative procedure. Convergence is reached relatively fast, and typically 3 or 4 iterations are sufficient. To check if this procedure is sufficiently conservative, a comparison with the database of experiments is made. The predicted value for S_{max} is determined as:

$$S_{max} = \frac{S_{max,EC} - 1}{6} \log N_i + 1 \text{ for } N_i \leq 10^6 \qquad (58)$$

and $S_{max,EC}$ as given by Eq. (57). A comparison between the experimental results with S_{min} = 0,05 and the proposed *S*-*N* curves is found in Fig. 69. For other values of S_{min}, the comparison to the *S*-*N* curves can be found in Fig. 70, Fig. 71, Fig. 72, Fig. 73, Fig. 74 and Fig. 75 Comparing all results from the database to the proposal results in an average value of the tested to predicted S_{max} of 1,22 with a standard deviation of 0,155 and a coefficient of variation of 12,7%. The characteristic value based on a normal distribution is then 0,962 and based on a lognormal distribution 0,993. The histogram of the tested to predicted value of S_{max} is given in Fig. 76. The 5% lower bound of this measured distribution is 1,017 and since this value is larger than 1, the method is conservative enough for design.

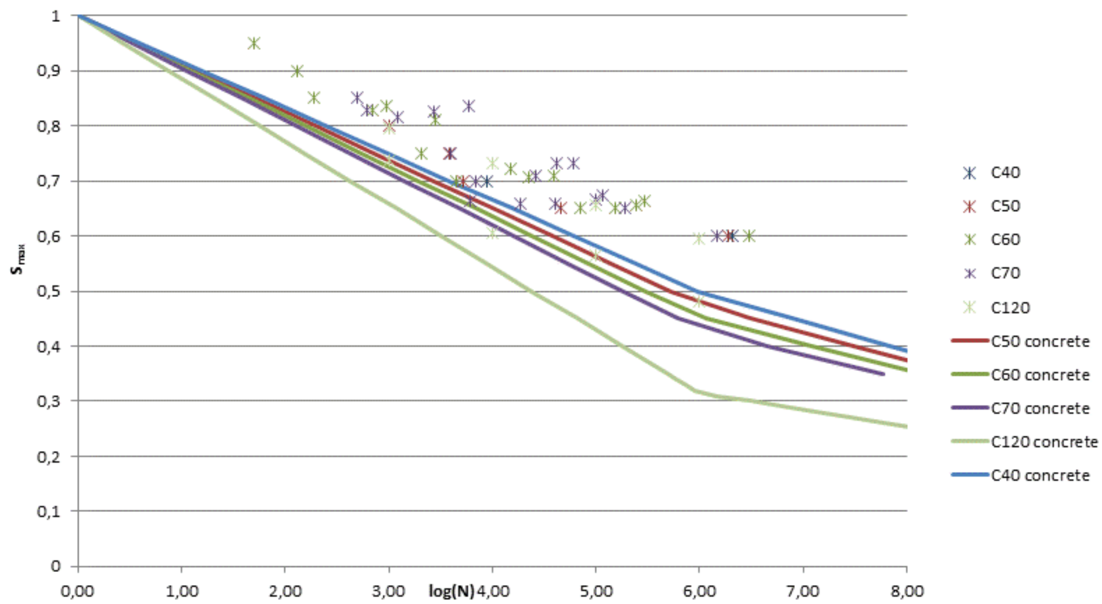

Fig. 69: Proposed S-N curves as compared to experiments with S_{min} = 0,05.

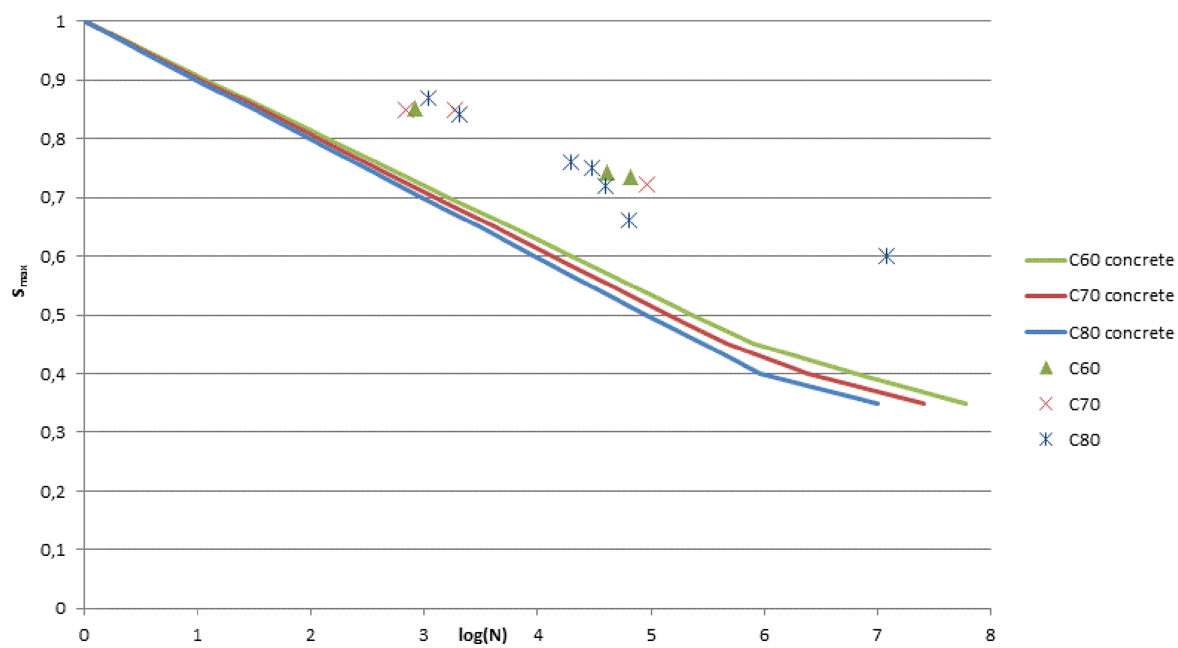

Fig. 70: Proposed S-N curves as compared to experiments with S_{min} = 0,02.

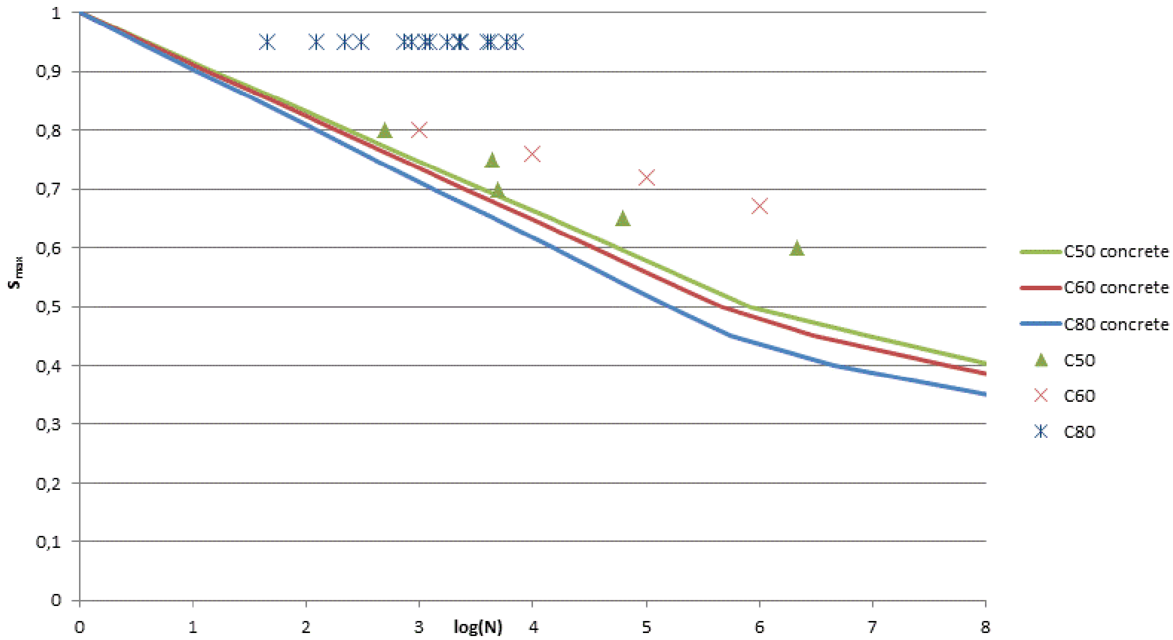

Fig. 71: Proposed S-N curves as compared to experiments with S_{min} = 0,1.

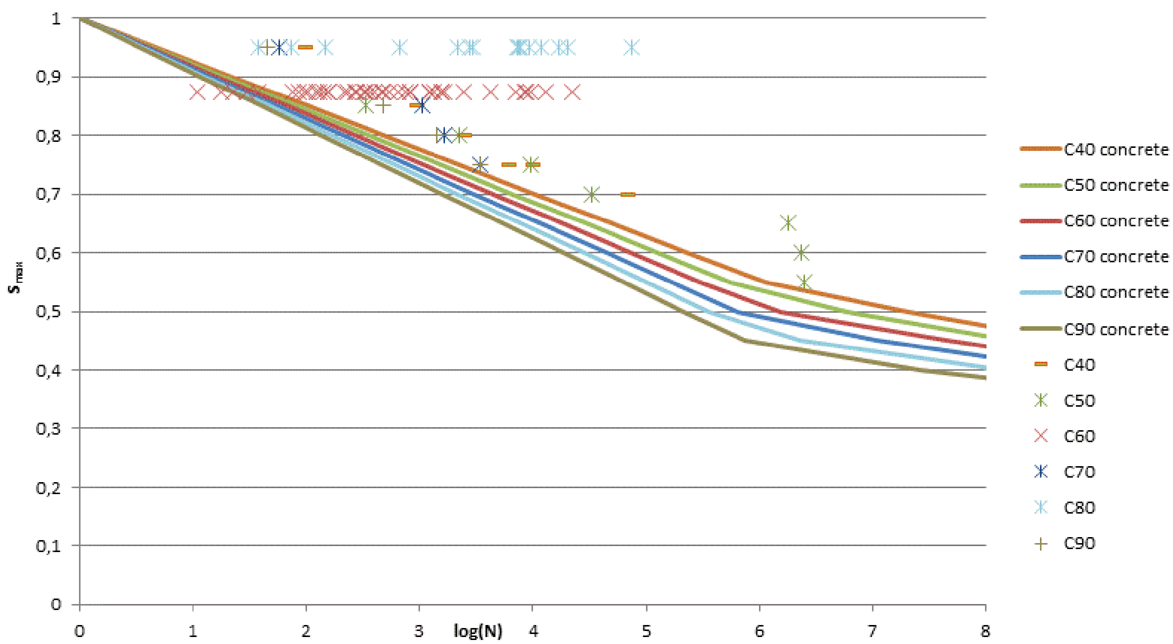

Fig. 72: Proposed S-N curves as compared to experiments with S_{min} = 0,2.

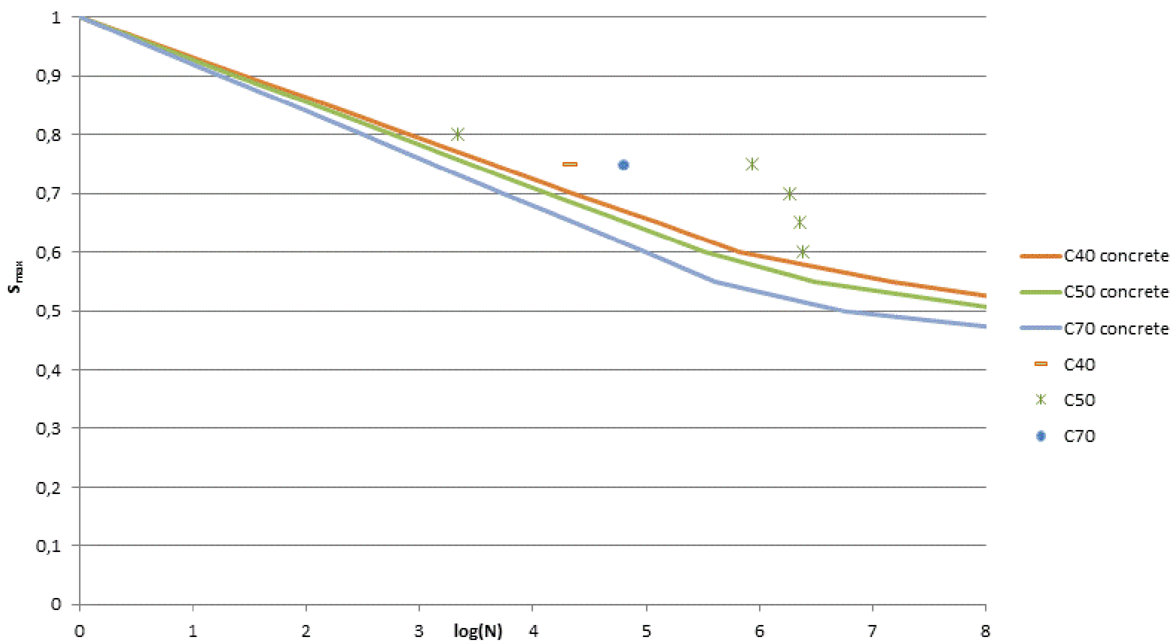

Fig. 73: Proposed S-N curves as compared to experiments with S_{min} = 0,3.

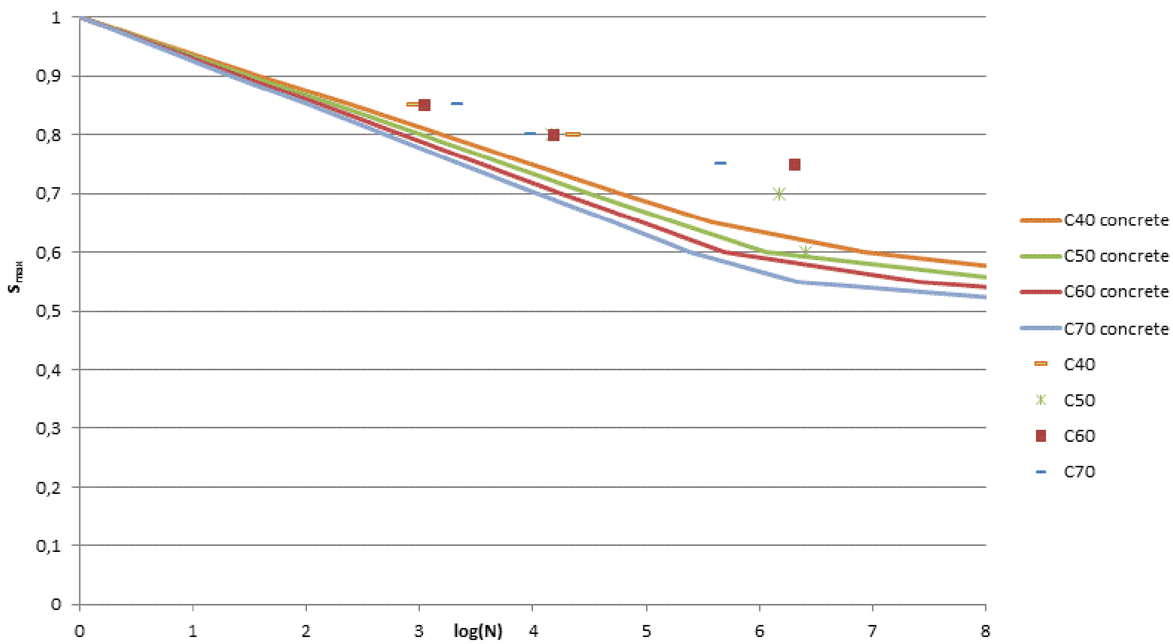

Fig. 74: Proposed S-N curves as compared to experiments with S_{min} = 0,4.

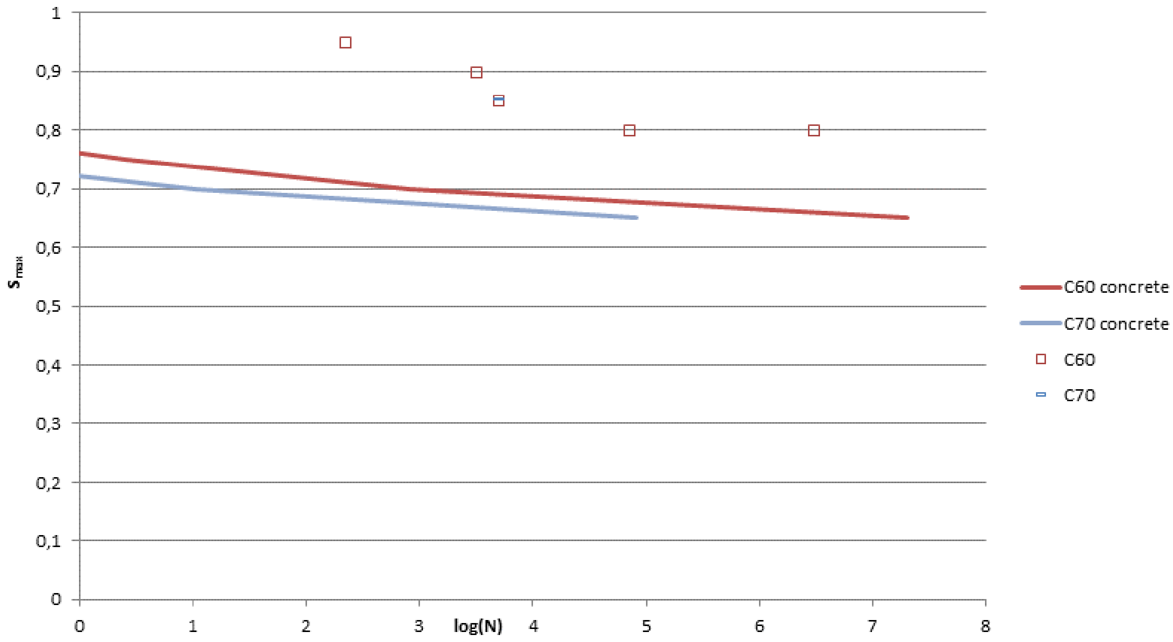

Fig. 75: Proposed S-N curves as compared to experiments with S_{min} = 0,6.

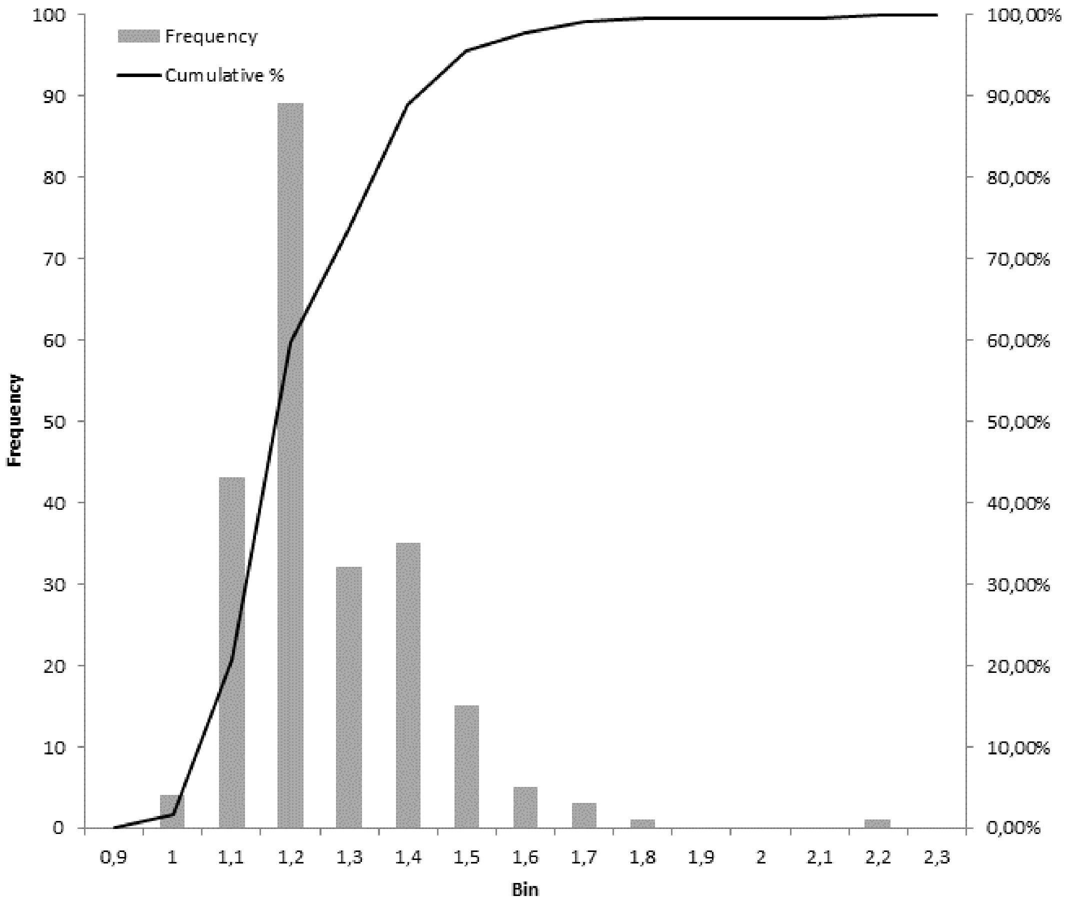

Fig. 76: Histogram of results of tested to predicted $S_{max.}$

5.6 Improved proposal suitable for higher concrete classes

In §5.2 it was shown that the conservatism of the code and proposal for the higher strength concrete classes can be reduced by modifying the reduction factor. This modification is now applied to the proposal, for which k_1 = 1 and $\gamma_{c,fat}$ = 1,5:

$$\log N_i = \frac{6\left(S_{max} - 1\right)}{S_{max,EC} - 1} \text{ for } N_i \leq 10^6 \tag{59}$$

$S_{max,EC}$ is here the value of S_{max} which is found for 10^6 cycles, and can be expressed as:

$$S_{max,EC} = \left(1 - \frac{f_{ck}}{400}\right)\left(1 - \frac{3}{7}\sqrt{1 - R_i*}\right) \tag{60}$$

with $R_i* = \frac{S_{min}}{S_{max,EC}}$, and

$$\log N_i = 14\frac{1 - E_{cd,max,i}}{\sqrt{1 - R_i}} \text{ for } N_i > 10^6 \tag{61}$$

$$E_{cd,max,i} = \frac{\sigma_{cd,max,i}}{f_{cd,fat}} \text{ for } N_i > 10^6 \tag{62}$$

with

$$f_{cd,fat} = f_{cd}\left(1 - \frac{f_{ck}}{400}\right) \tag{63}$$

A comparison between the experimental results with S_{min} = 0,05 and the proposed *S-N* curves is found in Fig. 77. Comparing all results from the database to the proposal results in an average value of the tested to predicted S_{max} of 1,15 with a standard deviation of 0,112 and a coefficient of variation of 9,7%. The characteristic value based on a normal distribution is then 0,965 and based on a lognormal distribution 0,979. The histogram of the tested to predicted value of S_{max} is given in Fig. 84. The 5% lower bound of this measured distribution is 1,004 and since this value is larger than 1, the method is conservative enough for design.

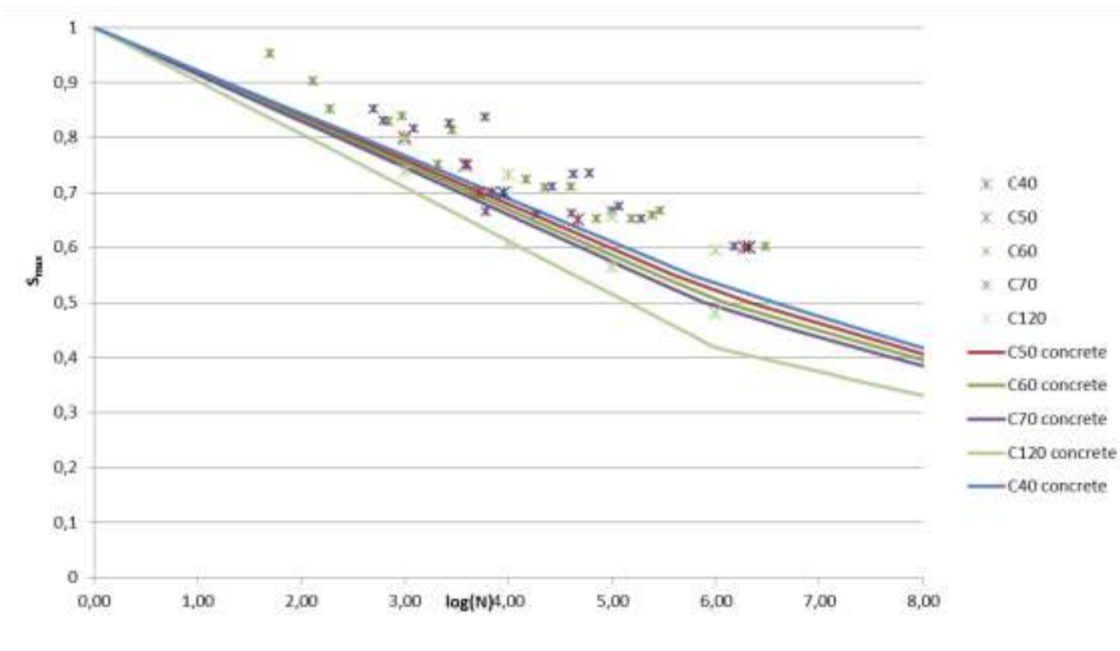

Fig. 77: Proposed S-N curves for higher strength concrete as compared to experiments with S_{min} = 0,05.

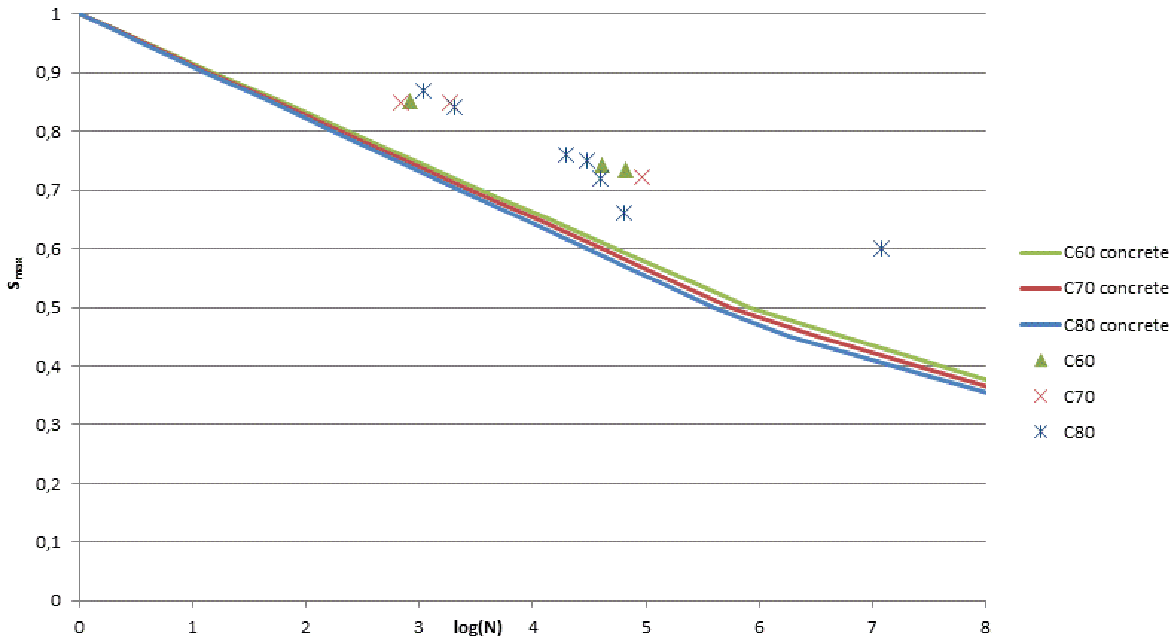

Fig. 78: Proposed S-N curves for higher strength concrete as compared to experiments with S_{min} = 0,02.

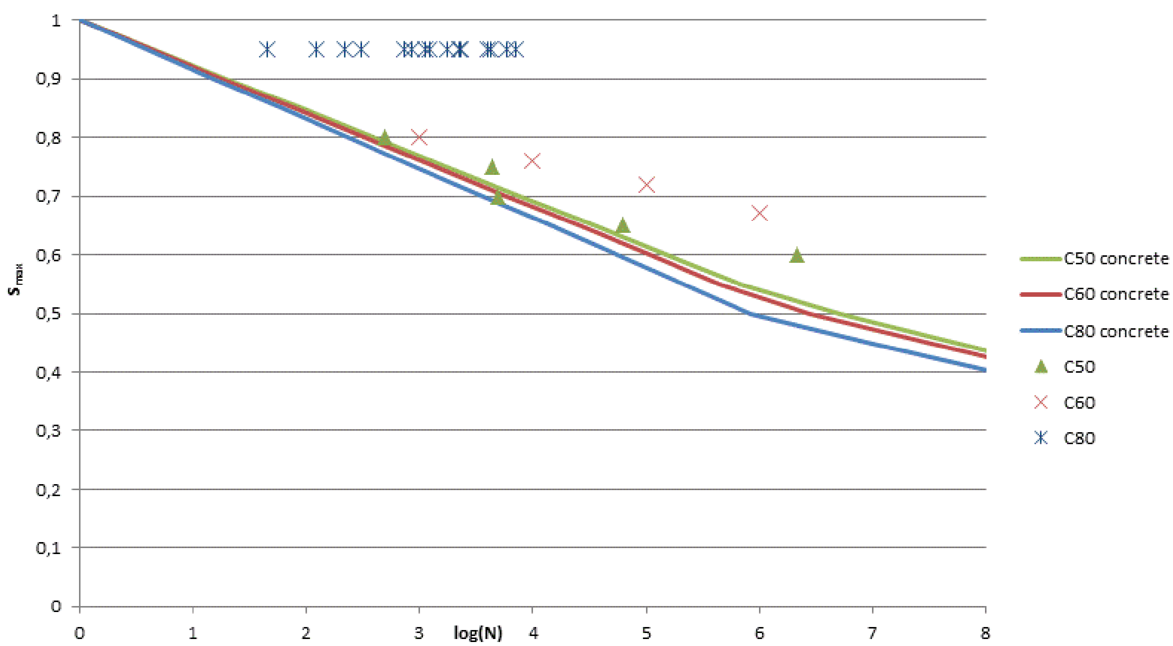

Fig. 79: Proposed S-N curves for higher strength concrete as compared to experiments with S_{min} = 0,1.

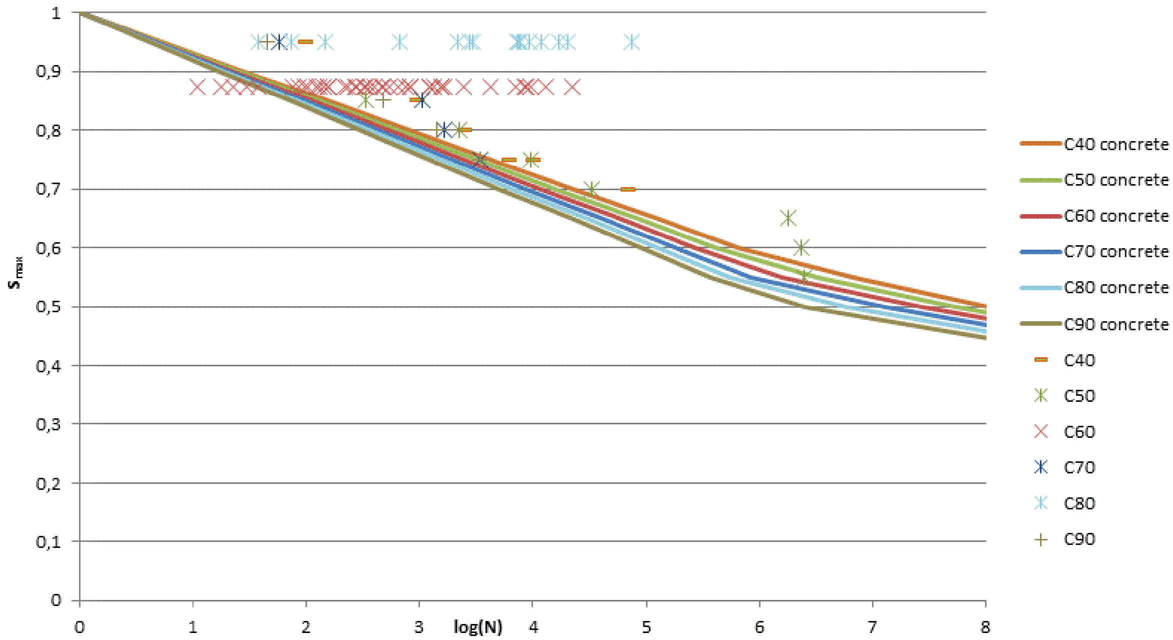

Fig. 80: Proposed S-N curves for higher strength concrete as compared to experiments with S_{min} = 0,2.

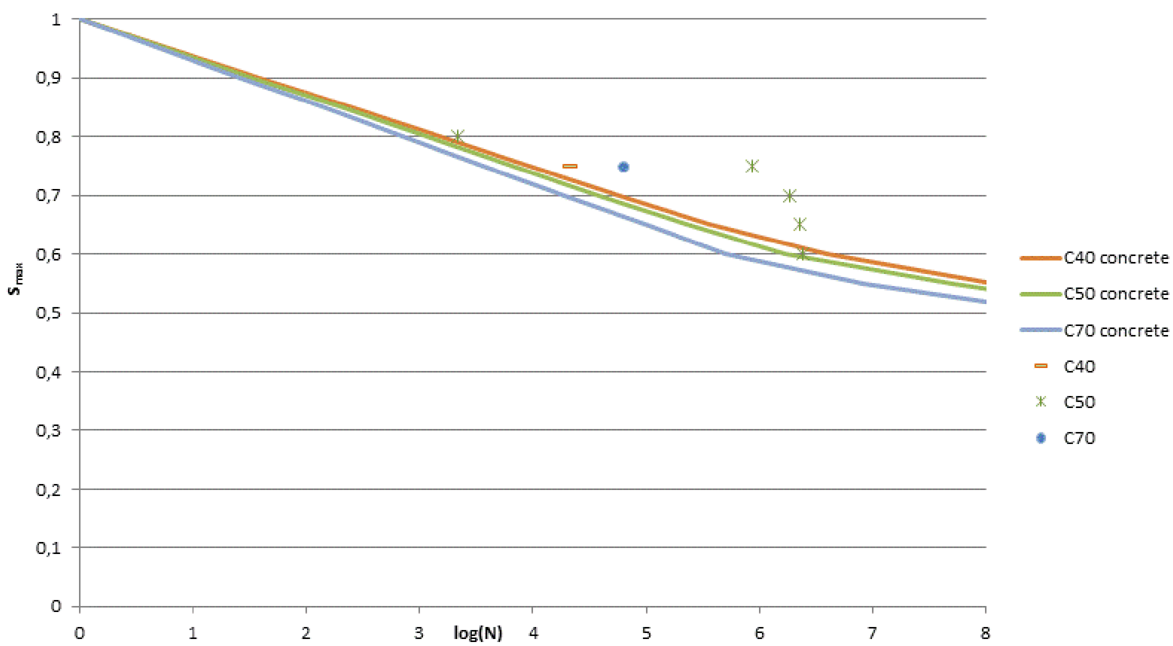

Fig. 81: Proposed S-N curves for higher strength concrete as compared to experiments with S_{min} = 0,3.

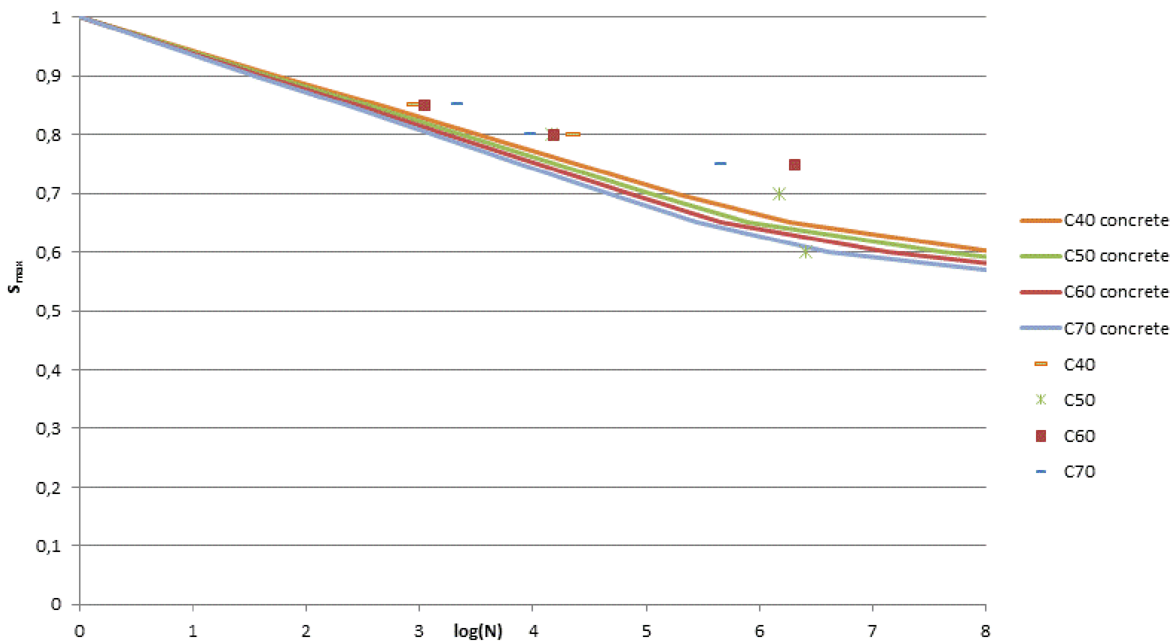

Fig. 82: Proposed S-N curves for higher strength concrete as compared to experiments with S_{min} = 0,4.

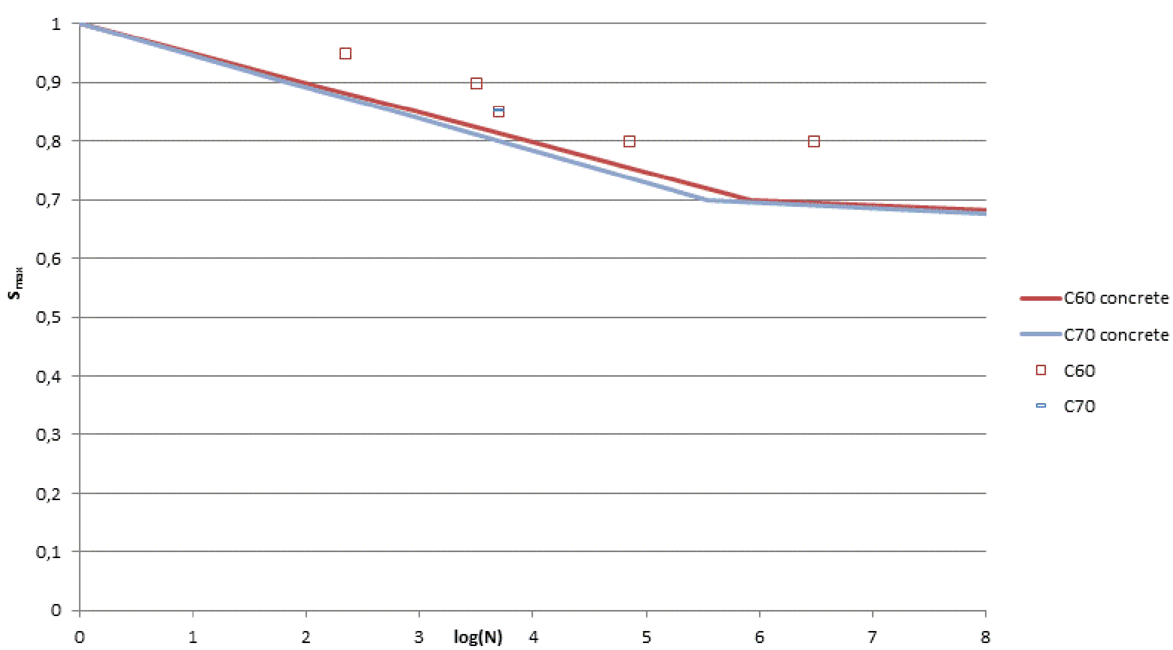

Fig. 83: Proposed S-N curves for higher strength concrete as compared to experiments with S_{min} = 0,6.

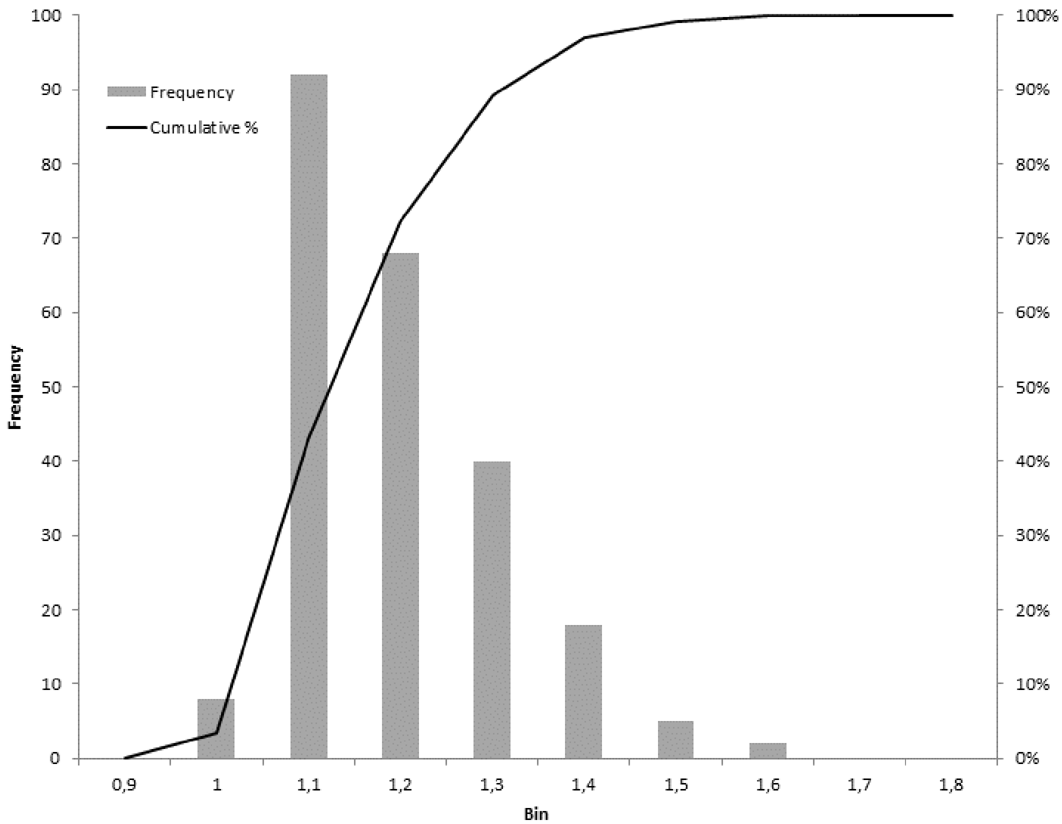

Fig. 84: Histogram of results of tested to predicted $S_{max.}$

5.7 Comparison between methods

An overview of the statistical parameters for the different methods is given in Table 15. The method with the best prediction is the new proposal, suitable for high strength concrete, as detailed in §5.6. This method gives the smallest coefficient of variation, which indicates the least scatter on the predicted values as compared to the experimental results. In all cases, replacing $f_{ck}/250$ by $f_{ck}/400$ results in a better correspondence between the prescribed *S-N* curves and the experimental results, as reflected by the lower values for the coefficient of variation for all proposals denoted "HSC" (meaning adjusted to take high strength concrete into account). For the last two rows, in which the results for the new proposal are given, the 5% lower bound is determined based on the assumption of a normal distribution ("Char") as well as based on the 5% lower bound in the histogram with the results of tested to predicted values for S_{max} ("5%"). Since the real distribution of these results does not follow a normal distribution, a more conservative 5% lower bound is seen when a normal distribution is assumed, and therefore checking based on the real distribution can be used, and –as can be seen in Table 15 – leads to satisfactory results for the new proposal.

Table 15: Overview of the statistical parameters from the different methods

Method	**§**	$\gamma_{c,fat}$	**AVG**	**STD**	**COV**	**Char**	**5%**
NB_corr	5.1	1,35	1,56	0,275	17,6%	1,11	
NB_corr + HSC	5.2	1,35	1,37	0,175	12,8%	1,081	
EC, k_1 = 1	5.3	1,5	1,45	0,230	15,8%	1,075	
EC, k_1 = 1, HSC	5.4	1,5	1,27	0,139	10,9%	1,044	
Proposal	5.5	1,5	1,22	0,155	12,7%	0,962	1,017
Proposal + HSC	5.6	1,5	1,15	0,112	9,7%	0,965	1,004

Table 16: Overview of the statistical parameters from the different methods for C60 concrete

Method	**§**	$\gamma_{c,fat}$	**AVG**	**STD**	**COV**	**Char**	**5%**
NB_corr	5.1	1,35	1,534	0,116	7,5%	1,344	
NB_corr + HSC	5.2	1,35	1,349	0,100	7,4%	1,184	
EC, k_1 = 1	5.3	1,5	1,422	0,081	5,7%	1,289	
EC, k_1 = 1, HSC	5.4	1,5	1,250	0,071	5,6%	1,135	
Proposal	5.5	1,5	1,162	0,116	10%	0,971	0,988
Proposal + HSC	5.6	1,5	1,108	0,084	7,6%	0,970	0,976

In a next step, the comparison is carried out for the separate concrete classes for which sufficient test results are available. For C60 concrete, there are 70 experimental results for specimens without fibers. The results are shown in Table 16. For C70 concrete, there are 28 experimental results. The results are given in Table 17. For C70 concrete, there are 37 experimental results. The results are given in Table 18. Most of the results that have a value of the tested to predicted value for S_{max} of less than 1 are found in the experiments by Saucedo et al. (2013), for C2 concrete (identified as class C60). These experiments were carried out on specimens that were not cylinders, but instead cubes with a side of 100mm. When these results are omitted from the analysis, 28 test results remain for C60 concrete. The results are then shown in Table 19, showing that a characteristic value of larger than 1 can be obtained when the results of the cube specimens by Saucedo et al. (2013) are eliminated from the analysis. Finally, to see if the conservatism of the method increases for increasing concrete compressive strengths, the results of these tables are graphically represented in Fig. 85 (all results) and Fig. 86 (results without C2 results) for the average values of the tested to predicted S_{max}, and in Fig. 87 (all results) and Fig. 88 (results without C2 results) for the characteristic values of the tested to predicted S_{max}.

Table 17: Overview of the statistical parameters from the different methods for C70 concrete

Method	**§**	$\gamma_{c,fat}$	**AVG**	**STD**	**COV**	**Char**	**5%**
NB_corr	5.1	1,35	1,472	0,076	5,2%	1,347	
NB_corr + HSC	5.2	1,35	1,279	0,067	5,2%	1,170	
EC, k_1 = 1	5.3	1,5	1,437	0,075	5,2%	1,314	
EC, k_1 = 1, HSC	5.4	1,5	1,249	0,065	5,2%	1,141	
Proposal	5.5	1,5	1,207	0,101	8,4%	1,041	1,070
Proposal + HSC	5.6	1,5	1,129	0,074	6,6%	1,007	

Table 18: Overview of the statistical parameters from the different methods for C80 concrete

Method	**§**	$\gamma_{c,fat}$	**AVG**	**STD**	**COV**	**Char**	**5%**
NB_corr	5.1	1,35	1,977	0,168	8,5%	1,701	
NB_corr + HSC	5.2	1,35	1,654	0,134	8,1%	1,435	
EC, k_1 = 1	5.3	1,5	1,794	0,140	7,8%	1,565	
EC, k_1 = 1, HSC	5.4	1,5	1,501	0,110	7,3%	1,320	
Proposal	5.5	1,5	1,373	0,140	10,2%	1,142	1,174

Proposal + HSC	5.6	1,5	1,285	0,106	8,2%	1,111	

Table 19: Overview of the statistical parameters from the different methods for C60 concrete, without the C2 results from Saucedo et al. (2013)

Method	**§**	$\gamma_{c,fat}$	**AVG**	**STD**	**COV**	**Char**	**5%**
NB_corr	5.1	1,35	1,451	0,071	4,9%	1,335	
NB_corr + HSC	5.2	1,35	1,281	0,066	5,2%	1,172	
EC, $k_1 = 1$	5.3	1,5	1,403	0,056	4,0%	1,312	
EC, $k_1 = 1$, HSC	5.4	1,5	1,238	0,050	4,0%	1,156	
Proposal	5.5	1,5	1,209	0,107	8,8%	1,034	
Proposal + HSC	5.6	1,5	1,129	0,069	6,1%	1,016	

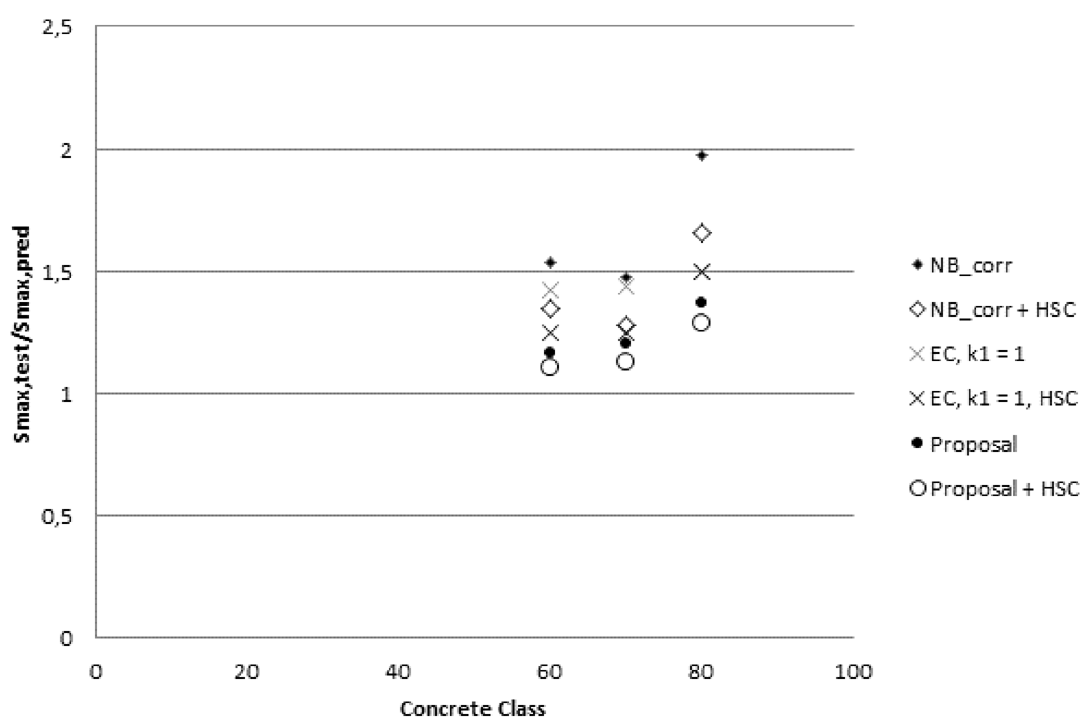

Fig. 85: Comparison between unity checks (average value) for different concrete classes

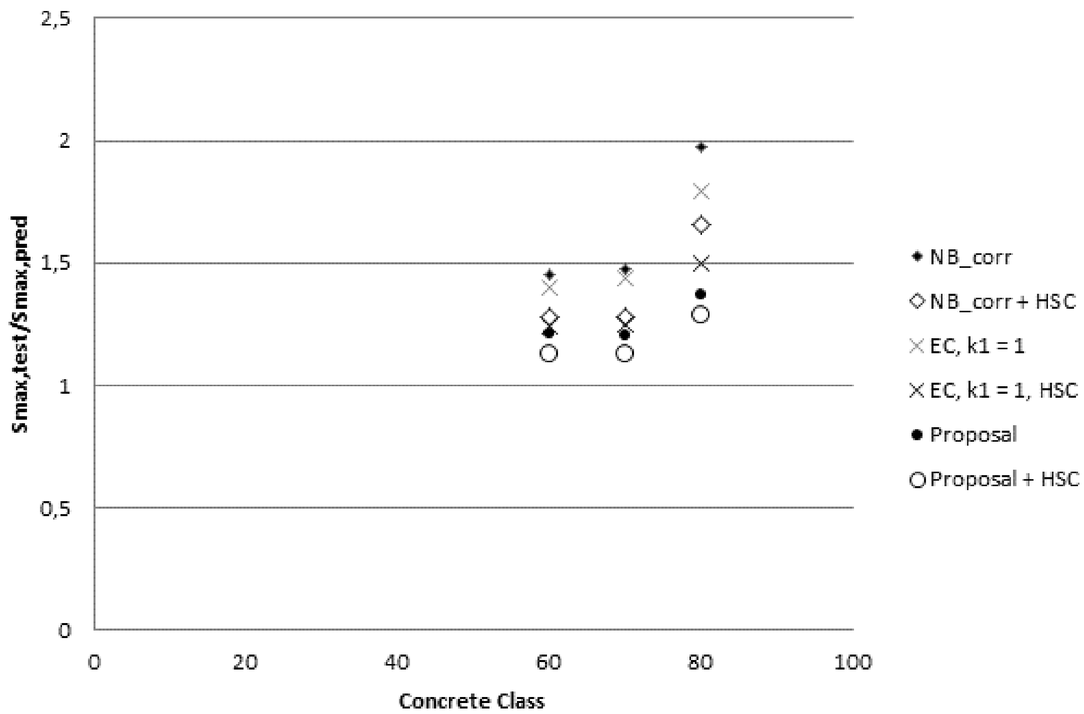

Fig. 86: Comparison between unity checks (average value) for different concrete classes, without the C2 results from Saucedo et al. (2013) for C60 concrete.

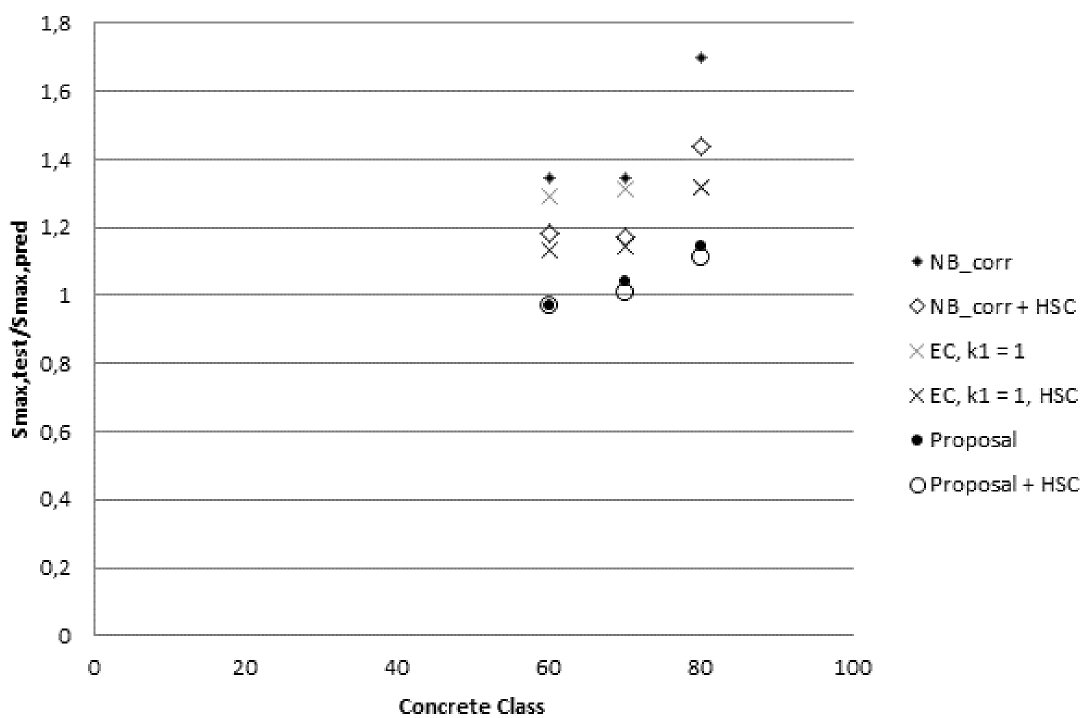

Fig. 87: Comparison between unity checks (characteristic value) for different concrete classes

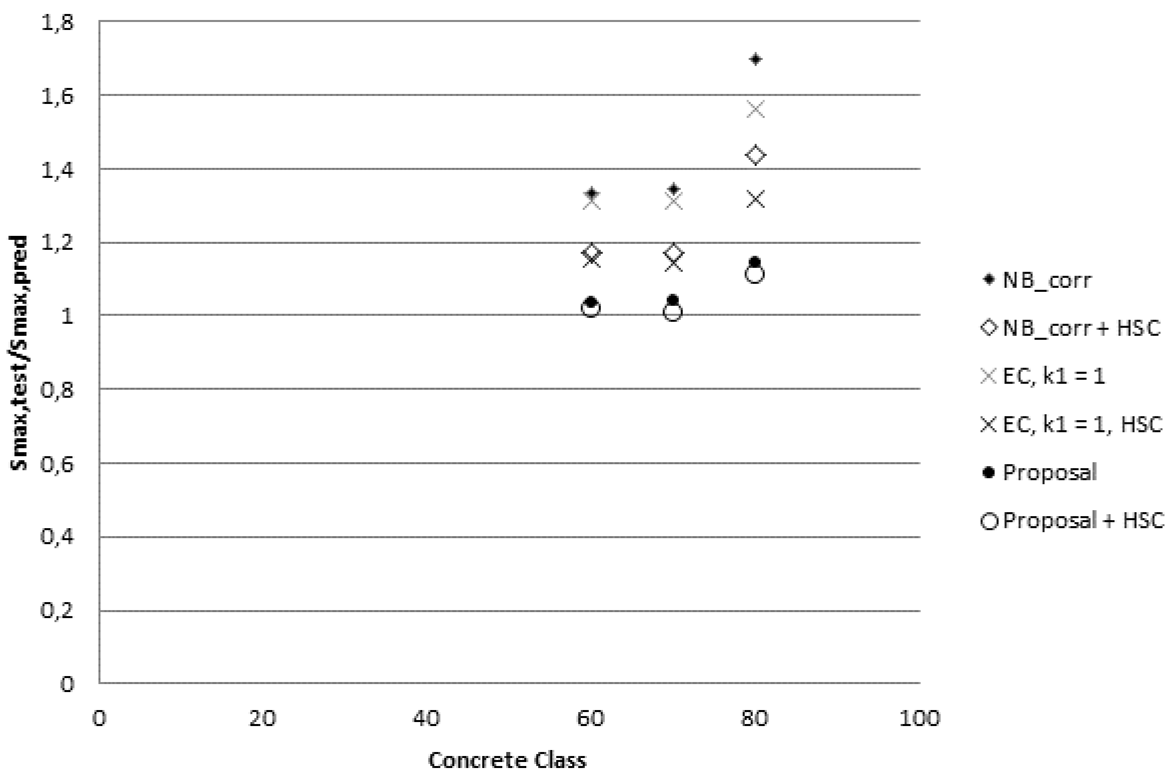

Fig. 88: Comparison between unity checks (characteristic value) for different concrete classes, without the C2 results from Saucedo et al. (2013) for C60 concrete.

All previous comparisons were based on S_{max}, which is a dimensionless unit, in which the maximum stress σ_{max} is divided by f_{cd}. A final overview is based on $\sigma_{max,}$ Fig. 89. From this figure, the following observations can be made:

- The effect of $\gamma_{c,fat}$ is mostly noticeable in the range of > 10^6 cycles, as can be seen from the results of "NB_corr" and "NB_corr, HSC" as compared to the approaches that use $\gamma_c = \gamma_{c,fat}$ = 1,5.
- The original Dutch National Annex "EC2-2 + NB" and the new proposal all are based on reaching the static compressive strength for a single load cycle (based on γ_c = 1,5).
- The original EC2-2 approach is on the conservative side.

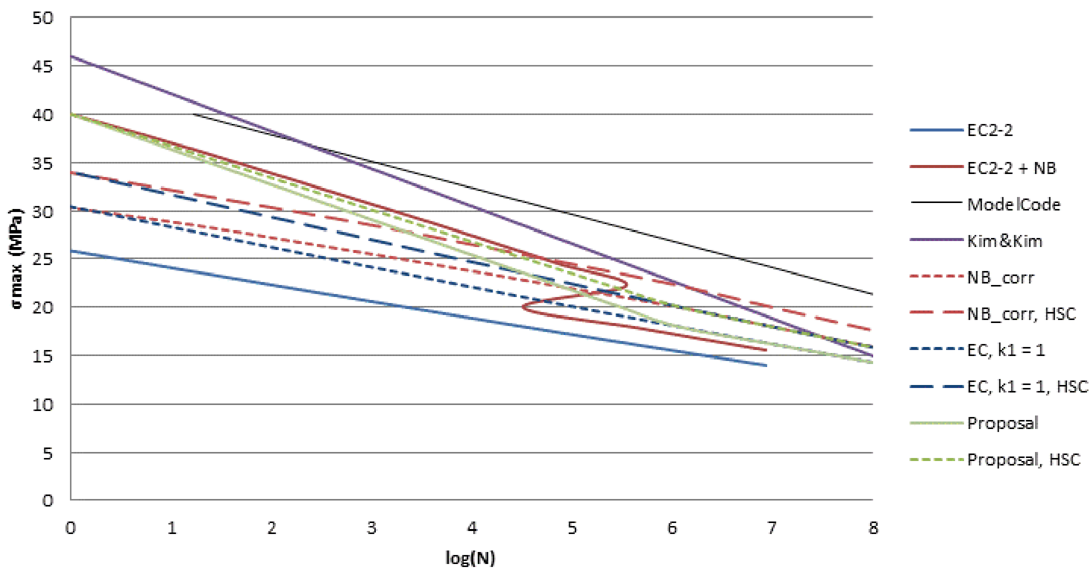

Fig. 89: Comparison between the different methods in terms of design maximum stresses.

5.8 Validation with normal strength concrete

In a final step, to check if the recommendations can be used for normal strength concrete as well, and can be used in the codes as generally applicable methods, a verification with a separate database of experiments on normal strength concrete is used. The experimental results from this database are given in Annex 2. These results are from Darmstadt (Klausen, 1978). Since these tests are on normal strength concrete, they are not discussed in Chapter 4 of this report. Only the experiments with a constant amplitude are used, the experiments with a variable amplitude are not considered. The specimens were cylinders with a diameter of 50mm and a height of 100mm.

Table 20: Overview of the statistical parameters from the different methods for the experiments from Klausen (1978).

Method	**§**	$\gamma_{c,fat}$	**AVG**	**STD**	**COV**	**Char**	**5%**
EC, k_1 = 1	5.3	1,5	1,297	0,142	10,9%	1,065	
EC, k_1 = 1, HSC	5.4	1,5	1,220	0,133	10,9%	1,002	
Proposal	5.5	1,5	1,187	0,152	12,8%	0,938	0,967
Proposal + HSC	5.6	1,5	1,144	0,132	11,5%	0,928	0,957

The results in Table 23 show that the Eurocode approaches with k_1 = 1 are suitable for the design for normal strength concrete. The influence of the term f_{ck}/250 or f_{ck}/400 is small, as can be seen when comparing the results of "EC, k_1 = 1" and "EC, k_1 = 1, HSC". The results in Table 20 have a larger scatter than when analyzing the database of high strength concrete, even though these test results are only from a single source. For experiments with a set value for S_{min} and S_{max} a number of cycles between 100 and 10^7 was found, which results in the large scatter from this dataseries. This conclusion is shown graphically in Fig. 90. As a result of this higher scatter, the 5% lower bound is relatively farther away from the average value of the tested to predicted value of S_{max}. For the prediction based on the proposal, the characteristic value based on the normal distribution and based on histogram of the values of the tested to predicted S_{max} becomes slightly smaller than 1.

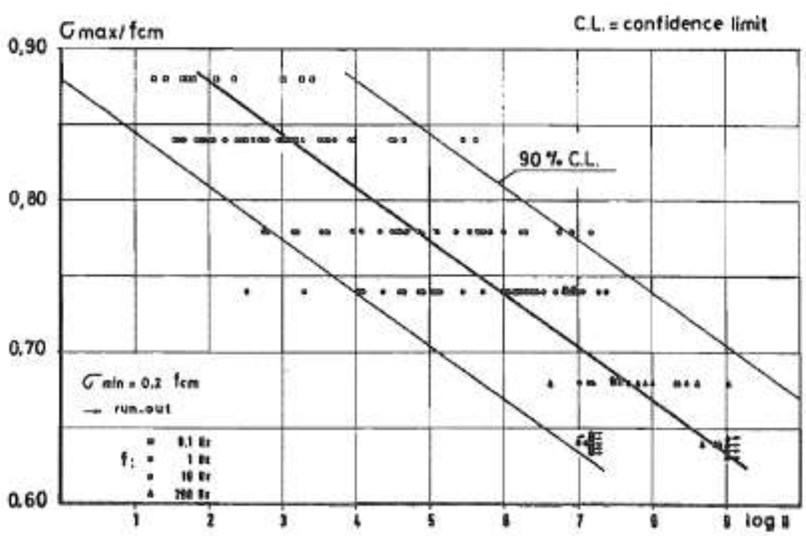

Fig. 90: Large scatter on the results by Klausen (1978).

Since the scatter on the experiments by Klausen is rather large, additional experiments are sought in the literature. Results by Assimacopoulos et al., as cited by Hsu (1981) are used, as well as results by Tepfers and Kutti (1979). These experimental results have been added to the database for normal strength concrete, Annex 2. The experiments by Tepfers and Kutti were carried out on 300mmcylinders with a concrete compressive strength of 45,4MPa and a stress ratio R = 0,2. The experiments by Assimacopoulos were carried out with a frequency of 150 Hz, and the specimens were cylinders of 51 by 102mm. Normal weight concrete with fc' = 41 MPa was used. The geometric average of 5 experiments is used for the reported S-N curve from which the datapoints are read. The results of the comparison between these experimental results and the proposals are shown in Table 21. Next, the results by Klausen are added to this database. For the first two series of experiments, the geometric mean of the data is used. While taking this approach means that some of the inherent uncertainty and variability on the model is lost, it is necessary to have a balanced database. In other words, having 39 results from the first series and 35 from the second series makes that the weight of these experiments becomes relatively larger, as for the next 13 series only the average of a number of experiments is reported. By using the average in the first and second series, all results in the database are averaged values, and we are not comparing different types of results. The results of this database are then given in *Table 22*. It can be seen that the proposal leads to satisfactory results.

Table 21: Overview of the statistical parameters from the different methods for the experiments from Hsu (1981) and Tepfers and Kutti (1979)

Method	**§**	$\gamma_{c,fat}$	**AVG**	**STD**	**COV**	**Char**	**5%**
EC, k_1 = 1	5.3	1,5	1,291	0,062	4,8%	1,190	
EC, k_1 = 1, HSC	5.4	1,5	1,212	0,063	5,2%	1,109	
Proposal	5.5	1,5	1,206	0,102	8,5%	1,039	
Proposal + HSC	5.6	1,5	1,135	0,081	7,1%	1,002	

Table 22: Overview of the statistical parameters from the different methods for the experiments from Hsu (1981) and Tepfers and Kutti (1979) and Klausen (1978)

Method	**§**	$\gamma_{c,fat}$	**AVG**	**STD**	**COV**	**Char**	**5%**
EC, k_1 = 1	5.3	1,5	1,293	0,086	6,7%	1,151	
EC, k_1 = 1, HSC	5.4	1,5	1,215	0,084	6,9%	1,077	
Proposal	5.5	1,5	1,198	0,106	8,8%	1,025	
Proposal + HSC	5.6	1,5	1,137	0,086	7,5%	0,996	1,003

5.9 Validation with normal strength concrete tested under water

In a final step, the comparison to the results of the IRO-Mats research and the proposals is given. The experimental results from this database are given in Annex 3. These results are taken from CUR reports 112 (CUR Committee 33, 1983) and 163 (CUR Committee 33, 1993). Since these tests are on normal strength concrete, they are not discussed in Chapter 4 of this report. Only the experiments with a constant amplitude are used, the experiments with rest period or with a variable amplitude or random loading are not considered. The experiments with eccentric loading were not considered for this analysis. The specimens were cylinders with a diameter of 150mm and a height of 450mm, which were cured in water. For the test results from CUR report 163, 6 specimens were used to find the value of the number of cycles given in Annex 3. For the results from CUR report 112, at least 7 experiments were used to find each value for the number of cycles. In Table 23 the results are given assuming that $f_{ck} = f_{c,mean} - 8$MPa, and in ***Error! Reference source not found.*** assuming that $f_{ck} = f_{c,mean} - 1{,}64\sigma_{meas}$ with σ_{meas} the measured standard deviation.

Since these specimens were tested under water, the fatigue life of these specimens is lower than the fatigue life of dry concrete. As such, it is not surprising that smaller values are found. Interesting to notice here is that the scatter on the tested to predicted values for S_{max} remains small, and that a coefficient of variation of 8,6% is achieved, which is in line with the results from the high strength concrete database as compared to the different proposals. However, the results err on the unsafe side, because the studied models are for dry concrete (as used in bridges) and not for wet concrete (as used in offshore construction and as described in the CUR reports). A reduction factor should be used on the fatigue strength of wet concrete. From these results it seems that a reduction factor of 0,8 is suitable.

Table 23: Overview of the statistical parameters from the different methods for the experiments from the CUR reports.

Method	**§**	$\gamma_{c,fat}$	**AVG**	**STD**	**COV**	**Char**	**5%**
EC, $k_1 = 1$	5.3	1,5	1,040	0,089	8,6%	0,893	
EC, $k_1 = 1$, HSC	5.4	1,5	0,995	0,086	8,6%	0,855	
Proposal	5.5	1,5	0,975	0,084	8,6%	0,838	
Proposal + HSC	5.6	1,5	0,956	0,081	8,5%	0,823	

Table 24: Overview of the statistical parameters from the different methods for the experiments from the CUR report with f_{ck} based on the measured standard deviation of the static compressive strength tests.

Method	**§**	$\gamma_{c,fat}$	**AVG**	**STD**	**COV**	**Char**	**5%**
EC, k_1 = 1	5.3	1,5	1,044	0,090	8,6%	0,897	
EC, k_1 = 1, HSC	5.4	1,5	0,998	0,086	8,6%	0,857	
Proposal	5.5	1,5	0,977	0,084	8,6%	0,840	
Proposal + HSC	5.6	1,5	0,957	0,081	8,4%	0,824	

6 Recommendations

The smallest coefficient of variation, and thus the best correspondence with the experiments is found for the proposal that consists of the following expressions:

$$\log N_i = \frac{6\left(S_{max} - 1\right)}{S_{max,EC} - 1} \text{ for } N_i \leq 10^6 \tag{64}$$

$S_{max,EC}$ is here the value of S_{max} which is found for 10^6 cycles, and can be expressed as:

$$S_{max,EC} = \left(1 - \frac{f_{ck}}{400}\right)\left(1 - \frac{3}{7}\sqrt{1 - R_i *}\right) \tag{65}$$

with $R_i * = \dfrac{S_{min}}{S_{max,EC}}$, and

$$\log N_i = 14\frac{1 - E_{cd,max,i}}{\sqrt{1 - R_i}} \text{ for } N_i > 10^6 \tag{66}$$

$$E_{cd,max,i} = \frac{\sigma_{cd,max,i}}{f_{cd,fat}} \text{ for } N_i > 10^6 \tag{67}$$

with

$$f_{cd,fat} = f_{cd}\left(1 - \frac{f_{ck}}{400}\right) \tag{68}$$

These equations have the following characteristics:

- for 1 loading cycle, the static compressive strength is found
- at 10^6 cycles, the connection between Eqs. (59) and (61) is smooth
- for higher strength concrete classes, the method is not overly conservative.

The disadvantage of this method is the need for iteration to determine $S_{max,EC}$. This method is recommended for the assessment of existing structures. Note that when an existing structures is assessed and the measured concrete compressive strength is taken into account, also the measured scatter on the tested cores needs to be taken into account to find the characteristic value of the concrete compressive strength f_{ck}.

Since the expression from NEN-EN 1992-2+C1:2011 in which $f_{ck}/250$ is replaced by $f_{ck}/400$ (with k_1 = 1) is easy to use and does not require iterations, it can be recommended for the design of new structures:

$$f_{cd,fat} = k_1\beta_{cc}(t_0) f_{cd}\left(1 - \frac{f_{ck}}{400}\right) \tag{69}$$

$$N_i = 10^{\left(14\frac{1 - E_{cd,max,i}}{\sqrt{1 - R_i}}\right)} \tag{70}$$

$$R_i = \frac{E_{cd,min,i}}{E_{cd,max,i}} \tag{71}$$

$$E_{cd,min,i} = \frac{\sigma_{cd,min,i}}{f_{cd,fat}} \tag{72}$$

$$E_{cd,max,i} = \frac{\sigma_{cd,max,i}}{f_{cd,fat}} \tag{73}$$

7 Summary and conclusions

In this report, concrete under compressive fatigue is studied. The following elements were studied in this report:

- A literature review of concrete in compression under repeated cycles is carried out, with an emphasis on the latest developments related to higher strength concrete.
- The existing code provisions and some proposals from the literature are studied and the influence of the concrete compressive strength (concrete class) is highlighted.
- A database of experiments in compressive fatigue, with an emphasis on high strength concrete is compiled.
- The results from the database are used to develop a proposal for the Dutch National Annex of the Eurocode.
- The resulting proposal for existing structures is conservative, is suitable for higher strength concrete and results in the static compressive strength for a single load cycle.
- The resulting improved version of the Eurocode expression is easy to use and does not require iterations. As such, it is mostly suitable for the design of new structures.

8 References

CEB Committee GTG 15, 1988, "Fatigue of Concrete Structures," CEB Bulletin d'information No 188.

CEN, 2005, "Eurocode 2: Design of Concrete Structures - Part 1-1 General Rules and Rules for Buildings. NEN-EN 1992-1-1:2005," Comité Européen de Normalisation, Brussels, Belgium, 229 pp.

CEN, 2011a, "Eurocode 2: Design of Concrete Structures - Part 1-1 General Rules and Rules for Buildings. NEN-EN 1992-1-1+C2:2011," Comité Européen de Normalisation, Brussels, Belgium, 246 pp.

CEN, 2011b, "Eurocode 2: Design of concrete structures - Concrete bridges - Design and detailing rules. NEN-EN 1992-2+C1:2011," Comité Européen de Normalisation, Brussels, Belgium, 113 pp.

Code Committee 351 001, 2011a, "National Annex to NEN-EN 1992-1-1+C2, Eurocode 2: Design of concrete structures – Part 1-1: General rules and rules for buildings. NEN-EN 1992-1-1+C2:2011/NB:2011," Nederlands Normalisatie-instituut, Delft, The Netherlands, 39 pp.

Code Committee 351 001, 2011b, "National Annex to NEN-EN 1992-2+C1, Eurocode 2: Design of concrete structures - Concrete bridges - Design and detailing rules. NEN-EN 1992-2+C1:2011/NB:2011," Nederlands Normalisatie-instituut, Delft, The Netherlands, 24 pp.

Code Committee 351 001 "Technical Foundations for Structures", 2009, "Regulations for concrete - Bridges - Structural requirements and calculation methods, NEN 6723:2009," 72 pp.

CUR-onderzoekcommissie C 33 "Wisselbelasting", 1983, "Vermoeiing van beton, deel 1: drukspanningen," V. CUR Rapport 112, pp.

CUR-onderzoekcommissie C 33 "Wisselbelasting", 1993, "Vermoeiing van beton, deel 4: drukspanningen (2)," V. CUR Rapport 163, pp.

del Viso, J. R., Carmona, J. R. and Ruiz, G., 2008, "Shape and size effects on the compressive strength of high-strength concrete," *Cement and Concrete Research*, V. 38, No. 3, Mar, pp. 386-395.

Fehling, E., Schmidt, M., Teichmann, T., Bunje, K., Bornemann, R. and Middendorf, B., 2005, "Entwicklung, Dauerhaftigkeit und Berechnung Ultrahochfester Betone (UHPC)," V. Forschungsbericht DFG FE 497/1-1, Universitat Kassel, 132 pp.

Fehling, E., Schmidt, M., Walraven, J., Leutbecher, T. and Fröhlich, S., 2013, "Betonkalender: IX - UHPC."

fib, 2012, "Model code 2010: final draft," International Federation for Structural Concrete; Lausanne, 676 pp.

fib Task Group 8.2, 2008, "Constitutive modelling of high strength/ high performance concrete," fib bulletin 42.

Holmen, J. O., 1982, "Fatigue of concrete by constant and variable amplitude loading," *ACI SP-75: Fatigue of Concrete Structures*, pp. 71-110.

Hordijk, D. A., 1994, "Vergelijkend onderzoek naar een aantal materiaaleigenschappen van grindbeton en kalksteenbeton. Fase II: Vermoeiing," V. 94-CON-R0270, TNO, Delft, 59 pp.

Hordijk, D. A., Wolsink, G. M. and de Vries, J., 1995, "Fracture and fatigue behaviour of a high strength limestone concrete as compared to gravel concrete," *Heron*, V. 40, No. 2, pp. 125-146.

Hsu, T. T. C., 1981, "Fatigue of Plain Concrete," *Journal of the American Concrete Institute*, V. 78, No. 4, 1981, pp. 292-305.

Kim, J. K. and Kim, Y. Y., 1996, "Experimental study of the fatigue behavior of high strength concrete," *Cement and Concrete Research*, V. 26, No. 10, Oct, pp. 1513-1523.

Klausen, D., 1978, "Festigkeit und Schädigung von Beton bei häufig wiederholter Beanspruchung," PhD, Technische Hochschule Darmstadt, pp. 85.

Lohaus, L. and Anders, S., 2006, "High-cycle Fatigue of Ultra-high Performance Concrete – Fatigue Strength and Damage Development," *Proceedings of the 2nd International Congress*, Naples, Italy, pp. 10pp.

Lohaus, L., Wefer, M. and Oneschkow, N., 2011, "Ermüdungsbemessungsmodell für normal-, hoch- und ultrahochfeste Betone," *Beton- und Stahlbetonbau*, V. 106, No. 12, pp. 836-846.

Petkovic, G., Lenschow, R., Stemland, H. and Rosseland, S., 1990, "Fatigue of high-strength concrete," *ACI SP-121: High-strength concrete*, pp. 505-525.

Saucedo, L., Yu, R. C., Medeiros, A., Zhang, X. and Ruiz, G., 2013, "A probabilistic fatigue model based on the initial distribution to consider frequency effect in plain and fiber reinforced concrete," *International Journal of Fatigue*, V. 48, Mar, pp. 308-318.

Snijders, A. M. M., 2013, "Fatigue and shear forces: Differences between NEN and Eurocode," MSc. Thesis, Delft University of Technology, pp. 172.

Tepfers, R. and Kutti, T., 1979, "Fatigue strength of plain, ordinary and lightweight concrete," *ACI Journal Proceedings*, V. 76, No. 3, pp. 635-652.

Tue, N. V. and Mucha, S., 2006, "Ermüdungsfestigkeit von hochfestem Beton unter Druckbeanspruchung," *Bautechnik*, V. 83, No. 7, pp. 497-504.

van der Veen, C. and Gijsbers, F. B. J., 2011, "Werkset factoren voor bestaande betonnen kunstwerken - Notitie Dwarskrachtbeoordeling bestaande kunstwerken," 6 pp.

Wefer, M., 2010, "Materialverhalten und Bemessungswerte von ultrahochfestem Beton unter einaxialer Ermudungsbeanspruchung," PhD Thesis, Leibniz Universitat Hannover, Hannover.

9 Annex 1: Database of fatigue tests

Ref	Specimen	fccyl,mean (MPa)	Smin	Smax	N	Opmerkingen
Petkovic et al., 1990	ND65	55	0,050	0,700	9000	Resultaten afgelezen uit S-N curves p, 519, individuele resultaten niet gekend
		55	0,050	0,600	2100000	De waarden zijn ook gemiddeldes van 2 of 3 proeven
		55	0,200	0,750	6200	
		55	0,200	0,700	70000	
		55	0,300	0,750	22000	
		55	0,400	0,850	900	
		55	0,400	0,800	23000	
	ND95	75	0,050	0,950	50	
		75	0,050	0,900	130	
		75	0,050	0,850	190	
		75	0,050	0,750	2100	
		75	0,050	0,700	4500	
		75	0,050	0,650	71000	
		75	0,050	0,600	3000000	Geen bezwijken na 3*10^6 wisselingen
		75	0,600	0,950	220	
		75	0,600	0,900	3100	
		75	0,600	0,850	5000	
		75	0,600	0,800	71000	dit specimen, of 2 specimens gemiddeld bezweken wel voor deze Smin en Smax
		75	0,600	0,800	3000000	niet gegeven hoeveel van de 3 specimens niet bezweken bij 3E6 wisselingen
		75	0,200	0,750	8700	
		75	0,400	0,850	1100	
		75	0,400	0,800	15000	
		75	0,400	0,750	2000000	Geen bezwijken
	LWA	80	0,050	0,850	500	

		80	0,050	0,750	4000	
		80	0,050	0,700	7000	
		80	0,050	0,650	190000	
		80	0,050	0,600	1500000	
		80	0,300	0,750	62000	
		80	0,400	0,850	2100	
		80	0,400	0,800	9200	
		80	0,400	0,750	450000	
		80	0,600	0,850	5000	
Fehling et al., 2005	UHPC σu = 0,06 bis 0,075	226	0,068	0,826	3200	Smin was tussen 0,06 - 0,075 => de gemiddelde waarde is gebruikt
		226	0,068	0,768	6300	De proefresultaten zijn afgelezen uit de S-N curves, de individuele resultaten zijn niet gegeven
		226	0,068	0,726	18000	Smax was niet gegeven, de y-as is functie van Δσ
		226	0,068	0,726	51000	De specimens bevatten volgens de tekst soms wel en soms geen vezels, maar de mengselbeschrijving geeft aan dat B3Q mengsel steeds staalvezels bevat
		226	0,068	0,715	18000	
		226	0,068	0,715	31000	
		226	0,068	0,656	51000	
		226	0,068	0,656	120000	
		226	0,068	0,656	450000	
		226	0,068	0,609	22000	
		226	0,068	0,609	40000	
		226	0,068	0,591	2000000	geen bezwijken
		226	0,068	0,503	5000000	geen bezwijken
		226	0,230	0,830	10000	
		226	0,230	0,659	2000000	geen bezwijken
Kim & Kim, 1996	LS	26	0,250	0,950	123	resultaten zijn gemiddeldes van een aantal (+- 6) specimens
		26	0,250	0,850	1363	
		26	0,250	0,800	5738	

		26	0,250	0,750	55739	
	MS	52	0,250	0,950	100	
		52	0,250	0,850	968	
		52	0,250	0,800	2528	
		52	0,250	0,750	10117	
	HS	84	0,250	0,950	58	
		84	0,250	0,850	1045	
		84	0,250	0,800	1644	
		84	0,250	0,750	3484	
	VHS	103	0,250	0,950	46	
		103	0,250	0,850	481	
		103	0,250	0,800	1419	
		103	0,250	0,750	3394	
Hordijk et al., 1995	Gravel // GD-3	78,2	0,052	0,829	622	Opgelet: dit zijn geen proeven op cylinders maar prismas van 250mm x 100mm x 100mm
Hordijk, 1994	GD-1	78,2	0,051	0,835	5900	de betondruksterkte is gemeten op prismas van 250mm x 100mm x 100mm
	GC-4	78,2	0,052	0,825	2701	frequentie f=6Hz
	GA-3	78,2	0,051	0,815	1227	
	GC-3	78,2	0,051	0,731	42379	
	GD-4	78,2	0,051	0,733	60537	
	GF-1	78,2	0,055	0,659	18939	
	GA-4	78,2	0,056	0,710	26494	
	GF-2	78,2	0,055	0,673	116908	
	GE-3	78,2	0,058	0,665	98664	
	GC-2	78,2	0,023	0,723	92885	
	GA - 2	78,2	0,022	0,849	1894	
	GB - 3	78,2	0,024	0,848	693	
	GE-1	78,2	0,054	0,664	6037	
	GE-2	78,2	0,055	0,660	40665	

	Limestone // KB-3	73,1	0,053	0,828	697	
	KC - 3	73,1	0,022	0,852	830	
	KD-4	73,1	0,053	0,837	945	
	KA-2	73,1	0,055	0,811	2836	
	KB - 4	73,1	0,026	0,743	40461	
	KC-2	73,1	0,029	0,735	65790	
	KD-3	73,1	0,053	0,722	14842	
	KA-3	73,1	0,056	0,707	22366	
	KA-4	73,1	0,053	0,709	39840	
	KD-1	73,1	0,059	0,665	292573	
	KF-1	73,1	0,055	0,657	243419	
	KE-1	73,1	0,059	0,651	155331	
Saucedo et al., 2013	C1	94,7	0,285	0,950	150	op kubussen van 80mm
		94,7	0,285	0,950	2927	
		94,7	0,285	0,950	2149	
		94,7	0,285	0,950	667	
		94,7	0,285	0,950	7600	
		94,7	0,285	0,950	75378	
		94,7	0,285	0,950	7839	
		94,7	0,285	0,950	20426	
		94,7	0,285	0,950	38	
		94,7	0,285	0,950	73	
		94,7	0,285	0,950	17172	
		94,7	0,285	0,950	11863	
		94,7	0,285	0,950	9218	
		94,7	0,285	0,950	7288	
		94,7	0,285	0,950	2798	
		94,7	0,095	0,950	2265	

	94,7	0,095	0,950	4276	
	94,7	0,095	0,950	2352	
	94,7	0,095	0,950	222	
	94,7	0,095	0,950	46	
	94,7	0,095	0,950	125	
	94,7	0,095	0,950	731	
	94,7	0,095	0,950	1106	
	94,7	0,095	0,950	7153	
	94,7	0,095	0,950	3961	
	94,7	0,095	0,950	1231	
	94,7	0,095	0,950	1753	
	94,7	0,095	0,950	302	
	94,7	0,095	0,950	858	
	94,7	0,095	0,950	5988	
C2	76,1	0,262	0,873	8411	op kubussen van 100mm
	76,1	0,262	0,873	821	voor f= 4Hz
	76,1	0,262	0,873	2485	
	76,1	0,262	0,873	1660	
	76,1	0,262	0,873	22570	
	76,1	0,262	0,873	9521	
	76,1	0,262	0,873	4192	
	76,1	0,262	0,873	13020	
	76,1	0,262	0,873	170256	
	76,1	0,262	0,873	1578	
	76,1	0,262	0,873	1222	
	76,1	0,262	0,873	133	
	76,1	0,262	0,873	7038	
	76,1	0,262	0,873	282	voor f=1Hz

76,1	0,262	0,873	23	
76,1	0,262	0,873	759	
76,1	0,262	0,873	1351	
76,1	0,262	0,873	85	
76,1	0,262	0,873	157	
76,1	0,262	0,873	479	
76,1	0,262	0,873	368	
76,1	0,262	0,873	833	
76,1	0,262	0,873	1571	
76,1	0,262	0,873	98	voor f=0,25Hz
76,1	0,262	0,873	1242	
76,1	0,262	0,873	535	
76,1	0,262	0,873	157	
76,1	0,262	0,873	18	
76,1	0,262	0,873	30	
76,1	0,262	0,873	219	
76,1	0,262	0,873	650	
76,1	0,262	0,873	122	
76,1	0,262	0,873	400	
76,1	0,262	0,873	339	voor f=0,0625
76,1	0,262	0,873	473	
76,1	0,262	0,873	102	
76,1	0,262	0,873	234	
76,1	0,262	0,873	11	
76,1	0,262	0,873	142	
76,1	0,262	0,873	76	
76,1	0,262	0,873	275	
76,1	0,262	0,873	329	

		76,1	0,262	0,873	38	
Lohaus et al., 2011	M2Q-1	170	0,050	0,900	9979	proeven op cylinders van 60mm x 180mm
		170	0,050	0,900	11478	afgelezen van SN curve
		170	0,050	0,900	1112	specimens met staalvezels 2,5vol%, 9mm lengte, l/d = 60
		170	0,050	0,900	3352	frequentie f=10Hz
		170	0,050	0,800	37559	
		170	0,050	0,800	1966	
		170	0,050	0,800	26137	
		170	0,050	0,800	13009	
		170	0,050	0,800	25679	
		170	0,050	0,800	1703	
		170	0,050	0,800	28756	
		170	0,050	0,800	19376	
		170	0,050	0,800	16154	
		170	0,050	0,800	9692	
		170	0,050	0,800	39098	
		170	0,050	0,800	29367	
		170	0,050	0,800	15700	f = 1Hz
		170	0,050	0,800	46074	f= 5Hz
		170	0,050	0,800	30503	f = 15Hz
		170	0,050	0,700	2460014	
		170	0,050	0,700	3206760	
	M2Q-2	170	0,200	0,900	182	
		170	0,200	0,900	385	
		170	0,200	0,900	1184	
		170	0,200	0,850	1864	
		170	0,200	0,850	416	
		170	0,200	0,850	7628	

	170	0,200	0,850	2630	
	170	0,200	0,800	11393	
	170	0,200	0,800	17086	
	170	0,200	0,800	12157	
	170	0,200	0,800	5310	
	170	0,200	0,800	24292	
	170	0,200	0,800	10387	
	170	0,200	0,750	161879	
	170	0,200	0,750	109604	
	170	0,200	0,750	356657	
	170	0,200	0,750	107516	
	170	0,200	0,700	2000933	
	170	0,200	0,650	14250000	f = 65Hz
	170	0,200	0,650	12000000	f = 65Hz
	170	0,200	0,650	15000000	f = 65Hz
	170	0,200	0,650	14250000	f = 65Hz
M2Q-3	170	0,050	0,800	4093	
	170	0,050	0,800	12786	
	170	0,050	0,800	5444	
	170	0,200	0,800	5948	
	170	0,200	0,800	53187	
	170	0,200	0,800	5680	
	170	0,200	0,800	43285	
	170	0,400	0,900	1099	
	170	0,400	0,900	1555	
	170	0,400	0,900	375	
	170	0,400	0,800	48253	
	170	0,400	0,800	48374	

	170	0,400	0,800	62487	
	170	0,400	0,800	187652	
	170	0,400	0,800	108130	
	170	0,400	0,800	1573078	
	170	0,400	0,800	1002066	
	170	0,400	0,800	570378	proef vroeger gestopt
	170	0,400	0,800	2980484	
	170	0,500	0,800	2600148	
	170	0,500	0,800	2600217	
M2Q-4	170	0,050	0,750	25290	in normaal klimaat
	170	0,050	0,750	25117	
	170	0,050	0,750	16651	
	170	0,050	0,750	35469	
	170	0,050	0,750	13390	
	170	0,050	0,750	16515	
	170	0,050	0,750	22517	
	170	0,050	0,750	28200	
	170	0,050	0,750	21224	
	170	0,050	0,750	20644	
	170	0,050	0,750	66544	proefstukken met warmte behandeld
	170	0,050	0,750	50057	
	170	0,050	0,750	46247	
	170	0,050	0,750	30344	
	170	0,050	0,750	23410	
	170	0,050	0,750	48848	
	170	0,050	0,750	12377	
	170	0,050	0,750	38706	
	170	0,050	0,750	18286	

	170	0,050	0,750	45208	
B4Q-1	170	0,050	0,900	398	
	170	0,050	0,900	408	
	170	0,050	0,900	881	
	170	0,050	0,900	573	
	170	0,050	0,850	1483	
	170	0,050	0,850	2732	
	170	0,050	0,850	2750	
	170	0,050	0,850	661	
	170	0,050	0,800	27124	
	170	0,050	0,800	8395	
	170	0,050	0,800	15178	
	170	0,050	0,800	24268	
	170	0,050	0,800	10405	
	170	0,050	0,750	71836	
	170	0,050	0,750	105872	
	170	0,050	0,750	105543	
	170	0,050	0,750	177219	
	170	0,050	0,750	83637	
	170	0,050	0,700	395209	
	170	0,050	0,700	263454	
	170	0,050	0,700	208683	
	170	0,050	0,700	608759	
	170	0,050	0,700	548557	
	170	0,050	0,700	133411	f= 65Hz
	170	0,050	0,700	232092	f= 65Hz
	170	0,050	0,700	295706	f= 65Hz
	170	0,050	0,700	116891	f= 65Hz

	170	0,050	0,700	86182	f= 65Hz
	170	0,050	0,700	91905	f= 65Hz
	170	0,050	0,650	1469117	f= 65Hz
	170	0,050	0,650	1066419	f= 65Hz
	170	0,050	0,650	1452126	f= 65Hz
	170	0,050	0,650	329531	f= 65Hz
	170	0,050	0,650	1793320	f= 65Hz
	170	0,050	0,600	2000000	f= 65Hz
	170	0,050	0,600	2000000	f= 65Hz
	170	0,050	0,600	10000000	f= 65Hz
	170	0,050	0,600	10808000	f= 65Hz
	170	0,050	0,600	2884371	f= 65Hz
B4Q-2	170	0,050	0,900	2109	
	170	0,050	0,900	5920	
	170	0,050	0,900	1119	
	170	0,050	0,900	1490	
	170	0,050	0,900	2674	
	170	0,050	0,900	184	
	170	0,050	0,900	2235	
	170	0,050	0,900	234	
	170	0,050	0,900	454	
	170	0,050	0,800	19821	
	170	0,050	0,800	35327	
	170	0,050	0,800	4729	
	170	0,050	0,800	35921	
	170	0,050	0,800	6629	
	170	0,050	0,800	13164	
	170	0,050	0,800	3350	

	170	0,050	0,800	9523	
	170	0,050	0,800	26307	
	170	0,050	0,800	21683	
	170	0,050	0,800	9166	
	170	0,050	0,700	458588	
	170	0,050	0,700	313607	
	170	0,050	0,700	1507732	
	170	0,050	0,700	616697	
	170	0,050	0,700	828554	
	170	0,050	0,700	65885	
	170	0,050	0,700	475276	
	170	0,050	0,700	773128	
B4Q-3	170	0,050	0,800	34409	
	170	0,050	0,800	35254	
	170	0,050	0,800	44748	
	170	0,050	0,800	28786	
	170	0,050	0,800	26533	
	170	0,050	0,800	33426	
	170	0,050	0,700	525053	
	170	0,050	0,700	2384388	
	170	0,050	0,700	40018	
	170	0,050	0,700	236371	
	170	0,050	0,700	587998	
	170	0,050	0,700	652383	
	170	0,050	0,700	3462190	
NB	38	0,050	0,900	4135	normale sterkte beton, zonder vezels
	38	0,050	0,900	229	
	38	0,050	0,900	9166	

		38	0,050	0,900	1266	
		38	0,050	0,900	931	
		38	0,050	0,900	2400	
		38	0,050	0,900	567	
		38	0,050	0,900	782	
		38	0,050	0,900	845	
		38	0,050	0,900	251	
		38	0,050	0,800	26425	
		38	0,050	0,800	73543	
		38	0,050	0,800	103386	
		38	0,050	0,800	19131	
		38	0,050	0,800	14260	
		38	0,050	0,800	12417	
		38	0,050	0,800	98015	
		38	0,050	0,800	165910	
		38	0,050	0,800	133152	
		38	0,050	0,800	29323	
		38	0,050	0,700	1272231	
		38	0,050	0,700	2342911	
		38	0,050	0,700	3003765	
		38	0,050	0,700	2301902	
		38	0,050	0,700	2414014	
Lohaus & Anders, 2006	Reference	140	0,050	0,738	1000	enkel de SN curve is gegeven, 3 punten zijn afgelezen
		140	0,050	0,605	10000	de cylinderszijn 70mm diameter, lengte 210mm
		140	0,050	0,564	100000	
		140	0,050	0,480	1000000	
	Reference	145	0,050	0,795	1000	met warmtebehandelink
	Heat Treated	145	0,050	0,732	10000	

		145	0,050	0,657	100000	
		145	0,050	0,595	1000000	
	SF 0,75	140	0,050	0,717	1000	staalvezels, 0,75vol%, 6mm lengte, l/d=37,5
		140	0,050	0,632	10000	
		140	0,050	0,532	100000	
		140	0,050	0,435	1000000	
	SF 1,75	130	0,050	0,738	1000	staalvezels, 1,75vol%, 6mm lengte, l/d=37,5
		130	0,050	0,665	10000	
		130	0,050	0,572	100000	
		130	0,050	0,495	1000000	
	AR S 3,0	120	0,050	0,738	1000	alkali-resistente glasvezels, 3,0kg/m^3, 13mm lengte, despersible
		120	0,050	0,646	10000	
		120	0,050	0,557	100000	
		120	0,050	0,465	1000000	
	AR Y 6,0	130	0,050	0,717	1000	alkali-resistente glasvezels, 6,0kg/m^3, 13mm lengte,integral
		130	0,050	0,632	10000	
		130	0,050	0,532	100000	
		130	0,050	0,435	1000000	
Tue &Mucha, 2006	Leipzig proeven	65	0,400	0,800	14489	resultaten als gemiddelde van een aantal specimens gegeven
		65	0,400	0,700	1471316	
		65	0,400	0,600	2540240	
		65	0,300	0,800	2203	
		65	0,300	0,750	878830	
		65	0,300	0,700	1832482	
		65	0,300	0,650	2263330	
		65	0,300	0,600	2393031	
		65	0,200	0,850	338	
		65	0,200	0,800	2229	

		65	0,200	0,750	9691	
		65	0,200	0,700	33536	
		65	0,200	0,650	1808836	
		65	0,200	0,600	2316853	
		65	0,200	0,550	2495845	
		65	0,100	0,800	500	
		65	0,100	0,750	4428	
		65	0,100	0,700	4871	
		65	0,100	0,650	62483	
		65	0,100	0,600	2115172	
		65	0,050	0,800	1000	
		65	0,050	0,750	3847	
		65	0,050	0,700	5179	
		65	0,050	0,650	46402	
		65	0,050	0,600	1908925	
Zhao et al., 1996	NS	30,75	0,100	0,810	1000	frequentie f=10Hz
		30,75	0,100	0,770	10000	proefresultaten op basis van enkel SN curve, geen datapunten
		30,75	0,100	0,750	100000	
		30,75	0,100	0,720	1000000	
	HS	69,454	0,100	0,800	1000	
		69,454	0,100	0,760	10000	
		69,454	0,100	0,720	100000	
		69,454	0,100	0,670	1000000	
Hohberg, 2004	B25	28	0,080	0,840	1800	datapunten afgelezen van een grafiek
		28	0,080	0,750	20000	frequentie f=10Hz
		28	0,080	0,730	95000	
		28	0,080	0,710	120000	
		28	0,080	0,660	1100000	

	28	0,080	0,640	1700000
	28	0,080	0,600	7000000
B45	43	0,040	0,840	1400
	43	0,040	0,750	11000
	43	0,040	0,670	80000
	43	0,040	0,660	110000
	43	0,040	0,585	1100000
B95	88	0,020	0,870	1100
	88	0,020	0,840	2050
	88	0,020	0,760	20000
	88	0,020	0,750	30000
	88	0,020	0,720	40000
	88	0,020	0,660	65000
	88	0,020	0,600	12000000

10 Annex 2: Verification database of normal strength concrete

Ref	Specimen	fccyl,mean (MPa)	Smin	Smax	log N	N
Klausen, 1978	1	44,1	0,205	0,745	2,5186	330
	2	44,1	0,205	0,745	3,2923	1960
	3	44,1	0,205	0,745	4,0584	11439
	4	44,1	0,205	0,745	4,0746	11874
	5	44,1	0,205	0,745	4,1097	12874
	6	44,1	0,205	0,745	4,3756	23747
	7	44,1	0,205	0,745	4,601	39902
	8	44,1	0,205	0,745	4,648	44463
	9	44,1	0,205	0,745	4,8465	70226
	10	44,1	0,205	0,745	4,9025	79891
	11	44,1	0,205	0,745	5,0615	115213
	12	44,1	0,205	0,745	5,0688	117166
	13	44,1	0,205	0,745	5,1667	146791
	14	44,1	0,205	0,745	5,4588	287607
	15	44,1	0,205	0,745	5,7281	534687
	16	44,1	0,205	0,745	5,9661	924911
	17	44,1	0,205	0,745	6,0109	1025416
	18	44,1	0,205	0,745	6,0712	1178148
	19	44,1	0,205	0,745	6,1685	1474009
	20	44,1	0,205	0,745	6,1939	1562788
	21	44,1	0,205	0,745	6,2124	1630797
	22	44,1	0,205	0,745	6,2909	1953890
	23	44,1	0,205	0,745	6,3194	2086412
	24	44,1	0,205	0,745	6,3802	2399938
	25	44,1	0,205	0,745	6,4173	2613966
	26	44,1	0,205	0,745	6,4349	2722074

27	44,1	0,205	0,745	6,5355	3431626
28	44,1	0,205	0,745	6,7016	5030371
29	44,1	0,205	0,745	6,8295	6753051
30	44,1	0,205	0,745	6,8366	6864359
31	44,1	0,205	0,745	6,8441	6983932
32	44,1	0,205	0,745	6,8512	7099046
33	44,1	0,205	0,745	6,9366	8641716
34	44,1	0,205	0,745	6,9472	8855233
35	44,1	0,205	0,745	6,9518	8949525
36	44,1	0,205	0,745	6,9561	9038576
37	44,1	0,205	0,745	7,1595	14437766
38	44,1	0,205	0,745	7,1985	15794286
39	44,1	0,205	0,745	7,3987	25043787
1	44,1	0,205	0,845	1,5564	36
2	44,1	0,205	0,845	1,6021	40
3	44,1	0,205	0,845	1,6628	46
4	44,1	0,205	0,845	1,8389	69
5	44,1	0,205	0,845	1,8977	79
6	44,1	0,205	0,845	1,9295	85
7	44,1	0,205	0,845	1,9543	90
8	44,1	0,205	0,845	2	100
9	44,1	0,205	0,845	2,0414	110
10	44,1	0,205	0,845	2,2305	170
11	44,1	0,205	0,845	2,398	250
12	44,1	0,205	0,845	2,4624	290
13	44,1	0,205	0,845	2,4915	310
14	44,1	0,205	0,845	2,6129	410
15	44,1	0,205	0,845	2,6991	500

16	44,1	0,205	0,845	2,732	540
17	44,1	0,205	0,845	2,8062	640
18	44,1	0,205	0,845	2,9822	960
19	44,1	0,205	0,845	2,9912	980
20	44,1	0,205	0,845	3,0645	1160
21	44,1	0,205	0,845	3,1524	1420
22	44,1	0,205	0,845	3,1584	1440
23	44,1	0,205	0,845	3,2042	1600
24	44,1	0,205	0,845	3,3161	2071
25	44,1	0,205	0,845	3,5144	3269
26	44,1	0,205	0,845	3,5856	3851
27	44,1	0,205	0,845	3,6213	4181
28	44,1	0,205	0,845	3,7269	5332
29	44,1	0,205	0,845	3,9451	8813
30	44,1	0,205	0,845	3,9677	9283
31	44,1	0,205	0,845	4,4899	30896
32	44,1	0,205	0,845	4,5381	34522
33	44,1	0,205	0,845	4,6701	46784
34	44,1	0,205	0,845	5,4727	296961
35	44,1	0,205	0,845	5,6419	438430
1	44,1	0,05	0,805	2,6837	483
2	44,1	0,05	0,685	4,7115	51464
3	44,1	0,05	0,585	6,4388	2746629
4	44,1	0,2	0,88	1,9705	93
5	44,1	0,2	0,84	3,1116	1293
6	44,1	0,2	0,78	4,8233	66573
7	44,1	0,2	0,74	5,9644	921298
8	44,1	0,2	0,68	7,6761	47435120

	9	44,1	0,35	0,89	3,0992	1257
	10	44,1	0,35	0,85	5,0807	120420
	11	44,1	0,4	0,91	2,0232	105
	12	44,1	0,4	0,875	4,7214	52650
	13	44,1	0,4	0,835	7,8051	63841047

Ref	Specimen	fccyl,mean (MPa)	Smin	Smax	log N	N	
Tepfers & Kutti	1	54,3	0,18	0,9	0,477121	3	
	2	54,3	0,192	0,96	0,60206	4	
	3	54,3	0,192	0,96	2	100	
	4	54,3	0,168	0,84	3,021189	1050	
	5	54,3	0,168	0,84	3,30103	2000	
	6	54,3	0,16	0,8	3,477121	3000	
	7	54,3	0,16	0,8	3,799341	6300	
	8	54,3	0,14	0,7	3,913814	8200	
	9	54,3	0,1492	0,746	4,50515	32000	
	10	54,3	0,1492	0,746	4,60206	40000	
	11	54,3	0,1386	0,693	5,812913	650000	
Hsu	Assimacolpoulos et al	41	0,09495	0,633	6,079181	1,20E+06	elk punt is geometrisch gemiddelde van 5 tot 14 proeven
	2	41	0,10005	0,667	6,021189	1,05E+06	
	3	41	0,105	0,7	5,875061	750000	
	4	41	0,1125	0,75	5,50515	320000	
	5	41	0,271065	0,71333	6,60206	4,00E+06	
	6	41	0,285	0,75	6,146128	1,40E+06	
	7	41	0,285	0,75	6	1,00E+06	
	8	41	0,304	0,8	5,90309	8,00E+05	
	9	41	0,323	0,85	5,342423	2,20E+05	
	10	41	0,492	0,82	6,146128	1,40E+06	

11	41	0,5202	0,867	5,778151	6,00E+05
12	41	0,54	0,9	4,662758	4,60E+04
13	41	0,54	0,9	5,50515	3,20E+05
14	41	0,66759	0,867	6,30103	2,00E+06
15	41	0,672441	0,8733	6,612784	4,10E+06
16	41	0,682759	0,8867	6,342423	2,20E+06
17	41	0,693	0,9	6,176091	1,50E+06
18	41	0,7084	0,92	6,491362	3,10E+06
19	41	0,7084	0,92	5,361728	2,30E+05
20	41	0,7315	0,95	5,30103	2,00E+05
21	41	0,7744	0,88	6,322219	2,10E+06
22	41	0,792	0,9	6,30103	2,00E+06
23	41	0,792	0,9	6,50515	3,20E+06
24	41	0,8096	0,92	5,20412	1,60E+05
25	41	0,836	0,95	4,845098	7,00E+04

11 Annex 3: CUR experiments

Ref	Specimen	fccyl,mean (MPa)	Smin	Smax	N	Opmerkingen
CUR 163	I-1	34,44	0,08	0,8	955	f = 6Hz
	I-2	34,44	0,07	0,7	6026	de resultaten zijn het gemiddelde van 6 proeven
	I-3	34,44	0,06	0,6	49545	ongewapend betonnen cilinders met een diameter
	I-4	34,44	0,32	0,8	2432	van 150 mm en een van ongeveer 450 mm;
	I-5	34,44	0,28	0,7	32137	natte verharding
	I-6	34,44	0,56	0,8	18365	geen resultaten van random belastingsproeven meegenomen
	I-7	34,44	0,08	0,8	298	geen resultaten meegenomen van proeven met rustperiodes
	I-8	34,44	0,07	0,7	1683	geen resultaten meegenomen van proeven met excentrische belasting
	I-9	34,44	0,06	0,6	11535	
	I-10	34,44	0,32	0,8	757	
	I-11	34,44	0,28	0,7	6166	
	I-12	34,44	0,56	0,8	2254	
	I-13	34,44	0,08	0,8	89	
	I-14	34,44	0,07	0,7	441	
	I-15	34,44	0,06	0,6	2667	
	I-16	34,44	0,32	0,8	140	
	I-17	34,44	0,28	0,7	1462	
	I-1	34,44	0,08	0,8	298	f=0,6Hz
	I-2	34,44	0,07	0,7	1683	natte verharding
	I-3	34,44	0,06	0,6	11535	
	I-4	34,44	0,32	0,8	757	
	I-5	34,44	0,28	0,7	6166	
	I-6	34,44	0,56	0,8	2254	
	I-1	34,44	0,08	0,8	89	f=0,06Hz
	I-2	34,44	0,07	0,7	441	natte verharding

I-3	34,44	0,06	0,6	2667	
I-4	34,44	0,32	0,8	140	
I-5	34,44	0,28	0,7	1462	
II-2	36,408	0,07	0,7	5260	f = 6Hz
II-3	36,408	0,06	0,6	44157	serie 1, nat, B45
II-4	36,408	0,32	0,8	4498	
II-5	36,408	0,28	0,7	76384	
II-6	36,408	0,56	0,8	70795	run-out specimens
II-15	36,408	0,06	0,6	6699	f=0,06Hz
II-2	24,026	0,07	0,7	6546	serie 2, nat, B30
II-3	24,026	0,06	0,6	95499	
II-4	24,026	0,32	0,8	5395	
II-5	24,026	0,28	0,7	539511	
II-6	24,026	0,56	0,8	67453	
II-15	24,026	0,06	0,6	7345	f=0,06Hz
II-2	30,996	0,07	0,7	85704	serie 3, droog
II-1	30,996	0,08	0,8	6501	
II-38	30,996	0,09	0,9	1067	
II-40	30,996	0,36	0,9	4898	
II-41	30,996	0,63	0,9	81283	
II-13	30,996	0,08	0,8	925	f=0,06Hz
II-2	33,784	0,07	0,7	7112	serie 4, nat, B45 gewijzigd
II-3	33,784	0,06	0,6	58749	
II-4	33,784	0,32	0,8	3793	
II-5	33,784	0,28	0,7	80353	
II-6	33,784	0,56	0,8	95940	
II-15	33,784	0,06	0,6	3565	f=0,06Hz
II-2	44,362	0,07	0,7	4140	serie 5, nat, B45, 26 weken

	II-3	44,362	0,06	0,6	48084	
	II-4	44,362	0,32	0,8	3828	
	II-5	44,362	0,28	0,7	78163	
	II-6	44,362	0,56	0,8	85310	
	II-15	44,362	0,06	0,6	3428	f=0,06Hz
	III-2	35	0,07	0,7	8147	f=6Hz
	III-3	35	0,06	0,6	44259	nat, B45
	III-5	35	0,28	0,7	67764	
	III-8	35	0,07	0,7	1524	f=0,6Hz
	III-9	35	0,06	0,6	21878	
	III-11	35	0,28	0,7	6209	
	III-14	35	0,07	0,7	5358	f=0,06Hz
	III-15	35	0,06	0,6	527	
	III-17	35	0,28	0,7	4385	
CUR 112		36,9	0	0,9	129	ongewapend betonnen cilinders met een diameter
		36,9	0	0,8	465	van 150 mm en een van ongeveer 450 mm;
		36,9	0	0,7	1959	gemiddelde waarde van minstens 7 proeven is genomen voor N te bepalen
		36,9	0	0,6	16904	
		36,9	0	0,5	167109	
		36,9	0,36	0,9	245	
		36,9	0,32	0,8	2032	
		36,9	0,28	0,7	31696	
		36,9	0,72	0,9	465	
		36,9	0,64	0,8	25293	
		36,9	0,6	0,75	981748	